CRL4 Ubiquitin Ligase Promotes Fanconi Anemia Pathway-Induced Single-Stranded DNA Signaling at Interstrand Crosslinks

---

Dissertation

zur

Erlangung der naturwissenschaftlichen Doktorwürde

(Dr. sc. nat.)

vorgelegt der

Mathematisch-naturwissenschaftlichen Fakultät

der Universität Zürich

von

Tamara Codilupi

von

Rupperswil AG

Promotionskommission

Prof. Dr. Hanspeter Naegeli (Vorsitz und Leitung)

PD Dr. Pavel Janscak

Prof. Dr. Lorenza Penengo

Prof. Dr. Martin Pruschy

Zürich, 2017

Table of contents

Summary

Crosslinking agents like cisplatin are extensively used for the treatment of many solid malignancies including lung, testicular, ovarian and cervical cancer. The cytotoxic effect of cisplatin is mediated by its ability to form DNA interstrand crosslinks (ICLs), which lead to cell death primarily by interfering with DNA replication. Despite the high potency of cisplatin, its clinical use is limited due to the fast emergence of resistances in most of the patients. A common mechanism by which cancer cells evade ICL-induced cell death involves the activation of the DNA damage response (DDR) that coordinates cell cycle progression with DNA repair. Many factors involved in the DDR are tightly regulated by ubiquitination and, therefore, the ubiquitin-proteasome system presents a promising target for the sensitization of cancer cells toward ICL-agents. MLN4924, an inhibitor of cullin-RING E3 ubiquitin ligases (CRLs) is currently investigated in several clinical trials against different malignancies. Importantly, preclinical studies demonstrated that MLN4924 sensitizes cancer cells toward ICL-agents, suggesting that CRL inhibitors may mitigate clinical resistances. However, the mechanisms of this synergy and which of the many CRL complexes are implicated in the cellular response to cisplatin remain poorly understood.

Here, I could demonstrate that the effect of MLN4924 is in particular mediated via inhibition of CRL4. Moreover, I identified CRL4 as a major player that promotes survival of HeLa cells following cisplatin treatment by supporting the S-phase checkpoint response. Inhibition of the CRL4 complex by concomitant depletion of the partially redundant scaffold proteins CUL4A and CUL4B suppresses the formation of ICL-induced single-stranded DNA (ssDNA) and, consequently, the assembly of the ssDNA-RPA platform required for ATR-dependent checkpoint activation. Accordingly, phosphorylation levels of the ATR target proteins RPA2, CHK1 and H2AX are significantly reduced in CRL4-deficient cells. In addition, CUL4A/B depletion stabilizes the replication licensing factor CDT1, thus stimulating DNA re-replication in cisplatin exposed cells. These findings suggest that re-initiation of DNA replication interferes with the damage-induced checkpoint response by masking the ICL-induced ssDNA. Collectively, these findings highlight the importance of CRL4 in the signaling of ICLs and inhibition of CRL4 might present a possible strategy to enhance the efficacy of cisplatin or other chemotherapeutics.

Zusammenfassung

Platinalaloga wie zum Beispiel Cisplatin gehören zu den wirksamsten Chemotherapeutika, die zur Behandlung einer Vielzahl von Krebserkrankungen eingesetzt werden. Der zytotoxische Effekt von Cisplatin basiert hauptsächlich auf seiner Fähigkeit, den DNA-Doppelstrang kovalent zu verlinken. Dies hemmt die DNA-Replikation und führt dadurch zum Zelltod. Trotz diesem äusserst effizienten Wirkungsmechanismus ist die klinische Verwendung sehr stark eingeschränkt, da es in den meisten Fällen zur schnellen Resistenzbildung führt. Eine wichtige Rolle bei der Entstehung von Resistenzen spielt die zelluläre Antwort auf DNA-Schäden, wie zum Beispiel die Hemmung des Zellzyklus und die Aktivierung der DNA Reparatur. Viele der in diesen Signalwegen involvierten Faktoren werden durch Ubiquitinierung reguliert, somit stellt das Ubiquitin-Proteasom-System ein vielversprechendes therapeutisches Ziel dar, um die Wirkung von Cisplatin in Krebszellen zu erhöhen. MLN4924 ist ein Inhibitor der Cullin-RING-E3 Ubiquitin-Ligasen (CRLs), der zur Zeit in klinischen Studien für die Behandlung von soliden Tumoren geprüft wird. Interessanterweise haben präklinische Studien ergeben, dass MLN4924 die Wirksamkeit von Cisplatin in Krebszellen verstärken kann. Dies deutet darauf hin, dass CRL-Inhibitoren die Entwicklung von klinischen Resistenzen vermindern könnten. Die Mechanismen dieser Synergie und welcher der vielen CRL-Komplexen diesen vermittelt, ist aber noch weitgehend unbekannt.

In dieser Arbeit konnte ich zeigen, dass der Effekt von MLN4924 hauptsächlich auf die Inhibition von CRL4 beruht. Darüber hinaus wird eine entscheidende Rolle von CRL4 im Überleben von HeLa-Zellen nach Cisplatin-Behandlung demonstriert, indem es den S-Phasen Zellzyklus-Checkpoint fördert. Die Inhibierung der CRL4-Aktivität durch gleichzeitige Depletion der beiden Gerüstproteinen CUL4A und CUL4B verminderte die Bildung von Cisplatin-induzierter Einzelstrang-DNA (ssDNA) und folglich auch die Bildung des ssDNA-RPA-Komplexes. Dementsprechend ist die ATR-abhängige Checkpoint-Aktivierung in den CRL4-defizienten Zellen vermindert, was durch die reduzierte Phosphorylierung von RPA2, CHK1 und H2AX bestätigt wird. Zusätzlich wird in den CRL4-defizienten Zellen der Replikations-Lizenzierungsfaktor CDT1 stabilisiert, was zur Stimulierung der DNA Re-Replikation in den Zellen nach Cisplatin-Behandlung führt. Diese Ergebnisse deuten darauf hin, dass die Über-Replizierung der DNA die Aktivierung der Checkpoints vermindert, indem sie die ssDNA als auslösendes Signal

maskiert. Zusammenfassend zeigen diese Resultate deutlich, dass CRL4 eine wichtige Rolle im Signalweg von Cisplatin-DNA-Schäden spielt und als mögliches therapeutisches Ziel dienen könnte, um die Effizienz von Cisplatin oder anderen Chemotherapeutika zu erhöhen.

Abbreviations

6-4PP	6-4 photoproduct
ALC1	Amplified in liver cancer 1
ATM	Ataxia telangiectasia mutated
ATR	Ataxia telangiectasia and rad3-related protein
BCL-2	B-cell lymphoma 2
BRG1	Brahma-related gene 1
CAND1	Cullin-associated and neddylation-dissociated 1
CDDP	Cisplatin
CDT1/2	Cell division cycle protein 1/2
CHD1	Chromodomain helicase DNA-binding 1
CHK1/2	Checkpoint kinase 1/2
CPD	Cyclobutane pyrimidine dimer
CRL	Cullin-RING ubiquitin E3 ligase
CSB	Cockayne syndrome group B
CSN	COP9 signalosome complex
CTR1	Copper transporter 1
CUL	Cullin
DCAF	DDB1 and CUL4-associated factors
DDB1	Damaged DNA-binding 1
DDB2	DNA damage-binding protein 2
DDR	DNA damage response
DSB	Double strand breaks
DUB	Deubiquitinating enzymes
EdU	5-ethynyl-2′-deoxyuridine
EMT	Epithelial-mesenchymal transitions
FA	Fanconi anemia
GG-NER	Global-genome nucleotide excision repair
GSH	Gutathione
GSK-3	Glycogen synthase kinase 3
HIPK2	Homeodomain-interacting protein kinase 2
HUWE	HECT, UBA and WWE domain containing 1, E3 ubiquitin protein ligase
ICL	Interstrand crosslink
INO80	Inositol requiring 80
JNK	c-Jun N-terminal kinase
KEAP1	Kelch like ECH associated protein 1
MAPK	Mitogen-activated protein kinase
Mcl-1	Myeloid cell leukemia 1
MMC	Mitomycin C
MMR	Mismatch repair
Mnase	Micrococcal nuclease
MnSOD	Manganese-dependent superoxide dismutase
mTOR	Mammalian target of rapamycin

NEDD8	Neural precursor cell expressed, developmentally downregulated 8
NEM	N-ethylmaleimide
NER	Nucleotide excision repair
NFκB	Nuclear factor kappa B
NRF2	Nuclear respiratory factor 1
NSCLC	Non-small cell lung cancer
PARC	p53-associated, parkin-like cytoplasmic protein
PCNA	Proliferating cell nuclear antigen
RBX1	RING box 1
RING	Really interesting new gene
ROS	Reactive oxygen species
RPA	Replication protein A
SCF	SKP1-Cullin1-F-Box protein
siRNA	Small-interfering RNA
SKP	S-phase kinase-associated protein
SOX9	Sex determining region Y-box 9
ssDNA	Single-stranded DNA
SWI/SNF	Switch/sucrose non-fermenting
TC-NER	Transcription-coupled NER
TFIIH	Transcription factor IIH
TGF beta	Transforming growth factor beta 1
TLS	Translesion synthesis
UPS	Ubiquitin-proteasome system
UV	Ultraviolet
WSB1	WD repeat and SOCS box containing 1
XPC	Xeroderma pigmentosum group C

1 Introduction

1.1 The DNA damage response maintains genome integrity

Genomic integrity is constantly challenged by chemical and physical agents that cause various types of DNA damage. The genotoxic sources can be endogenous, like for example reactive oxygen species arising from metabolism, or exogenous including ultraviolet (UV) light, ionizing radiation and a variety of chemicals that attack the DNA. Lesions in the DNA double helix cause cell death and mutations that favor the development of aging and cancer. A specific cellular network, collectively termed as DNA damage response (DDR), has evolved to coordinate the sensing of DNA damage, their repair and activation of appropriate cellular responses (Bartkova et al., 2005; Li et al., 2000; Matsuoka et al., 2007; Myung et al., 2001 and reviewed by Ciccia and Elledge, 2010). Depending on the kind and severity of the damage, the DDR mediates transient cell cycle arrest and repair or, if damage cannot be repaired, cell death or senescence will be induced to prevent the generation and propagation of potentially deleterious mutations.

On the other hand, DNA damaging agents also provide therapeutic opportunities (Bando et al., 2003; Day et al.; Moding et al., 2015; Shukuya et al., 2015; Patricia M. Takahara et al.; Wu et al., 2011 and reviewed by Cheung-Ong et al., 2013). In fact, they have been the mainstay of cancer therapy since decades and include DNA crosslinking agents (e.g. cisplatin), antimetabolites (e.g. 5-fluorouracil) and topoisomerase inhibitors (e.g. doxorubicin). The mechanism of action of those drugs is to block DNA replication, thereby inducing cell death or senescence particularly in cancer cells as they have in general a higher replication rate compared to the normal tissue leading to a more pronounced replication stress. However, the DNA repair responses that protect cells from mutagenic lesions also counteract the mechanism of genotoxic chemotherapeutics, thereby lowering their efficacy (Donawho et al., 2007; Duan et al., 2014; Li et al., 2016a; Miknyoczki et al., 2003; Sokol et al., 2013; Toledo et al., 2011).

In order to deal with the vast diversity of DNA lesions, a variety of specialized DNA repair systems have evolved. UV light induces DNA helix-distorting intrastrand base crosslinks including cyclobutane pyrimidine dimers (CPD) and 6-4 photoproducts (6-4PP) that are removed by the nucleotide excision repair (NER) pathway (Naegeli and Sugasawa, 2011; Puumalainen et al., 2016; Rüthemann et al., 2016). Non-helix distorting damage like single

strand breaks (SSBs), oxidation products and alkylated bases are repaired by the base excision repair (BER) pathway, whereas the mismatch repair pathway removes mis-incorporated bases arising from DNA replication (Li et al., 2016b; Liu et al., 2016; Markkanen et al., 2016; Parsons and Dianov, 2013; Tubbs et al., 2009). Other DNA damage represent double strand breaks (DSBs) that are primarily caused by ionizing radiation or radiomimetic drugs such as bleomycin (Mladenov et al., 2016). During G2 and S phase of the cell cycle, DSBs are repaired by homologous recombination (HR) that uses the corresponding sister chromatid as repair template and is therefore mostly error-free. Repair by non-homologous end-joining (NHEJ) is not dependent on homologous chromatin, thus it is not restricted to a certain phase of the cell cycle. NHEJ is a very efficient and flexible system by directly processing and rejoining broken DNA ends but it is considered to be error-prone (Biehs et al., 2017; Cortez et al., 1999; Ghezraoui et al., 2014; Yun and Hiom, 2009). One of the most complex DNA lesions consist of DNA interstrand crosslinks (ICLs) that are formed by natural metabolic intermediates like aldehydes and by chemotherepeutics such as cisplatin or mitomycin C. Resolving of ICLs is a multistep mechanism as crosslinks have to be excised from both DNA strands and requires the cooperative action of multiple repair systems. ICL removal is usually initiated by the Fanconi anemia (FA) complex followed by the coordinated engagement of HR, NER and dedicated DNA polymerases for translesion synthesis (TLS) (Joo et al., 2011; Knipscheer et al., 2009; Moldovan and D'Andrea, 2009; van Twest et al., 2017 and reviewed by Ceccaldi et al. 2016 and Clauson et al. 2013).

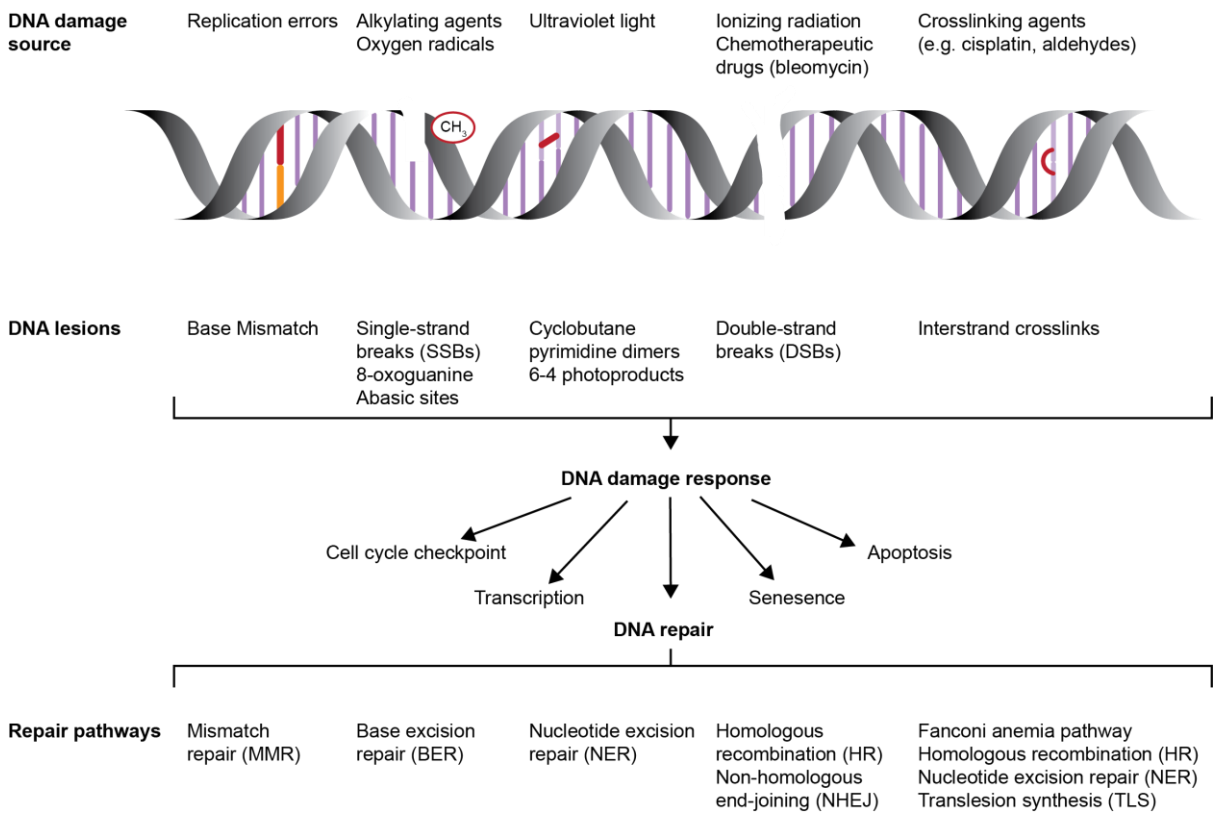

Figure 1. DNA damage response coordinates repair of DNA damage.

Endogenous and exogenous sources cause distinct DNA damage including base mismatches, single and double strand breaks, cyclobutane pyrimidine dimers, 6-4 photoproducts, modified bases and crosslinks. Upon recognition of the damage, the DNA damage response (DDR) is activated to regulate cellular processes like cell cycle control, transcription, DNA repair, senescence and apoptosis. Specialized DNA repair mechanisms are responsible for the removal of the lesions.

1.2 Function of cullin-RING ubiquitin ligases in the cellular response to cisplatin

– Can cullins modulate cisplatin sensitivity?

Tamara Codilupi and Hanspeter Naegeli

Institute of Pharmacology and Toxicology, University of Zurich-Vetsuisse,
Winterthurerstrasse 260, 8057 Zurich

Corresponding author: Hanspeter Naegeli (naegelih@vetpharm.uzh.ch)

Manuscript in preparation.

Section 1.2 constitutes a review article. I prepared the figures and wrote the manuscript together with H. Naegeli.

Abstract

Despite impressive advances in the development of protein kinase inhibitors and monoclonal antibodies, conventional chemotherapeutics are still the most widely exploited drugs against human cancer. A paradigmatic case consists of platinum-based small molecules active against many advanced solid malignancies. Although these tumors respond initially to platinum, its clinical use is limited by the fast development of resistances. In addition, platinum-based therapy is accompanied by severe side effects. Clearly, novel strategies are needed to improve the response of cancer cells to chemotherapeutics, thereby overcoming resistance and reducing deleterious side effects. The ubiquitin-proteasome system contributes to cellular responses to DNA damaging agents and, hence, may represent an amenable target for optimization of chemotherapy. Indeed, many reactions to chemotherapeutics, including DNA repair, DNA damage tolerance, cell cycle checkpoint regulation and apoptotic cell death, are tightly regulated by ubiquitination and subsequent proteolytic degradation. It is, in particular, important to develop tools to control the activity of cullin-dependent RING ubiquitin ligases (CRLs). A proof of concept is provided by the neddylation inhibitor Pevonedistat, currently under investigation in clinical trials, which like a scattergun collectively antagonizes numerous CRLs. However, each CRL has multiple substrates involved in distinct biological pathways and, depending on the tumor biology, its inhibition can have different effects and even support the development of resistance. The selection of the most effective drug combination for each patient is, therefore, challenging and biomarkers currently used for diagnosis do not reflect the whole tumor complexity. Novel functional diagnostic tests are now being investigated with promising results and might provide a suitable strategy to select the right CRL inhibitor to be combined with platinum-based drugs or other chemotherapeutic agents for the right patient.

1.2.1 Cisplatin: meachanism of action and molecular basis of resistances

The covalent reaction of platinum-based small molecules with DNA is exploited as a therapeutic principle against cancer. *Cis*-diamminedichloridoplatinum(II) (cisplatin) is one of the most widely used chemotherapeutic agents active against many solid malignancies including advanced testicular, cervical, ovarian and lung cancer (Dasari and Tchounwou, 2014). Since the discovery of cisplatin as a cytotoxic agent in the 1970s, numerous derivatives have been developed to reduce side effects and tumor resistances, the most prominent being carboplatin and oxaliplatin (Dilruba and Kalayda, 2016). Despite the slightly improved safety profile of newer platinum derivatives, cisplatin remained indispensable due to its high potency and is used as first line treatment primarily for advanced metastatic malignancies, often in combination with other chemotherapeutics or with radiation therapy (Apps et al., 2015; Wheate et al., 2010). Some neoplasms like non-small-cell lung cancer and late stage ovarian cancer are typically resected surgically followed by adjuvant treatment with platinum-based chemotherapy. Others like urothelial bladder carcinoma are treated for neoadjuvant purposes to achieve down staging of the tumor mass before surgery (Dash et al., 2008; Pignon et al., 2008; Silver et al., 2010).

The uptake of cisplatin into target cells occurs primarily through the copper transporter 1 (CTR1) (Howell et al., 2010). Once in the cytoplasm, cisplatin becomes activated by an aquation reaction, whereby the two chlorides are replaced by water molecules. This hydrolyzed intermediate is a potent electrophile that reacts with both proteins and nucleic acids. Cisplatin forms covalent bonds with purine bases, mostly with guanines, and thereby causes intra- and interstrand crosslinks. Formation of such DNA adducts interferes with vital cellular processes including DNA replication and transcription, which in turn activates the cellular DNA damage response and ultimately triggers apoptotic cell death (Basu and Krishnamurthy, 2010). Susceptibility to apoptosis is enhanced by the mismatch repair (MMR) pathway, which recognizes and signals cisplatin-DNA damage (Sawant et al., 2015). However, intra- and interstrand crosslinks can be repaired by nucleotide excision repair (NER) and the Fanconi anemia (FA) pathway, respectively. Moreover, certain DNA polymerases (e.g. Polη) are able to bypass cisplatin-DNA adducts during replication by translesion synthesis (TLS), thereby preventing replication fork stalling and subsequent damage signaling (Albertella et al., 2005; Mouw and D'Andrea, 2014; Schaerer, 2013; Wang and Lippard, 2005). Conversely, an elevated oxidative stress contributes to the cytotoxicity of cisplatin. Mitochondrial dysfunction as a consequence of

cisplatin-adducts on the mitochondrial DNA increases the generation of reactive oxygen species (ROS). Moreover, binding of cisplatin to the nucleophilic glutathione (GSH) and metalloproteins like for example manganese-dependent superoxide dismutase (MnSOD), which are important cellular antioxidants, further aggravates the cellular damage (Brown et al., 2009; Chen and Kuo, 2010; Marullo et al., 2013).

Although many tumors respond initially to cisplatin treatment, its clinical use is limited by the fast development of chemotherapy resistance. The mechanisms contributing to cisplatin resistance have been intensely studied and are typically caused by a combination of distinct processes, which include 1) alterations in the drug transporter CTR1 leading to reduced cellular uptake, 2) enhanced drug detoxification due to elevated levels of glutathione and metallothioneins, 3) reduced oxidative stress by up regulation of antioxidant proteins (for example MnSOD), 4) removal of DNA adducts by enhanced activity of the NER and FA pathways, 5) changes in DNA damage tolerance reactions, including TLS during DNA replication or loss of MMR and finally 6) abrogation of apoptotic cell death (Clauson et al., 2013; Galluzzi et al., 2012; Kelland, 2007). In addition to these problems related to the high incidence of resistance, cisplatin therapy is accompanied by severe side effects including dose-limiting nephrotoxicity, which often causes treatment failure (Miller et al., 2010).

Clearly, novel therapeutic strategies are needed to improve the response of cancer cells to cisplatin, thereby overcoming resistance and reducing deleterious side effects. The ubiquitin-proteasome system plays a pivotal role in the cellular response to DNA damaging agents and, hence, may represent an amenable target for optimization of cisplatin treatment. Indeed, many cellular responses to cisplatin including DNA repair, DNA damage tolerance, cell cycle checkpoint regulation and apoptotic cell death are tightly regulated by ubiquitination and subsequent proteolytic degradation processes. In this review, we discuss the role of cullin-dependent RING ubiquitin ligases (CRLs) in the cellular response to cisplatin.

1.2.2 The ubiquitin-proteasome system

The ubiquitin-proteasome system (UPS) is the major pathway regulating protein homeostasis in eukaryotic cells. It has a key function in many biological processes by controlling the turnover of rate-limiting proteins (Ciechanover, 1998). The attachment of

ubiquitin, a polypeptide of 8.5 kDa, to target proteins occurs via a sequence of enzymatic events. In the first step, ubiquitin is activated by the ubiquitin-activating enzyme (E1) by an ATP-dependent reaction. In a second step, ubiquitin is transferred from the E1 enzyme to an ubiquitin-conjugating enzyme (E2). The E2 enzymes then form a complex with one of multiple E3 ubiquitin ligases and, in a subsequent reaction, ubiquitin is transferred to a lysine residue on the substrate protein (Komander and Rape, 2012). The specificity in this cascade is primarily conferred by the numerous E3 ligases. Mammalian cells possess several hundred distinct E3 ligases, which are classified into three classes according to the nature of their specific core domain: HECT (homologous to E6-AP carboxy terminus), RING (really interesting new gene) finger, and U-box E3s (Sarikas et al., 2011). Ubiquitinated proteins are degraded by the 26S proteasome and ubiquitin is released by deubiquitinating enzymes (DUBs), making ubiquitin conjugation to target substrates a reversible process (Wilkinson, 1997).

Deregulation of the UPS is frequently encountered in cancer cells, thereby not only contributing to disease progression but also influencing drug resistance (Huang and Dixit, 2016). A first proof for UPS being a target for cancer therapy is provided by the proteasome inhibitor bortezomib that is successfully used in the treatment of hematological malignancies (Dou and Zonder, 2014). However, analogous beneficial effects of proteasome inhibition in solid malignancies is still missing. The use of bortezomib in combination with conventional chemotherapeutics including cisplatin has been investigated in several clinical studies that, in the majority of cases, failed to identify an advantage over the standard therapy. Nevertheless, promising responses have been observed in non-small cell lung cancer by a combination of bortezomib with platinum agents, implying that the treatment response highly depends on the tumor type (Chao and Wang, 2016; Davies et al., 2009; Piperdi et al., 2012). In this respect, it should be considered that proteasome inhibition reflects a rather unspecific approach that affects the stability of many if not most cellular proteins. Further research has therefore focused on potential therapeutic targets upstream of the proteasome, namely the E3 ligases whose inhibition may provide higher specificity and efficacy.

1.2.3 CRL complexes

1.2.3.1 General structure

CRLs are multiprotein complexes representing the largest family of E3 ubiquitin ligases and are responsible for ubiquitination of ~20% of cellular proteins degraded through UPS (Soucy et al., 2009; Zhao and Sun, 2013). CRLs have a modular architecture, where the cullin protein serves as a structural scaffold. Each CRL contains one of the eight cullins (CUL1-3, 4A/B, 5, 7 and 9) present in mammalian cells to recruit the RING finger domain-containing protein RBX1/2 (also known as ROC1/2) and an adaptor protein on its carboxy- and amino terminal site, respectively (Figure 1). While RBX1/2 recruits the ubiquitin-containing E2 enzyme, the adaptor protein associates with interchangeable substrate receptors. Binding of the CRL complex to a substrate promotes the transfer of the ubiquitin from the E2 to the substrate, primarily resulting in proteasomal degradation of the ubiquitinated substrate. The numerous substrate receptors determine the specificity of CRLs that often function through selective recognition of preceding post-translational modifications like phosphorylation and hydroxylation. Considering all possible combinations, cullins form several hundreds distinct ubiquitin E3 ligases with diverse composition (Sarikas et al., 2011). Substrate receptors can potentially bind multiple different targets, thus expanding widely the functional range of CRLs (Chen et al., 2015; Petroski and Deshaies, 2005).

1.2.3.2 CRL1

The CRL1 ubiquitin ligase complex (also known as SCF for SKP1-Cullin1-F-Box protein) contains CUL1 as scaffold protein that interacts via its adaptor SKP1 with a number of F-box proteins, which constitute the specific substrate receptors (Cardozo and Pagano, 2004; Skaar et al., 2014). The 69 known F-box proteins target a variety of substrates in multiple pathways that are critical for biological functions including cellular proliferation, apoptosis and signaling. Accordingly, many F-box proteins exhibit oncogenic or tumor-suppressive activities (Heo et al., 2016; Randle and Laman, 2016; Skaar et al., 2013; Wang et al., 2014b). CRL1 complexes have also important functions in the regulation of chemosensitivity, especially by controlling the apoptotic response in cancer cells.

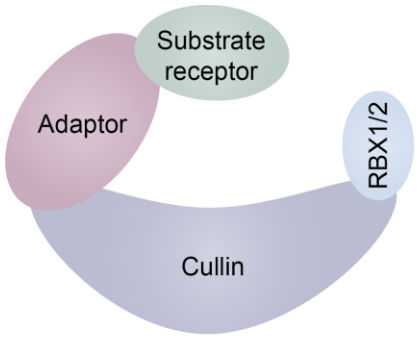

Cullin RING E3 ligase	Cullin	Adaptor	Substrate receptor	Example substrate receptor
CRL1 / SCF	CUL1	SKP1	F-box proteins	SKP2, beta-TrCP1, FBXW7
CRL2	CUL2	Elongin B Elongin C	VHL-box proteins	VHL
CRL3	CUL3	BTB-domain proteins		KEAP1
CRL4A	CUL4A	DDB1	DCAF	DDB2, CDT2
CRL4B	CUL4B	DDB1	DCAF	CDT2, HUWE1
CRL5	CUL5	Elongin B Elongin C	SOCS-box proteins	WSB1
CRL7	CUL7	SKP1	FBXW8	FBXW8
PARC	CUL9	Unknown	Unknown	Unknown

Figure 1. Cullin-RING E3 ubiquitin ligases.

Each CRL is composed of a cullin protein that serves as scaffold to recruit the RING-finger protein RBX1/2 to its C-terminal domain and an adaptor to its N-terminal domain. The adaptor protein can associate with different substrate receptors to build distinct CRLs.

Most of the F-box proteins have a context-specific function, acting either as tumor suppressor or oncogene depending on the tumor tissue. In contrast, SKP2 (S-phase kinase-associated protein 2, also known as FBXW11) and FBXW7 have well-defined biological function being a verified oncogene and tumor suppressor, respectively (Heo et al., 2016). SKP2 exhibit its tumorigenic function mostly by destruction of cell cycle inhibitors with p27 as its primary target. Its frequent overexpression in many human malignancies correlates clinically with poor prognosis and treatment outcome (Kitagawa et al., 2008; Kossatz et al., 2004; Zhang et al., 2016b). Conversely, FBXW7 targets various oncogenes, including c-Myc and cyclin E, for degradation thereby exhibiting a tumour-suppressive function (Kitagawa et al., 2009; Willmarth et al., 2004). The screening of > 500 primary tumours revealed an overall mutation frequency in *FBXW7* of 6%, with the highest frequency in tumours of the bile duct (35%) and blood (31%) (Akhoondi et al., 2007). In gastric cancer, FBXW7 expression is frequently suppressed by two micro-RNAs, miR-223

and miR363, that promote tumour proliferation and chemoresistance (Zhang et al., 2016a; Zhou et al., 2015).

1.2.3.3 CRL3

CUL3 ubiquitin ligases recruit BTB-domain proteins, which unusually function as both adapters and substrate receptors. In mammalian cells, 180 different BTB-proteins are present, although not all of those seem to be associated with the CRL3 complex. They interact through their BTB-domain with CUL3, whereas the substrates are recruited through a second protein interaction surface like the MATH, Znf or Kelch domains (Stogios et al., 2005; Xu et al., 2003). By targeting a broad range of regulatory proteins, CRL3s control different stress responses and are linked to several human pathologies including metabolic diseases, dystrophies and cancer (reviewed in Genschik et al., 2013). Especially $CUL3^{KEAP1}$ plays an important role in tumorigenesis and development of chemoresistance by regulating the antioxidant stress response via the NRF2 pathway (see below). As for the majority of CRLs, the function of CUL3 seems to depend on the tumor origin. Whereas depletion of CUL3 by siRNA treatment sensitizes ovarian cancer cells toward cisplatin, overexpression of CUL3 in human fibrosarcoma had no influence on cisplatin sensitivity (Jazaeri et al., 2013; Zhang et al., 2004).

1.2.3.4 CRL4

The CUL4 subfamily include CUL4A and CUL4B, which both serve as scaffold protein in CRL4 complexes. Despite an elongated amino terminus present in CUL4B, the two paralogs share more than 80% sequence identity and have mainly redundant functions (Fischer et al., 2011a). DDB1 (for damaged DNA-binding 1) is the adaptor protein that recruits WD40 repeat-containing proteins, also referred to as DCAFs (DDB1 and CUL4-associated factors), as substrate receptors to the CUL4 scaffold. A systematic search identified 90 distinct DCAFs associated with the CRL4 complex, but the function of the majority of these substrate receptors remains to be elucidated (Lee and Zhou, 2007). Targets of CRL4 include primarily proteins involved in cell cycle regulation and DNA damage responses that exert important functions in maintaining genome integrity (Abbas and Dutta, 2011). Altered expression levels of subunits of the CRL4 complex have been found in a variety of human malignancies and high CUL4A expression is associated with

their aggressiveness (Hannah and Zhou, 2015; Xu et al., 2014). Based on the analysis of a wide panel of cell lines, Olivero et al. (2014) proposed that cancer cells may generally be addicted to CRL4 complexes displaying CDT2 (cell division cycle protein 2) as the substrate receptor. Depletion of CDT2 in the examined panel of cancer cells conferred cytotoxicity without causing effects on normal cells, thus offering a possible target for cancer therapy (Olivero et al., 2014). Such tumorigenic properties of CUL4 were demonstrated in a conditional CUL4 transgenic mouse model of lung cancer (Yang et al., 2014): 32% of the mice with overexpressed CUL4A developed lung cancer at week 40 and further analysis revealed deregulated expression of several cell cycle-regulating factors including the cyclin-dependent kinase inhibitor p21 and replication licensing factor CDT1. In accordance with these findings, another study reported higher expression levels of CUL4 in clinical samples of non-small cell lung cancer (NSCLC) tissue compared to the corresponding healthy tissue, that is associated with decreased overall survival (Hung et al., 2016; Wang et al., 2014a). Depletion of CUL4A in a panel of NSCLC lines increased the cytotoxic effect of cisplatin, suggesting that CUL4 overexpression is associated with cisplatin resistant in lung cancer (Hung et al., 2016; Yang et al., 2014). Interestingly, also deregulated expression of the adaptor protein DDB1 has been associated with altered drug responsiveness. In a study that aimed to evaluate the utility of molecular data from the Cancer Genome Atlas (TCGA) to predict clinical drug responses, high DDB1 expression was found to be a strong indicator of poor response to cisplatin in 336 bladder urothelial carcinoma samples that further correlated with lower overall survival of these patients (Ding et al., 2016).

DNA damage-binding protein 2 (DDB2, encoded by the *XPE* gene) is the most intensively studied substrate receptor of CRL4. DDB2 binds with high affinity to UV-induced cyclobutane pyrimidine dimers (CPDs) and 6-4 photoproducts (6-4PPs), but also with minor affinity to damage caused by cisplatin and oxidative lesions (Jones et al., 2010). As a DNA damage recognition factor, DDB2 has a key role in the initiation of the global-genome nucleotide excision repair (GG-NER) pathway and mutations in the *XPE* gene cause sensitivity to UV light and confer a high risk of developing skin cancer (Moriwaki, 2016).

1.2.3.5 Further cullins

CRL2 and CRL5 are structurally related ubiquitin ligases that share the same adaptor, i.e., the elongin B/C complex. It is their association with distinct substrate receptors that divides them into two subclasses: CUL2 recruits VHL-box proteins with the tumor suppressor von Hippel Lindau as the most prominent member, whereas CUL5 uses SOCS-box proteins for substrate recognition (Kamura et al., 2004; Wang et al., 2016). However, generally the substrates of this large repertoire of CRL2 and CRL5 complexes remain poorly characterized (Okumura et al., 2012).

The least characterized cullins are CUL7 and CUL9, which share a high degree of sequence homology. CUL7 forms an E3 ligase by recruiting the adapter protein SKP1 and the F-box protein FBXW8 as substrate receptor but, to date, only few target proteins have been identified. Cullin 9 is so far considered as an atypical cullin protein and the components of a putative CRL9 complex, also known as PARC (p53-associated, Parkin-like cytoplasmic protein), remained elusive.

1.2.4 Role of cullins in the cisplatin response

The CRL complexes regulate many proteins with roles in cell cycle progression, DNA damage response, apoptosis, oxidative stress defense and signal transduction (Lee and Zhou, 2010; Zhao and Sun, 2013). These mechanisms play a pivotal role not only in cancer development but also in the cellular responses to anti-cancer chemotherapeutics. Jazaeri et al., (2013) investigated the contribution of cullins on the chemosensitivity to cisplatin of two ovarian carcinoma cell lines, SKOV3 and ES2, using a small-interfering RNA (siRNA) approach. Down regulation of each of the cullins changed the sensitivity towards cisplatin, either by promoting chemosensitivity or by conferring chemoresistance. In their study, depletion of CUL3 resulted in the strongest synergistic effect together with cisplatin by inducing cytotoxicity in both cell lines, whereas knockdown of CUL1 displayed an antagonistic effect on cisplatin-induced cell death. Down regulation of the other cullins had opposing effects in the two cell lines, suggesting a strong influence of the genetic background. A conditional CUL4A transgenic mouse model of lung cancer indicated that CUL4A overexpression exerts tumorigenic properties. In addition, depletion of CUL4A by siRNA in a panel of non-small-cell lung carcinoma cell lines increased the cytotoxic effect

of cisplatin, suggesting that CUL4 overexpression is associated with cisplatin resistance (Yang et al., 2014).

1.2.4.1 Regulation of CRL activity by neddylation

CRLs are tightly regulated in dynamic cycles of neddylation required for their activation, deneddylation by the COP9 signalosome complex (CSN) and substrate receptor exchange by CAND1 (cullin-associated and neddylation-dissociated 1) (Chung and Dellaire, 2015) (Figure 2). Neddylation refers to the attachment of the ubiquitin-like protein NEDD8 (for neural precursor cell expressed, developmentally downregulated 8) to a lysine residue at the carboxy terminus of cullins. In analogy to the ubiquitination pathway, neddylation requires an E1 NEDD8-activating enzyme, an E2 NEDD8-conjugating enzyme and an E3 NEDD8 ligase to covalently link NEDD8 to its substrate, which are primarily cullins (Enchev et al., 2014). Cullin neddylation results in the activation of their ligase activity by promoting conformational changes such that the carboxy-terminal domain moves closer to the substrate, thereby facilitating the ubiquitin transfer from the E2 enzyme to the substrate (Duda et al., 2008). The resulting decline of substrate concentration promotes binding of the CSN to the CRLs, which sterically blocks the interaction between substrate and CRL. This transient inhibition of the CRL activity can be reversed by increasing the substrate level, thus competing with the CSN for the cullins. In addition, the deneddylation activity of the CSN results in inactivation of the CRLs (Cavadini et al., 2016). Deneddylated CRLs are subsequently sequestered by CAND1. Based on *in vitro* studies, CAND1 was thought to be a CRL inhibitor by preventing the association of the cullin scaffold with the substrate receptors. However, further studies revealed that CAND1 is an exchange factor for substrate receptors. Depending on the available substrates, CRL complexes are reassembled through CAND1 by exchanging the substrate receptor, thereby providing a dynamic system for targeting a great number of diverse substrates (Pierce et al., 2013; Wu et al., 2013).

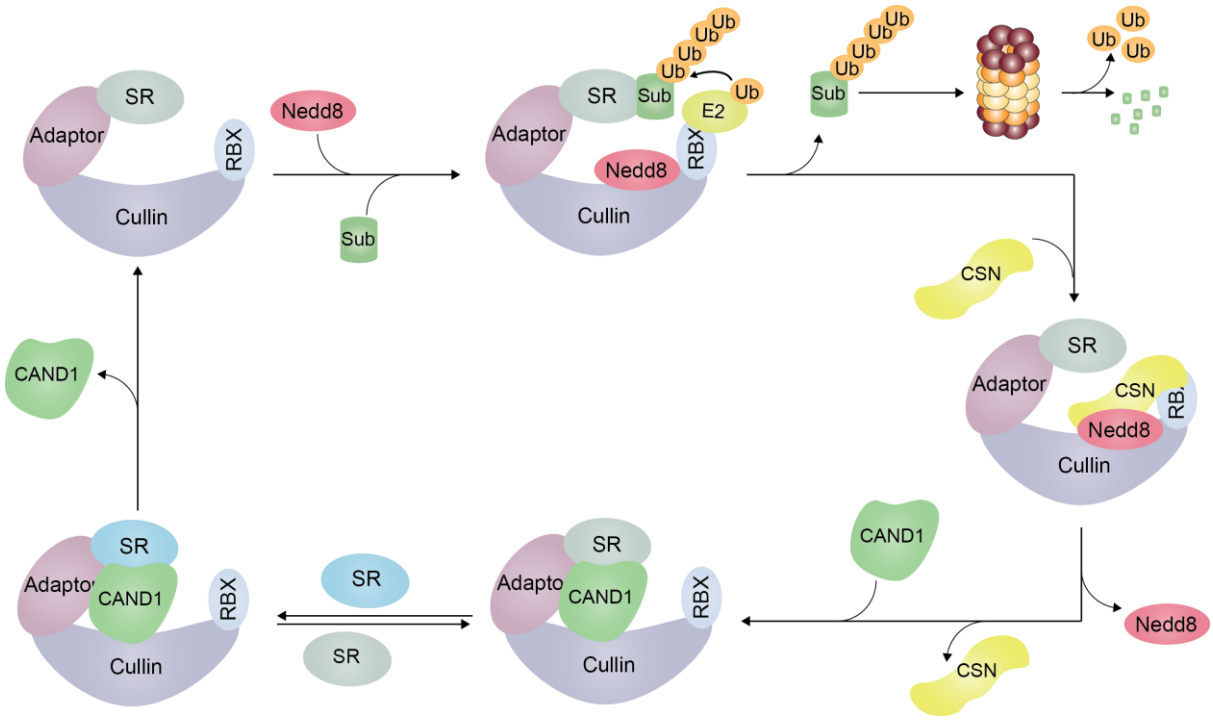

Figure 2. Dynamic regulation of CRLs.

CRLs are activated by neddylation and bind to their protein substrate via the substrate receptor. The cullin scaffold becomes neddylated and the E2-Ub is recruited to the CRL through RBX1/2 allowing transfer of the ubiquitin to the substrate. The protein substrate is subsequently degraded through the proteasome. A decrease in substrate concentration promotes the association with CSN and deneddylation of the CRLs results in their inactivation. The CRLs can re-enter the cycle or exchange its receptor via CAND1 that alters the substrate specificity.

1.2.4.2 Neddylation inhibitor MLN4924

A new class of antineoplastic agents has been developed that targets the NEDD8 conjugating pathway. MLN4924 (Pevonedistat), the first of this class of compounds, selectively inhibits the first step of the neddylation pathway by inactivating the NEDD8-activating enzyme. It thereby inhibits the ubiquitination activity of the downstream CRLs, resulting in the accumulation of unmodified CRL-substrates (Liao et al., 2011; Pan et al., 2013; Soucy et al., 2009). Given the pivotal role of certain cullin substrates in tumorigenesis, the NEDD8 degradation pathway is considered a promising target for cancer treatment.

MLN4924 is currently under investigation in multiple clinical trials. Interestingly, preclinical studies found that the combination of MLN4924 with cisplatin results in synergistic cytotoxicity, both in primary tumor cells and xenograft models. In

chemoresistant ovarian cancer cell lines, MLN4924 significantly increased the cytotoxic activity of cisplatin. The combination of these two drugs dramatically elevated oxidative stress, which caused higher levels of DNA damage including strand breaks and oxidative lesions that ultimately trigger apoptosis (Nawrocki et al., 2013). Proteomic analyses support the notion that inhibition of the NEDD8 pathway alters the cellular redox status (resulting in increased levels of oxidative stress proteins) and induces DNA damage (leading to elevated levels of p53 and other DNA damage response proteins). Furthermore, administration of MLN4924 to mice bearing ovarian tumor xenografts supported the efficacy of cisplatin against both cisplatin-sensitive and cisplatin-resistant cancer cells (Nawrocki et al., 2013). A synergistic effect of MLN4924 and cisplatin was also observed in cell lines derived from several types of ovarian tumors (Jazaeri et al., 2013). Depletion of CUL3 by siRNA reproduced the effect of MLN4924. CUL3 has an important role in oxidative stress response (see below), further supporting the impact of redox-related mechanisms in the cisplatin response (Jazaeri et al., 2013). Neddylation inhibition potentiated cisplatin induced apoptosis also in cervical (HeLa, ME-180) and bladder urothelial (NTUB1, T24) cancer cells (Ho et al., 2015; Lin et al., 2015). In bladder carcinoma cell lines, the combined treatment with MLN4924 and cisplatin strongly activated the c-Jun N-terminal kinase (JNK), resulting in decreased levels of the anti-apoptotic protein Bcl-xL and consequently, stronger induction of apoptosis. Cisplatin-induced activation of the checkpoint kinases ATR and ATM is suppressed by MLN4924, whereas the levels of phosphorylated histone H2AX (γ-H2AX, a marker of DNA damage) is increased. This suggests that persistent DNA damage due to disrupted cell cycle checkpoints are responsible for the JNK activation (Ho et al., 2015). An inhibition of the ATR pathway by MLN4924 is further indicated by a study of Kee et al. (2012). These authors showed that neddylation is required for sustained activation of the CHK1 signal transducer and ubiquitination of FANCD2, a key factor in the FA repair pathway acting downstream of CHK1.

1.2.4.3 CRLs with pro-apoptotic function

The effectiveness of cisplatin treatment depends highly on the ability of the cells to undergo apoptosis. This tightly regulated process involves numerous factors, of which some represent substrates of CRLs (Figure 3 and Table 1). Indeed, several CRLs are

essential for cisplatin induced cell death and in some malignancies, reduced expression levels are associated with chemoresistance. Mcl-1 (myeloid cell leukemia 1), a BCL-2 (B-cell lymphoma 2).-like protein with anti-apoptotic function, is a target protein of $CUL1^{beta\text{-}TrCP1}$ and $CUL1^{FBXW7}$. High levels of Mcl-1 negatively impact cancer cell responses to cisplatin in a variety of human cell lines, including those from gastric cancer and non-small-cell lung carcinoma (Akagi et al., 2013; Michels et al., 2014). In response to chemotherapeutic agents like cisplatin, Mcl-1 is phosphorylated by the glycogen synthase kinase 3 (GSK-3), thus generating a recognition motif for $CUL1^{beta\text{-}TrCP1}$ and $CUL1^{FBXW7}$. The ensuing ubiquitination of phospho-Mcl-1 results in its rapid degradation and induction of apoptosis (Ding et al., 2007; Koo et al., 2015). This pathway is counteracted by the mammalian target of rapamycin 2 (mTOR2), which associates with $CUL1^{FBXW7}$ and suppresses its activity resulting in delayed Mcl-1 degradation. This suppression could be relieved by mTOR inhibitors and, consequently, a combination of mTOR inhibitors with cisplatin resulted in enhanced cytotoxic effects (Koo et al., 2015).

In addition to apoptosis, FBXW7 promotes cell cycle arrest in gastric cancer by increasing the levels of the CDK inhibitors p14, p16 and p21, and decreasing the level of cyclin D. Expression levels of FBXW7 is markedly reduced in gastric cancer tissue compared to the adjacent healthy tissue and low levels of FBXW7 promote cell proliferation and cisplatin resistance (Zhou et al., 2015). The tumor suppressive function of FBXW7 is further confirmed by clinical data. High expression of miR-363, a microRNA targeting FBXW7 correlates with reduced survival in patients with gastric cancer and, in addition, those patients have a poor response to cisplatin treatment (Zhang et al., 2016a) .

$CUL4^{DDB2}$ increases cisplatin sensitivity by down regulation of the anti-apoptotic protein BCL-2. Accordingly, DDB2 expression is significantly lower in cisplatin-resistant ovarian cancer cell lines compared to the corresponding cisplatin-sensitive parental cells (Barakat et al., 2010). Mechanistically, DDB2 functions as a transcriptional repressor of *Bcl-2* by recruiting the histone deacetylase HDAC1 to the *Bcl-2* promoter, which results in the loss of histone H3 acetylation at positions K9 and K14 (Zhao et al., 2013). DDB2-deficient cells undergo cell cycle arrest but are resistant to apoptosis (Stoyanova et al., 2009).

Gigaxonin (also known as Kelch-like protein 16), an adapter/substrate receptor of CUL3, has been linked to cisplatin sensitivity in head and neck cancer by targeting the transcription factor NFκB (nuclear factor kappa B) for degradation. The interaction of

gigaxonin with NFκB is mediated by the tumor suppressor p16 and ubiquitination of NFκB results in apoptosis and senescence of head and neck squamous cell carcinoma cell lines. Nuclear expression of p16 in 103 analyzed primary tumor cells inversely correlates with NFκB expression. In addition, high p16 levels are associated with a more favorable clinical prognosis, an effect that may be related to increased cisplatin sensitivity (Veena et al., 2014).

The F-box protein FBXO32 (also known as Atrogin-1) was recently identified as tumor suppressor in ovarian cancer (Chou et al., 2010). Reduced expression levels of FBXO32 due to promoter hypermethylation is a common feature of advanced-stage ovarian cancers that correlates clinically with a shorter progression-free survival of these patients. Restored expression of FBXO32 reduced cell growth of a platinum-resistant ovarian cancer cell line both *in vitro* and in xenografts, and enhances the sensitivity toward cisplatin of this cell line by inducing apoptosis (Chou et al., 2010). The tumor suppressive function of FBXO32 via regulation of apoptosis was further identified in breast cancer cells (Tan et al., 2007; Zhou et al., 2017).

1.2.4.4 CRLs with anti-apoptotic function

In contrast to the abovementioned cases, several CRLs have anti-apoptotic functions that promote cisplatin resistances. SKP2, a substrate receptor of CUL1, forms a complex with the acetyltransferase CBP/p300, thereby suppressing p300-mediated acetylation of p53 and the transactivation ability of p53 protein. Thus, a high cellular level of SKP2 suppresses cell death and, consequently, down regulation of SKP2 expression in cancer cells significantly increases the efficiency of cisplatin by enhancing p53-dependent apoptosis (Kitagawa et al., 2008).

In melanoma cells, $CUL1^{FBXW11}$(also known as beta-TrCP2 / HOS) up regulates NFκB by targeting its inhibitor IκB for proteolytic degradation. NFκB is a transcription factor that induces the expression of genes that promote survival or suppress apoptosis. Therefore, inactivation of beta-TrCP2 results in the sensitization of human melanoma cells to cisplatin-triggered apoptosis (Fuchs et al., 1999; Lee et al., 2007; Soldatenkov et al., 1999; Tan et al., 1999).

A specific target of CRL4 includes HUWE1 (HECT, UBA And WWE Domain Containing 1, E3 Ubiquitin Protein Ligase), another E3 ubiquitin ligase that in turn triggers

degradation of the anti-apoptotic protein Mcl-1 upon DNA damage. It has accordingly been demonstrated that depletion of CUL4B stabilizes HUWE1 and thereby promotes the degradation of Mcl-1, leading to increased induction of apoptosis. As a consequence, cells deficient in CUL4B showed increased sensitivity toward cisplatin (Yi et al., 2015). $CUL4^{DDB2}$ may also have an apoptosis-suppressive function by activation of the mitogen-activated protein kinase (MAPK) pathway that reduces cell death signaling induced by TNF-α (Sun and Chao, 2005).

The ubiquitin ligase CRL5 displaying WSB1 (WD repeat and SOCS box containing 1) as the substrate receptor was shown to have a function in the DNA damage response by promoting the ubiquitination and degradation of HIPK2 (homeodomain-interacting protein kinase 2). HIPK2 in turn regulates the transcription of a number of key effectors including p53 and thereby stimulates apoptosis upon genotoxic stress (Möller et al., 2003a, 2003b). It has been demonstrated that HIPK2 is targeted for proteasomal degradation by CRL5 under normal conditions, but exposure of cells to cisplatin prevents this destruction. Consequently, HIPK2 remains active and stable for the induction of apoptosis (Choi et al., 2008). WSB1 supports pancreatic tumor progression and depletion of WSB1 increases the sensitivity of neuroblastoma cells toward cisplatin (Archange et al., 2008; Shichrur et al., 2014). However, WSB1 is expressed in different isoforms, which might result in distinct effects on tumor growth and chemosensitivity (Chen et al., 2006).

CUL7 and CUL9 alone, but also as a heterodimer, have been shown to sequester cytoplasmic p53, thus suppressing the apoptotic pathway (Kaustov et al., 2007; Skaar et al., 2007). It has been demonstrated that cisplatin-mediated down regulation of PARC results in increased nuclear and mitochondrial localization of p53 and subsequent apoptotic cell death. Interestingly, ovarian cancer cells could be sensitized toward cisplatin by depletion of PARC (Woo et al., 2012).

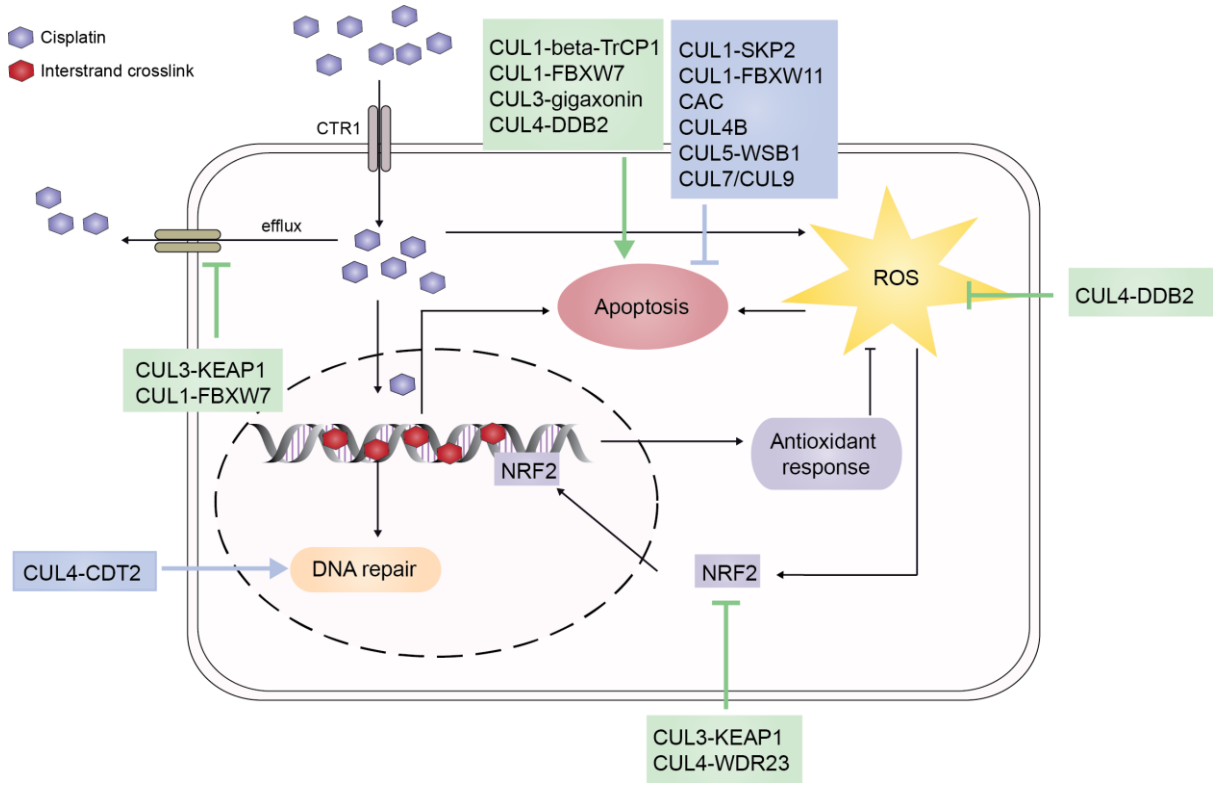

Figure 3. CRLs modulate the cellular response to cisplatin treatment.

Cisplatin is actively taken up by the copper transporter 1 (CTR1) and becomes activated in the cytoplasm. The subsequent binding to DNA, the major target of cisplatin, generates inter- and intrastrand crosslinks that interfere with DNA replication and transcription. If the DNA adducts remains unrepaired, the cell will ultimately undergo apoptotic cell death. Elevated ROS levels also contribute to the cytotoxic effect of cisplatin. Activation of the antioxidant response (e.g. by the transcription factor NRF2) counteracts the oxidative stress and prevents cell death. Numerous CRLs interfere with apoptosis, DNA repair, oxidative damage response or efflux mechanisms, thereby supporting either resistance (blue) or sensitivity (green) to the action of cisplatin.

1.2.4.5 Role of oxidative damage

An important role in chemoresistance to cisplatin has the KEAP1 (Kelch-like ECH-associated protein 1) adapter/substrate receptor, which targets NRF2 (nuclear factor E2-related factor) for degradation (Itoh et al., 1999). NRF2 is a master transcriptional activator of genes encoding cytoprotective enzymes that are induced in response to oxidative and xenobiotic stress, including membrane transporters, phase II detoxifying enzymes and antioxidant factors like NQO1 (NAD(P)H dehydrogenase (quinone 1)) and HO-1 (heme oxigenase 1). Although NRF2 counteracts oxidative stress and thereby protects from many diseases, it also provides a growth advantage for cancer cells and contributes to

chemoresistance (Furfaro et al., 2016). The loss of KEAP1-mediated degradation of NRF2 leads to its constitutive transcriptional activation. Mutations of *Keap1* and *NRF2* have been found in several malignancies including lung carcinoma as well as head and neck cancer (Ohta et al., 2008; Shibata et al., 2008). Interestingly, a strong cisplatin-resistant phenotype due to this disrupted KEAP1-NRF2 pathway and the resulting increase of antioxidant proteins have been found in many primary and cultured tumor cells. Their sensitivity to cisplatin could be restored by overexpression of KEAP1 (Jiang et al., 2010a; Tian et al., 2016; Wang et al., 2008). Other two mechanisms leading to reduced KEAP1 activity are its transcriptional repression due to down regulation of the transcriptional activator FoxO3 and degradation by autophagy-mediated processes initiated through nucleoporin p62, both conferring resistance to cisplatin by over activation of NRF2 (Bao et al., 2014; Guan et al., 2016; Xia et al., 2014). The clinical relevance of this KEAP1-NRF2 pathway is further supported by a study of human bladder cancer cases, where NRF2 expression negatively impacts the overall survival of patients who received cisplatin therapy (Hayden et al., 2014).

For many years, $CUL3^{KEAP1}$ was considered to be the sole regulator of NRF2. However, a recent study identified $CUL4^{WDR23}$ as an additional factor for NRF2 degradation independently of the canonical $CUL3^{KEAP1}$ system, indicating that control of NRF2 homeostasis is more complex than previously thought (Lo et al., 2017). Even though WDR23 recognizes a distinct binding motif within the NRF2 sequence than KEAP1, they seem to constitute redundant pathways. In the tested lung cancer cell line deficient for KEAP1, overexpression of WDR23 was able to enhance cellular sensitivity to cisplatin by suppressing NRF2. Moreover, tumor samples from lung cancer patients harboring KEAP1 mutations show an increased expression of WDR23. It will be of great interest to investigate how these two parallel pathways function together in the coordinated turnover of NRF2.

DDB2 is also an important repressor of the antioxidant system by inhibiting gene expression of MnSOD and catalase that ultimately induces premature senescence upon cisplatin. In both mouse embryonic fibroblasts and human carcinoma cells, a DDB2 deficiency reduced premature senescence triggered by ROS and, consequently, rendered the cells cisplatin-resistant (Roy et al., 2010).

1.2.4.6 Regulation of DNA repair

With regard to the response to chemotherapy, p53-induced DDB2 expression was demonstrated to enhance resistance by promoting the repair of cisplatin-induced DNA lesions (Barckhausen et al., 2013; Takimoto et al., 2002). The substrate receptor CDT2 promotes the repair of cisplatin-induced DNA crosslinks by targeting the endonuclease XPG, which cleaves the damaged DNA strands on the 3' side of the lesion. Subsequent degradation of XPG by CRL4 is required for the recruitment of DNA polymerase δ to the damaged site to ensure gap-filling DNA synthesis in the final step of repair (Han et al., 2015). In addition, CDT2 has been implicated in translesion DNA synthesis at cisplatin adducts in the presence of ubiquitinated PCNA (proliferating cell nuclear antigen) (Terai et al., 2010).

1.2.4.7 Regulation of other mechanisms

In addition to influencing the oxidative stress response, KEAP1 controls intracellular cisplatin concentrations by regulating drug transporters. A knockdown of *Keap1* in a HPV (human papilloma virus)-16 transformed human renal epithelial cell line increased the expression of multiple transporters, namely multidrug resistance protein 1-3 (MDR1-3), breast cancer resistance protein (BCRP), multidrug resistance-associated protein 2 and 3 (MRP2 and MRP3), which enhance cisplatin efflux (Jeong et al., 2015).

A recently identified target of FBXW7 is the master transcription factor SOX9 (sex determining region Y-box 9) that has diverse functions in embryonic development and maintenance of stem cell populations in adults. In multiple cancer cell lines, cisplatin induced the proteasomal degradation of SOX9 in a $CUL1^{FBXW7}$ dependent manner (Hong et al., 2016). The reaction depends on SOX9 phosphorylation by GSK3 that generates a recognition motif for FBXW7. A cohort study of 423 medullablastoma patients further revealed significantly lower expression of FBXW7 that correlates with high SOX9 protein levels. Importantly, failure to degrade SOX9 renders medullablastoma cell lines insensitive to cisplatin treatment (Suryo Rahmanto et al., 2016). The regulation of epithelial-mesenchymal transitions (EMT) represents an additional mechanism by which FBXW7 is thought to promote cisplatin chemosensitivity. In non-small cell-lung carcinoma, depletion of FBXW7 by siRNA induces a mesenchymal phenotype that renders the cells more cisplatin-resistant (Yu et al., 2013).

Another CUL1 substrate receptor, FBXO22 was shown to mediate ubiquitination and subsequent degradation of the oncoprotein CD147 (also known as extracellular matrix metalloproteinase inducer (EMMPRIN) or basigin) (Wu et al., 2017). CD147 is a transmembrane glycoprotein strongly implicated in tumour progression and development of chemo-resistance of cancer cells by regulating a plethora of cellular processes including drug transporters (reviewed in Xiong et al., 2014). Interestingly, cisplatin-resistant lung cancer cell lines contain markedly elevated levels of CD147 and overexpression of FBXO22 could reverse this cisplatin resistance by destabilization of CD147. However, the mechanism of how CD147 confers cisplatin resistance was not assessed in this study.

Table 1. Role of CRLs in the cellular sensitivity toward cisplatin treatment

CRLs which support cisplatin sensitivity

Cullin protein	Substrate receptor	Substrate / mechanism	Function	References
CUL1	beta-TrCP (FBXW1)	degradation of Mcl-1	pro-apoptotic	Ding et al., 2007
CUL1	FBXW7 (CDC4)	degradation of Mcl-1	pro-apoptotic	Koo et al., 2015
CUL1	FBXW7 (CDC4)	suppresses G1/S transition by increasing the expression levels of p14, p16, p21	cell cycle arrest	Zhou et al., 2015
CUL1	FBXW7 (CDC4)	downregulation promoted mesenchymal phenotype cells were more resistant to cisplatin	suppresses EMT	Yu et al., 2013
CUL1	FBXW7 (CDC4)	SOX9	EMT / efflux	Rahmanto et al. 2016; Hong et al., 2016
CUL1	FBXO22	degradation of the glycoprotein CD147	unknown	Wu et al., 2017
CUL1	FBXO32 (Atrogin)	target unknown	pro-apoptotic	Chou et al., 2010; Qin et al., 2009; Tan et al., 2007
CUL3	Gigaxonin (KLHL16)	degradation of NfκB	pro-apoptotic	Veena et al., 2014
CUL3	KEAP1 (KLHL19)	degradation of MDR1, MRP2/3, BCRP	enhanced efflux	Jeong et al., 2015
CUL3	KEAP1 (KLHL19)	degradation of NRF2	reduced oxidative defence	Bao et al., 2014; Guan et al., 2016; Xia et al., 2014
CUL4	DDB2	transcriptional repression of BCL2 by recruitment of HDAC to *BCL2* promoter	pro-apoptotic	Zhao et al., 2013
CUL4	DDB2	increased levels of ROS due to repression of antioxidant genes (MnSOD, catalase)	premature senescence	Roy et al., 2010
CUL4	WDR23	degradation of NRF2	reduced oxidative defence	Lo et al., 2017

CRLs which support cisplatin resistance

Cullin protein	Substrate receptor	Substrate / mechanism	Function	References
CUL1	FBXW11 (beta-TrCP2 / HOS)	activation of NF-κB by degradation of its inhibitor IκB	anti-apoptotic	Fuchs et al., 1999; Lee et al., 2007; Soldatenkov et al., 1999;
CUL1	CRLs which	binding to the acetyltransferase CBP/p300 inhibits the interaction of p300 and p53, thereby prevents activation of p53	anti-apoptotic	Kitagawa et al., 2008
CUL4	CDT2 (DTL)	degradation of XPG during NER	DNA repair	Han et al., 2015
CUL4	CDT2 (DTL)	mono-ubiquitination of PCNA promotes translesion synthesis	DNA repair (TLS)	Terai et al., 2010
CUL4	DDB2	activation of p38 MAPK pathway., reduces TNF-α induced apoptosis (target not known)	anti-apoptotic	Sun and Chao, 2005
CUL4B	unkown	degradation of HUWE1 (ubiquitin ligase that targets Mcl-1)	anti-apoptotic	Yi et al., 2015
CUL5	WSB1	degradation of HIPK2 (transcription factor for p53)	anti-apoptotic	Choi et al., 2008; Archange et al., 2008; Shichrur et al., 2014
CUL7 / CUL9		sequester p53	anti-apoptotic	Skaar et al., 2007; Woo et al., 2012

1.2.5 CRLs as therapeutic targets to overcome cisplatin resistance?

The ubiquitin-proteasome system is a promising target in cancer therapy and its inhibition provides a potential strategy to overcome drug resistances. CRLs build the biggest family of E3 ubiquitin ligases and display specificity in the selection of protein substrates designated for degradation. By suppressing apoptotic cell death or promoting DNA repair of cisplatin adducts, numerous CRLs have been linked to cisplatin resistance thereby providing a potential target for cancer therapy. On the other hand, several CRLs mitigate the cytotoxicity of cisplatin and inhibition of those ubiquitin ligases would diminish chemotherapy efficacy (Figure 3 and Table 1). These opposing mechanisms of distinct CRLs also question the effect of the newly developed neddylation inhibitor MLN4924, which collectively inhibits CRLs. Although preclinical studies are promising by showing synergistic effect with cisplatin, its clinical benefit remains to be confirmed and the treatment success might be highly dependent on the tumor characteristics of each individual patient. Accordingly, inhibition of a specific CRL may provide a more targeted approach to modulate cisplatin sensitivity. Indeed, in recent years many attempts have been made to develop small-molecule inhibitors targeting F-box proteins, the substrate receptors of CRL1 (Skaar et al., 2014). Among these, SKP2 is the most intently studied substrate receptor and its inhibition targets directly cancer stem cells, which are the major cause of drug resistance and treatment failure. Consequently, combined treatment with SKP2 inhibitors and chemotherapeutics including doxorubicin resulted in synergistic lethality in human cancer cell lines in vitro and in xenograft models (Chan et al., 2013). Nevertheless, development of CRL-targeted therapy and the identification of those patient who can benefit from such a therapy is challenging due to several reasons. First, only a part of the substrate receptors has established protein targets and even fewer have multiple confirmed substrates, which implies that many substrates remained undiscovered so far. Second, whereas some CRLs seem to have a clear defined biological function in either promoting or suppressing tumor progression by targeting substrates with similar biological function, other CRLs can regulate substrates with distinct or even opposing functions. This clearly complicates the prediction of a treatment response not only for different cancer types but also for individual patients. Finally, the abundance of a particular component of CRLs does not necessarily reflect biological functionality due to the modular architecture of these complexes. The assembly of a specific substrate receptor with the cullin scaffold is regulated by diverse players including the substrate receptor exchange factor CAND1,

neddylation and deneddylation and also the availability of substrates. This multifaceted regulation of CRL activity makes it difficult to identify components with the potential to serve as predictable biomarkers. Also the multifactorial nature of cisplatin resistance makes it more difficult to identify a subgroup of patients that will benefit from a certain therapy combination.

The principle of precision medicine is to match a fit-to-purpose drug with the most receptive patients. In recent years, technological advances in genomics, transcriptomics and proteomics have contributed substantially to the identification of molecular signatures of cancers that predict the responsiveness to a specific drug. However, the clinical relevance is restricted due to the incomplete biological understanding of the relationship between cancer phenotype and molecular alterations. Additionally, chemoresistance is strongly influenced by tumor microenvironment and the presence of cancer stem cells, which cannot be assessed by conventional screening methods. Recently, functional testing has come into the focus of cancer diagnosis by probing the tumor response to drugs directly on biopsies in order to guide the therapy (Friedman et al., 2015). These ex vivo drug exposure methods take into account the impact of tumor microenvironment and tumor stroma. A promising approach uses patient-derived organoids, which are grown in an extracellular matrix allowing for three-dimensional expansion. Organoid cultures established from colorectal cancer retained several features of the original malignancy, thus may potentially provide a suitable tool to test drug sensitivity (van de Wetering et al., 2015). Another approach uses patient-derived tissue to determine drug sensitivity after xeno-transplantation of the tumor cells into immuno-deficient mice, which might even more accurately represent the endogenous tumor environment. A pilot study with tumor xenografts from patients with advanced cancers showed very promising results. Eleven of 14 patients achieved partial remission with a selected therapy based on personalized tumor xenografts (Hidalgo et al., 2011). Although there are several challenges to be overcome in future, these models provide novel opportunities for precision cancer medicine and are very promising to improve combined chemotherapeutic approaches for the treatment of cancer patients.

1.2.6 Conclusion

Cisplatin, a very potent and widely used chemotherapeutic agent, often provokes rapidly the development of resistances, which is one of the biggest obstacles in cancer treatment. CRLs have been shown to play a crucial role in the regulation of diverse mechanisms that contribute to chemoresistance, thereby providing a potential target for cancer therapy. However, each CRL has multiple substrates involved in distinct biological pathways and, depending on the tumor biology, its inhibition can have different effects and even support the development of cisplatin resistances. The selection of the most effective drug combination for each patient is challenging and biomarkers currently used for diagnosis are mainly based on genetic variations that do not reflect the whole complexity of a tumor. Novel functional treatment optimization tests are now being investigated with promising results and might provide a suitable tool in future to select the right CRL inhibitor, to be combined with cisplatin, for the right patient.

2 Aim of the thesis

The ubiquitin-proteasome system (UPS) has emerged as a promising target in cancer therapy. A new class of compounds currently in clinical trials inhibits the neddylation pathway by inactivating the NEDD8-activating enzyme (Soucy et al., 2009). The best characterized and, so far the most relevant neddylation substrates are the family members of cullins (CUL1-5, CUL7 and CUL9). Cullins serve as a scaffold in the cullin-RING ubiquitin E3 ligase (CRL) complexes that recruit via an adaptor protein a variety of different substrate receptors for targeting specific proteins for ubiquitination. Due to the high number of substrate receptors that can be incorporated into the complex, CRLs build the largest family of ubiquitin ligases (>200 CRLs) that are responsible for ubiquitination of ~20% of cellular proteins degraded through UPS. They regulate a variety of biological processes including DNA replication, cell cycle, apoptosis and antioxidant stress (Emanuele et al., 2011; Iso et al., 2016; Koepp et al., 2001; Lee et al., 2009; Nishitani et al., 2006; Zhang and Wang, 2006 and reviewed by Sarikas et al., 2011).

The ubiquitination activity of CRLs requires attachment of NEDD8 to the cullin scaffold; therefore, inhibition of the neddylation pathway results in the accumulation of unmodified CRL substrates. MLN4924 (Pevonedistat) is the first neddylation inhibitor that is currently investigated in several clinical trials against different malignancies. Given the high amount of CRL substrates that are stabilized upon MLN4924 treatment, the detailed molecular mechanisms of how MLN4924 exerts its cytotoxicity remains largely unknown. Several CRL substrates have been proposed to mediate MLN4924-dependent cell death for example by inducing DNA re-replication resulting from accumulated CDT1 or SET8 (Benamar et al., 2016; Lin et al., 2010; Pan et al., 2013).

Several preclinical studies demonstrated that MLN4924 sensitizes cancer cells to the cytotoxic action of cisplatin (Jazaeri et al., 2013; Kee et al., 2012; Nawrocki et al., 2013). Cisplatin is one of the most widely used chemotherapeutic drugs used in clinics, but the fast development of resistances frequently results in treatment failure. The synergistic effect observed between MLN4924 and cisplatin suggest that CRL inhibitors may mitigate clinical resistances. However, the mechanism of this synergy remains poorly understood. In particular, it is not clear which of the many CRL complexes are implicated in the cellular response to cisplatin. The overall goal of my thesis was, therefore, to understand

how CRL inhibition modulates the cellular sensitivity to cisplatin. The specific aims were: (1) to verify whether the neddylation inhibitor MLN4924 synergizes with cisplatin, (2) to identify individual cullin-based ubiquitin ligases that enhance the cytotoxic effect of cisplatin, (3) to analyze specifically the function of the CUL4A/B ubiquitin ligases in the response to cisplatin.

In addition, I contributed to a second project that aimed to understand whether and how chromatin-remodeling complexes are operating during global genome nucleotide excision repair (GG-NER). UV induced lesions are either repaired by transcription-coupled or GG-NER, depending on the localization and detection of the damage. UV lesions formed in non-transcribed sequences are initially sensed by the damage recognition factors DDB2 and XPC. Binding of these two proteins initiate the repair process by recruitment of further downstream proteins to the damaged site (Naegeli and Sugasawa, 2011; Puumalainen et al., 2016; Rüthemann et al., 2016). In order to gain access to the highly condensed DNA wrapped around nucleosomes, chromatin reorganization is thought to precede the initial damage detection step. Chromatin remodelers have key functions in regulating the chromatin accessibility by moving or ejecting nucleosoms, thereby facilitating binding of repair proteins to the damage (Gospodinov and Herceg, 2013). In this project, we investigated the role of chromatin-remodeling in GG-NER. Specifically, we wanted to identify specific chromatin remodelers that support the repair of UV-lesions and how they mechanistically influence the repair process.

3 Results

3.1 CRL4 ubiquitin ligase promotes Fanconi anemia pathway-induced single-stranded DNA signaling at interstrand crosslinks

Tamara Codilupi, Doreen Taube and Hanspeter Naegeli

Institute of Pharmacology and Toxicology, University of Zurich-Vetsuisse,
Winterthurerstrasse 260, 8057 Zurich

Corresponding author: Hanspeter Naegeli (naegelih@vetpharm.uzh.ch)

Manuscript to be submitted.

This section describes the importance of CRL4 in supporting the ICL-induced S-phase cell cycle checkpoint required for proper repair. I designed, performed and analyzed the experiments, prepared the figures and drafted the manuscript.

Abstract

DNA-crosslinking agents like cis-diamminedichloroplatinum(II) (cisplatin) are indispensible for the treatment of many malignancies. These drugs generate interstrand crosslinks (ICLs) in the DNA double helix that block replication fork movement, ultimately leading to cell death. Many factors counteracting this ICL-induced replication stress, including the Fanconi anemia (FA) pathway, are regulated by ubiquitin and, therefore, ubiquitination reactions are promising targets for the sensitization of cancer cells to crosslinking agents. Here, we report that the cullin-RING ubiquitin ligase CRL4 promotes the survival of cisplatin-treated HeLa cells by supporting S-phase checkpoint responses. A simultaneous depletion of the partially redundant cullin paralogs CUL4A/CUL4B, which form the CRL4 scaffold, stabilizes the replication licensing factor CDT1, thus stimulating DNA re-replication in cisplatin-exposed cells. This CUL4A/B deficiency is sufficient to prevent the formation of FA pathway-dependent single-stranded DNA (ssDNA) and limit the recruitment of replication protein A (RPA), resulting in diminished RPA phosphorylation and impaired checkpoint activation. Taken together, our findings indicate that the extra DNA replication occurring upon CRL4 deficiency interferes with damage-induced checkpoint responses by camouflaging the deployment of ssDNA, thereby impeding ssDNA-RPA signaling. This unexpected consequence of CRL4 down regulation may be exploited to enhance the efficacy of cisplatin or other chemotherapeutics.

Introduction

Platinum-based drugs are extensively used against many solid malignancies including lung, testicular, ovarian and cervical cancer (Kelland, 2007). The distinctive mechanism of action of cis-diamminedichloroplatinum(II) (cisplatin) or related platinum chemotherapeutics involves the formation of DNA interstrand crosslinks (ICLs), which lead to cell death primarily by interfering with DNA replication (Siddik, 2003). A common cause of treatment failure is the emergence of platinum resistance emerging in most patients even after an initially favorable response. Cancer cells avoid ICL cytotoxicity by eliciting the DNA damage response (DDR) coordinating cell cycle progression with DNA repair (Zou and Elledge, 2003; Dobbelstein and Sorensen, 2015). A critical trigger of DDR signaling is DNA replication stress characterized by persistent stretches of single-stranded DNA (ssDNA) at stalled replication forks. This locally induced ssDNA is rapidly coated by replication protein A (RPA) giving rise to ssDNA-RPA complexes that provide a platform for engagement of the ataxia telangiectasia-mutated and Rad3-related (ATR) kinase. This serine/threonine kinase phosphorylates RPA as well as signaling intermediates like the checkpoint kinase 1 (CHK1) and histone H2AX to activate cell cycle checkpoints (Byun et al., 2005; Huang et al., 2010; Maréchal and Zou, 2015). Ultimately, the efficiency of checkpoint activation determines how cancer cells respond to chemotherapy (Deans and West, 2011; Lopez-Martinez et al., 2016) and, accordingly, RPA hyperphosphorylation has been associated with increased cisplatin resistance (Manthey et al., 2010).

The DDR cascade is driven by posttranslational modifications involving, besides phosphorylation, polypeptide modifiers like ubiquitin (Brown and Jackson, 2015; Dantuma and van Attikum, 2015). In particular, cullin-RING ubiquitin ligases (CRLs) regulate a variety of biological processes including cell cycle progression and DNA replication. CRLs contain one of several cullin scaffolds (CUL1-5, CUL7 or CUL9) that via an adaptor (for example DDB1) recruit substrate receptors targeting specific proteins for ubiquitination (Abbas and Dutta, 2011; Cavadini et al., 2016; Fischer et al., 2011; Jackson and Xiong, 2009; Lin et al., 2010). The activity of CRLs, except those containing CUL7, requires the covalent attachment of the ubiquitin-like modifier NEDD8 to the respective cullins, thus inducing conformational changes that facilitate the ubiquitin transfer to substrates (Bulatov and Ciulli, 2015; Duda et al., 2008). MLN4924 (pevonedistat) is a small-molecule antagonist of this neddylation reaction that inhibits CRLs, thereby preventing the ubiquitination of many proteins and stabilizing these targets against

ubiquitin-dependent turnover (Soucy et al., 2009). A critical CRL target under replication stress is the replication-licensing factor CDT1, whose function is to promote the initiation of replication forks. Normally, only one round of DNA synthesis is allowed during each somatic cell cycle (Abbas and Dutta, 2011; Arias et al., 2005; Kim et al., 2007). However, by preventing the ubiquitination and proteasomal degradation of CDT1, MLN4924 induces the superfluous initiation of extra replication forks, causing aberrant DNA re-replication. In turn, this uncontrolled DNA synthesis generates irreparable DNA damage culminating in cell death (Blank et al., 2012; Lin et al., 2010; Milhollen et al., 2011; Pan et al., 2013).

Previous reports demonstrated that MLN4924 also sensitizes cancer cells to the cytotoxic action of DNA-crosslinking agents (Garcia et al., 2014; Jazaeri et al., 2013; Kee et al., 2012; Nawrocki et al., 2013), implying that CRL inhibitors may mitigate cisplatin resistance. However, the mechanism of this synergy between MLN4924 inhibitors and crosslinking agents remained poorly understood. In particular, it was not clear which of the many CRL complexes susceptible to MLN4924-mediated inhibition are implicated in the response to platinum drugs and how these CRLs affect the detection or signaling of DNA damage inflicted by crosslinking agents. Finally, it was not known how the MLN4924-induced re-initiation of DNA synthesis impinges on the response to platinum treatment. Here, we identified CRL4 as a major player modulating the cellular sensitivity to cisplatin and found that the two cullin paralogs CUL4A and CUL4B have redundant functions in regulating the response to ICLs. Surprisingly, concomitant down regulation of CUL4A and CUL4B suppresses the formation of ICL-induced ssDNA and, consequently, the assembly of ssDNA-RPA complexes as well as RPA, CHK1 and H2AX phosphorylation upon cisplatin treatment. These results indicate a counterintuitive effect of replication fork re-initiation whereby the resultant DNA reduplication dampens DDR signaling and loosens checkpoint activation.

Results

CUL4A/B depletion potentiates the cytotoxicity of crosslinking agents

We first carried out short-term viability assays, based on the cell-mediated resazurin reduction, to establish that MLN4924 potentiates the cytotoxic effect of the crosslinking agents cisplatin and mitomycin C (MMC) in HeLa cells, as demonstrated before with several other cancer cell lines (Garcia et al., 2014; Jazaeri et al., 2013; Kee et al., 2012; Nawrocki et al., 2013). The presence of MLN4924 at a concentration of 10 μM reduces the

IC_{50} of cisplatin from ~10 to ~2.5 µM and the IC_{50} of MMC from ~4 to ~1.5 µM (Figure 1A). MLN4924 also increases the cytotoxicity of cisplatin and MMC in Skov3 ovarian carcinoma cells (Supplementary Figure S1).

Next, we depleted different cullins by short interfering (siRNA) transfections of HeLa cells to understand which of the possible MLN4924 targets actually modulate the susceptibility to DNA-crosslinking agents. Comparative cell viability assays were carried out in the presence of 5 µM cisplatin, thus confirming a potentiation of cisplatin toxicity upon down regulation of CUL3 as reported before for Skov3 and ES2 ovarian carcinoma cells (Jazaeri et al., 2013). The novel finding of this initial screening was that a very similar potentiation is detected upon simultaneous down regulation of the two scaffold paralogs of CRL4, i.e., CUL4A and CUL4B (Supplementary Figure S2A). Dose dependence experiments confirmed that the co-depletion of CUL4A/B mimics to a large extent the sensitizing effect of MLN4924 when HeLa cells are treated with cisplatin (Figure 1B). As expected, the same increase of cisplatin sensitivity was achieved in depletion assays targeting the DDB1 adapter protein instead of the CUL4A/B scaffold. Instead, no sensitization was elicited upon depletion of only one of the cullins, CUL4A or CUL4B individually, indicating that these two interchangeable scaffolds have an at least partially redundant function. These results where further confirmed using distinct siRNA sequences for targeting CUL4A and CULB (Supplementary Figure S2B and S2C). The simultaneous depletion of CUL4A and CUL4B also sensitized HeLa cells towards the cytotoxic action of MMC (Figure 1C). The efficiency of each protein down regulation in siRNA transfection experiments is documented in Supplementary Figure S3.

Combined experiments with siRNA transfections and the addition of MLN4924 suggest a predominant contribution to cisplatin sensitization due to the lack of CRL4 activity, with only a minor influence from other ubiquitin ligases including CLR3 containing CUL3 as the scaffold. Indeed, the measured IC_{50} was close to the value of ~3 µM regardless of whether the cisplatin exposure of HeLa cells occurred in the presence of MLN4924 alone or upon siRNA-mediated CUL4A/B depletion followed by the addition of MLN4924 (Figure 1D). Further assays measuring the release of lactate dehydrogenase as a marker of membrane disruption (Figure 1E) confirmed that the concomitant CUL4A/B depletion enhances cisplatin-induced cell death. Finally, the increased cytotoxicity of cisplatin upon combined CUL4A/B depletions, but not after down regulation of only one of the two cullins individually, was confirmed in a long-term colony-forming assay (Figure 1F).

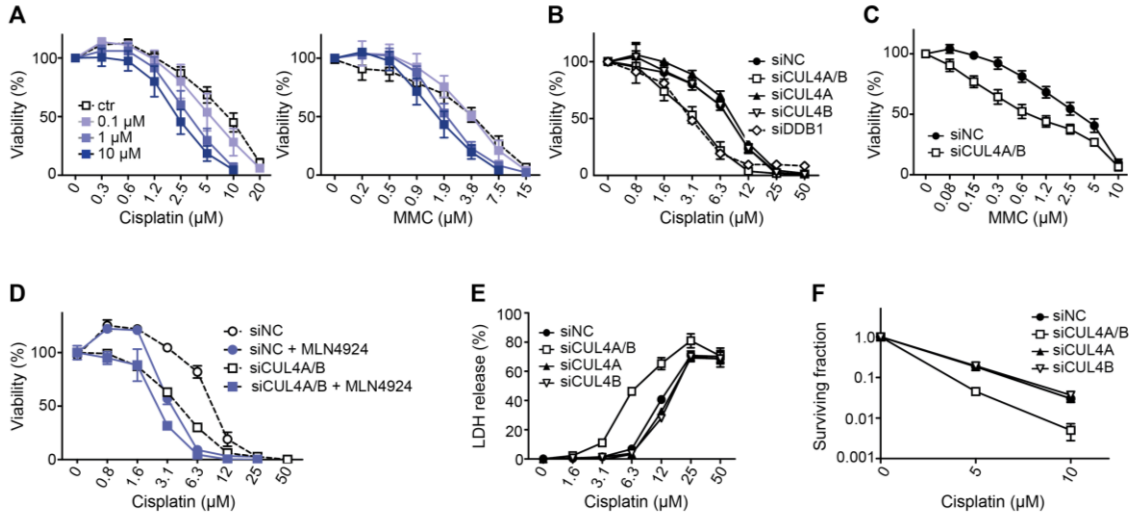

Figure 1. CUL4A/B depletion potentiates ICL cytotoxicity.

A) HeLa cells were incubated for 48 h with increasing concentrations of cisplatin (panel on the left) or mitomycin C (MMC, panel on the right) in combination with the indicated concentrations of MLN4924. Cell viability is expressed as the percentage of control values obtained in the absence of cisplatin (N = 5-10 experiments, error bars show s.e.m.). **B)** HeLa cells were transfected with siRNA to down regulate CUL4A, CUL4B (individually or in combination) or DDB1. Thereafter, cells were incubated with increasing cisplatin concentrations and tested for viability after 48 h (N = 5-10, siNC indicates non-coding control RNA). **C)** HeLa cells were transfected with siRNA to down regulate CUL4A and CUL4B (individually or in combination), incubated with the indicated MMC concentrations and tested for viability (N = 5). **D)** Combined experiments where HeLa cells were transfected with siRNA targeting CUL4A/B followed by incubation with cisplatin in the absence or the presence of MLN4924 as outlined (N = 5). **E)** Cytotoxicity assays measuring the cisplatin-induced release of lactate dehydrogenase (LDH) from HeLa cells during 48-h treatments with cisplatin (N = 3-5). Cells were pretreated with the indicated siRNA sequences. **F)** Colony-forming assays after exposure of siRNA-transfected HeLa cells to the indicated cisplatin concentrations.

CUL4A/B depletion stimulates DNA re-synthesis after ICL induction

Upon DNA damage, replication is inhibited by the S-phase checkpoint. To determine the effect of CUL4A/B depletion on this checkpoint response, HeLa cells were incubated for 24 h with a range of cisplatin concentrations. During the last 3 h of this cisplatin treatment period, the culture medium was additionally supplemented with the nucleoside analog 5-ethynyl-2′-deoxyuridine (EdU). Thereafter, DNA content and DNA synthesis were monitored by measuring 4',6-diamidino-2-phenylindole (DAPI) binding and EdU incorporation, respectively, in flow cytometry analyses. In control cells transfected with non-coding RNA, cisplatin inhibited the EdU incorporation, reflecting replicative DNA

synthesis, in a dose dependent manner (Figures 2A and 2B). At a cisplatin concentration of 5 µM, which reduces the viability of these control cells by ~30%, the EdU incorporation was decreased by nearly 90%. As expected from a previous report (Pan et al., 2013), siRNA-mediated down regulation of CRL4 activity by the combined CUL4A/B depletion elicited intra-S phase checkpoint responses lowering the rate of DNA synthesis relative to the respective non-coding RNA controls. However, this reduction of DNA synthesis relative to the non-coding RNA control was observed only as long as the cells were not exposed to cisplatin. Instead, the combined CUL4A/B depletion attenuated this inhibiting effect on DNA synthesis when the cells were challenged with cisplatin, such that CUL4A/B-depleted cells treated with cisplatin at 5 µM showed 2-fold higher EdU incorporations than cisplatin-exposed cells previously transfected with non-coding RNA (Figure 2B). The same response was observed when CUL4A/B-depleted HeLa cells were exposed to MMC. Indeed, as noted for cisplatin, the combined CUL4A/B depletion attenuated markedly the inhibiting effect of MMC on DNA synthesis (Figures 2C and 2D). Further analysis revealed that higher levels of the replication licensing factor CDT1, a known target of CRL4 (Jin et al., 2006), are likely responsible for the persistent DNA synthesis in cells damaged with crosslinking agents. Upon genotoxic stress caused by cisplatin, CDT1 is essentially completely degraded within 24 h in CRL4-proficient cells transfected with non-coding RNA. In contrast, the CUL4A/B co-depletion resulted in a pronounced stabilization of CDT1 and these cells maintained high CDT1 levels even after cisplatin exposure (Figures 2E and 2F). This persistent CDT1 indicates that the continued DNA synthesis detected in CUL4A/B-depleted cells is a consequence of an aberrant re-initiation of replication origins.

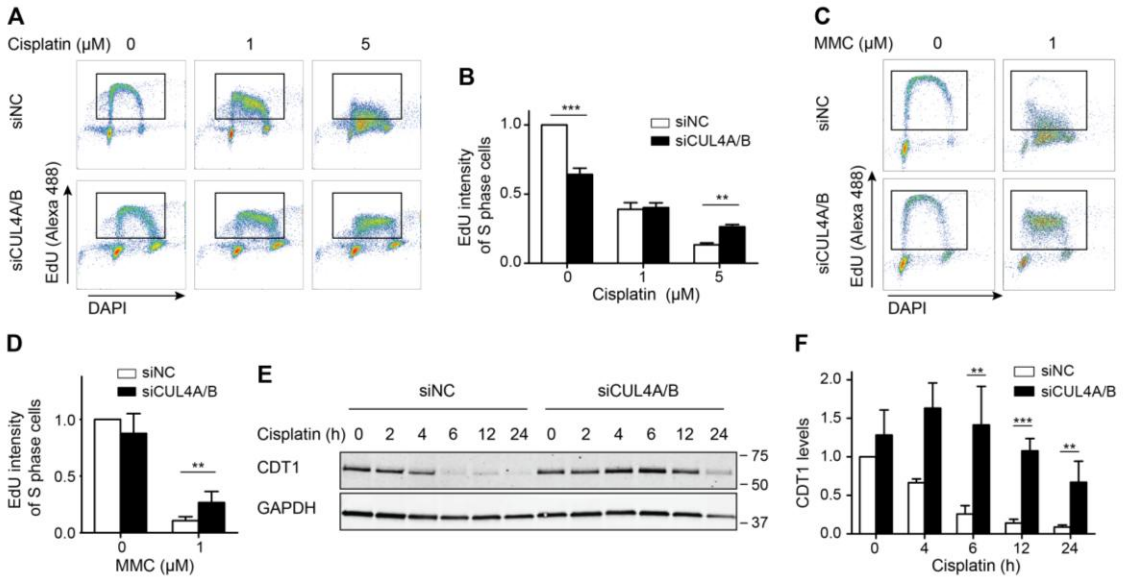

Figure 2. CRL4 depletion stimulates DNA re-synthesis upon ICLs

A) HeLa cells were transfected with siRNA and incubated for 24 h with the indicated cisplatin concentrations; 3 h before cell analysis by flow cytometry, the culture medium was supplemented with 5-ethynyl-2′-deoxyuridine (EdU). DNA content and DNA synthesis were monitored by 4',6-diamidino-2-phenylindole (DAPI) binding and EdU incorporation. The rectangles contain S-phase cells. **B)** Quantification of EdU incorporation in S-phase cells after treatment with the indicated cisplatin concentrations and comparison between CULA/B-proficient (siNC) and CUL4A/B-deficient cells (siCUL4A/B). N = 5; asterisks indicate significantly higher DNA synthesis in CUL4A/B-depleted cells relative to non-coding controls (***P < 0.0001, **P < 0.005, unpaired two-tailed t-test). **C)** HeLa cells were transfected with siRNA and incubated for 24 h with 1 μM MMC; 3 h before cell analysis by flow cytometry, the culture medium was supplemented with EdU. DNA content and DNA synthesis were monitored by DAPI binding and EdU incorporation. The rectangles contain S-phase cells. **D)** Quantification of EdU incorporations during S-phase after treatment with 1 μM MMC. N = 5; **P < 0.005. **E)** Representative immunoblot showing the time-dependent CDT1 levels in HeLa cells subjected to the indicated siRNA transfections and challenged with 20 μM cisplatin. Glyceraldehyde 3-phosphate dehydrogenase (GAPDH) was used as the loading control. **F)** Quantification of CDT1 levels normalized to GAPDH in HeLa cells challenged with 20 μM cisplatin. Values are expressed relative to the constitutive CDT1 level in untreated cells (N = 3-5); asterisks indicate significantly higher CDTI levels in CUL4A/B-depleted cells relative to non-coding controls.

Suppressed S-phase checkpoint in CUL4A/B-deficient cells

To elucidate the role of CRL4 in the ICL-initiated DDR cascade, we analyzed the activation of intra-S checkpoints by monitoring the phosphorylation of ATR and CHK1. In HeLa cells that were not exposed to cisplatin, we observed the expected increase of phosphorylated ATR (pATR) upon CUL4A/B depletion relative to non-coding RNA-treated controls, consistent with the pivotal role of this protein kinase in activating the

checkpoint machinery upon excessive CDT1 function and DNA re-replication (Lin & Dutta, 2007; Liu et al., 2007; Pan et al., 2013). Conversely, HeLa cells transfected with non-coding RNA react to a subsequent cisplatin exposure by ATR phosphorylation with a peak of pATR around 4 h after beginning of drug exposure (Figures 3A and 3B). As a consequence of ATR activation, these cells respond to cisplatin exposure by an increased phosphorylation of CHK1 with a plateau of pCHK1 at 12 hours after the beginning of drug treatment (Figures 3A and 3C). However, HeLa cells transfected with siRNA targeting CUL4A/B displayed lower levels of both pATR and pCHK1 upon cisplatin challenges. That this CUL4A/B depletion impedes partially CHK1 phosphorylation in response to ICL induction is confirmed in MMC-exposed HeLa cells (Figure 3D). Although CHK1 had been identified as a possible CRL4 target (Huh and Piwnica-Worms, 2013), we did not observe any overall changes of CHK1 protein level along with its differential phosphorylation. Despite the inhibitory effect of CUL4A/B depletions on the ATR-CHK1 pathway, this combined CUL4A/B deficiency had no statistically significant influence on the phosphorylation of ataxia telangiectasia-mutated (ATM) and CHK2 proteins in cisplatin-treated cells (Supplementary Figure S4).

We next tested whether the weakened S-phase checkpoint activation leads to an increase of the M-phase population. For that purpose, HeLa cells were again transfected with non-coding RNA or siRNA targeting CUL4A/B, followed by 24-h incubations with cisplatin. To determine a mitotic index, the cells were stained for DNA content and histone H3 phsphorylated at position Ser10 (pH3), a well-established marker of mitosis, and subsequently analyzed by flow cytometry (Figure 3E). These experiments revealed that cisplatin reduces the fraction of cells reaching the M phase in a dose-dependent manner. In the presence of cisplatin at 5 µM, however, the CUL4A/B co-depletion resulted in a doubling of the fraction of M-phase cells relative to the non-coding controls with proficient CRL4 activity (Figure 3F). Since this cisplatin concentration of 5 µM is highly toxic in CUL4A/B-depleted cells, we concluded that the CUL4A/B deficiency allows for entering mitosis despite irreparable ICLs, thereby causing mitotic catastrophe.

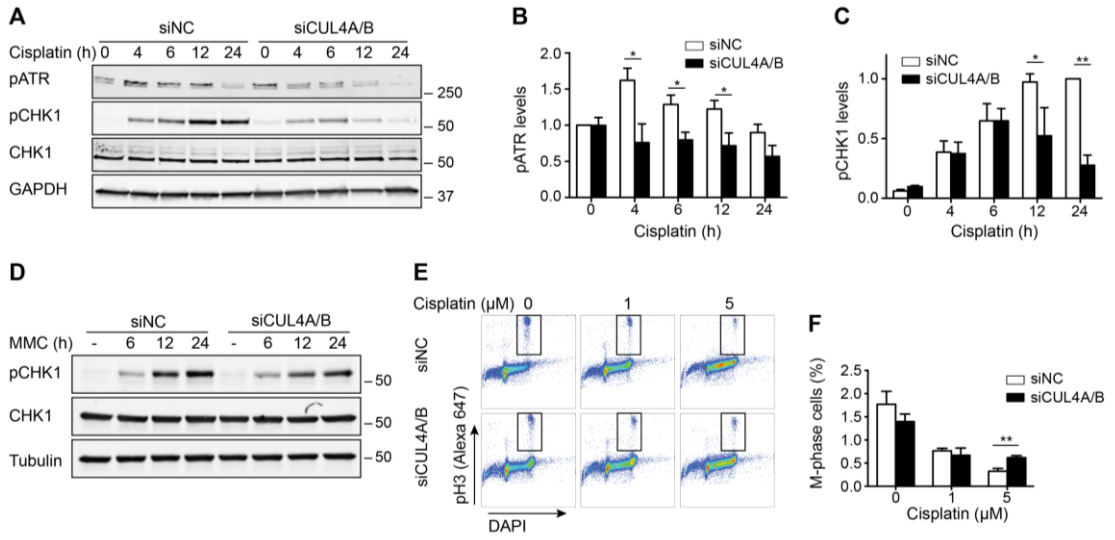

Figure 3. Suppression of the S-phase checkpoint upon CRL4 depletion
A) Representative immunoblot showing changes of phosphorylated ATR (pATR) and phosphorylated CHK1 (pCHK1) relative to GAPDH used as the loading control. HeLa cells were depleted of CUL4A/B as indicated and incubated with 20 μM cisplatin for different time periods. **B)** Quantification of pATR levels normalized to GAPDH in HeLa cells challenged with 20 μM cisplatin. Values are expressed relative to the constitutive pATR level in non-exposed counterparts (N = 3-5); asterisks indicate significantly lower pATR levels in CUL4A/B-depleted cells relative to non-coding controls (*P < 0.05, unpaired two-tailed t-test). **C)** Quantification of pCHK1 levels normalized to non-phosphorylated CHK1 in HeLa cells challenged with 20 μM cisplatin. Values are expressed relative to the constitutive pCHK1 level in non-exposed cells (N = 3-5). **D)** Representative immunoblot analysis showing pCHK1 changes induced by 1 μM MMC relative to non-phosphorylated CHK1 and tubulin used as loading standards. **E)** Staining for phospho-histone 3 (pH3). HeLa cells were CUL4A/B-depleted and challenged for 24 h with cisplatin as indicated. Mitotic cells characterized by high DNA and pH3 contents are indicated by rectangles. **F)** Percentage of mitotic cells after treatment with the indicated cisplatin concentrations compared to untreated untreated cell populations (N = 3-5); asterisks indicate a significantly higher percentage of mitotic cells upon CUL4A/B depletion relative to non-coding controls.

FANCD2-dependent ssDNA formation upon cisplatin treatment

To understand how CRL4 complexes support the S-phase checkpoint, we analyzed the ability of cisplatin-damaged HeLa cells to assemble a ssDNA-RPA signaling platform in response to ICL induction. First, the formation of stretches of ssDNA was assayed by incorporating 5-iodo-2′-deoxyuridine (IdU) and probing the cells with an antibody that binds to IdU exclusively in the ssDNA conformation. The fluorescence intensity elicited by these conformation-specific anti-IdU antibodies was detected by microscopy, thus

confirming as described (Clauson et al., 2013) that cisplatin leads to the accumulation of ssDNA foci (Figures 4A and 4B).

To understand the mechanism by which ICLs, although stabilizing covalently the duplex structure, can lead to the formation of ssDNA, we depleted by siRNA transfection different factors involved in ICL-processing, including distinct members of the Fanconi anemia (FA) pathway. Analyses of HeLa cells by immunofluorescence revealed that the depletion of FANCD2 is sufficient to abolish the ssDNA foci resulting from cisplatin treatment (Figures 4A and 4B). This observation is in line with the notion that FANCD2 constitutes a central member of the FA pathway recruited to ICLs to orchestrate downstream effector nucleases, which in turn are required for unhooking the crosslinked bases (Yamamoto et al., 2011; Klein Douwel et al., 2014; Pizzolato et al., 2015; Lachaud et al., 2016). Instead, FANCM and FAAP24 are dispensable for ssDNA induction in cisplatin-treated HeLa cells. Also, nucleotide excision repair (NER) activity is not involved in ssDNA induction upon cisplatin treatment, as no effect was seen after down regulation of XPA, which is a core NER factor.

A direct consequence of the observed ssDNA foci is the recruitment of RPA, which binds avidly to ssDNA. The RPA complex consists of three polypeptides, RPA1 (70 kDa), RPA2 (32 kDa) and RPA3 (14 kDa), whose middle subunit is phosphorylated on serine 33 (yielding pS33) upon replication stress. This reaction was tested through immunofluorescence microscopy by probing HeLa cells with phosphoprotein-specific antibodies (Figures 4A and 4C). These studies demonstrated that depletion of FANCD2 not only suppresses the formation of ssDNA but also the consequent foci of phosphorylated RPA2 in cisplatin-exposed cells. This result was further confirmed by Western blot analysis using two distinct siRNA sequences for targeting FANCD2 (Supplementary Figure S5). Instead, down regulation of FANCM, FAAP24 or XPA had no effect on pS33 foci. We conclude from these experiments that FANCD2, by recruiting downstream nucleases, is mainly responsible for eliciting stretches of ssDNA that subsequently serve as a hub for the initiation of RPA signaling at ICL sites.

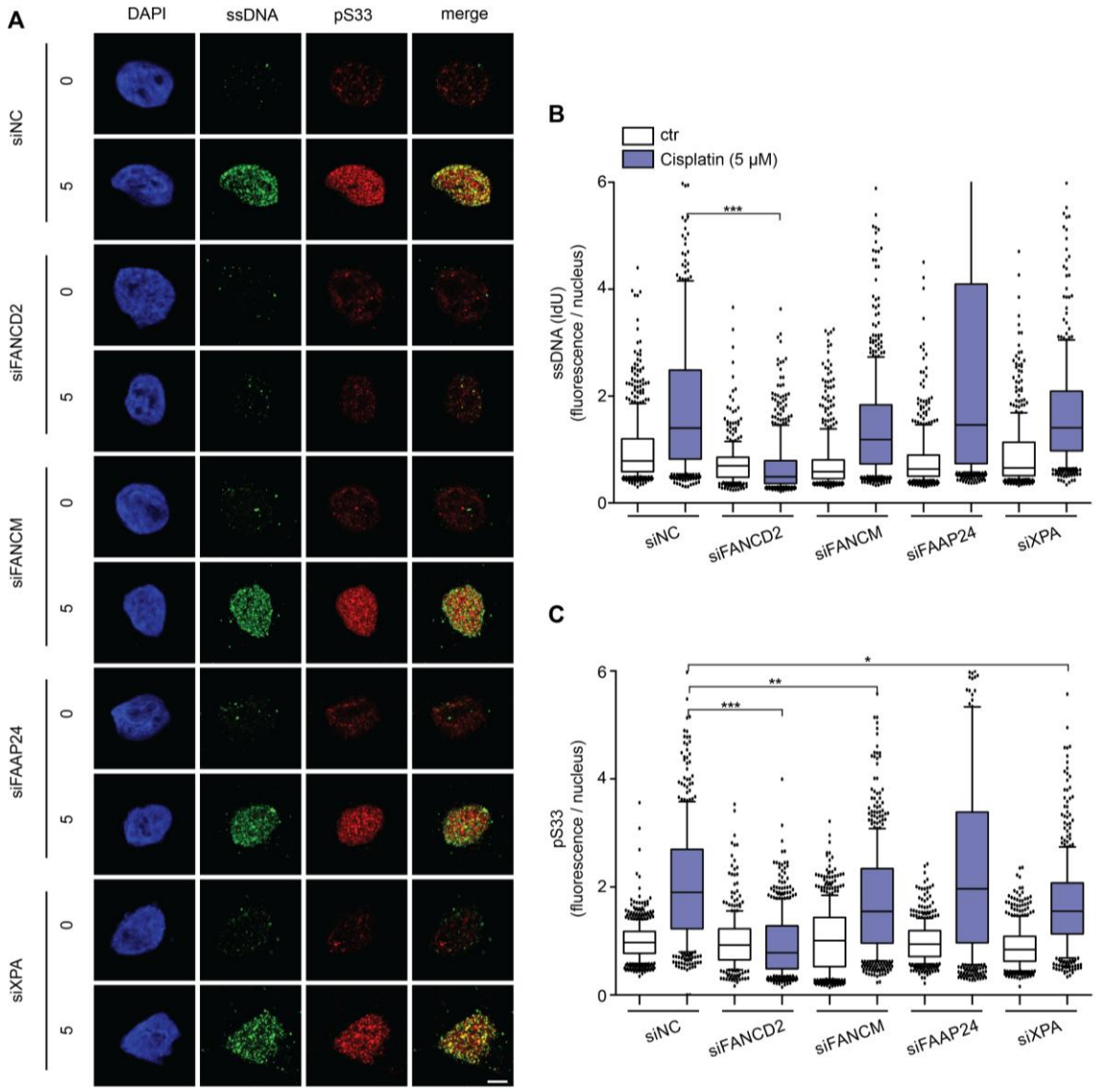

Figure 4. ICL-induced ssDNA formation

A) HeLa cells were transfected with the indicated siRNA and labeled for 30 h with 5-iodo-2′-deoxyuridine (IdU) before genotoxic treatment, which consisted of a 24-h exposure to cisplatin. Control cells were mock-treated. For the detection of ssDNA, the cells were fixed and stained with anti-IdU antibodies under native conditions. Concomitantly, the cells were stained for pS33 (phosphorylation of RPA on serine 33) using phospho-specific antibodies.. DAPI was employed to visualize the nuclei. **B)** Quantification of mean nuclear fluorescence intensities reflecting ssDNA formation (N > 200 nuclei from 2-4 experiments). Horizontal lines represent median values, boxes and whiskers show the 10-90th percentiles. The statistical analysis was carried out by 1-way ANOVA according to Kruskal-Wallis. Asterisks (***P < 0.0001) indicate significant differences between FANCD2-depleted cells and non-coding controls. **C)** Quantification of mean nuclear fluorescence intensities reflecting pS33 foci (N > 200 nuclei from 2-4 experiments). Asterisks indicate significant differences between cisplatin-treated samples. Scale bar: 10 µm.

CUL4A/B depletion suppresses ssDNA-RPA assembly

Next, we tested how the CRL4 ubiquitin ligase impinges on this FANCD2-dependent ssDNA-RPA signaling reaction. Besides demonstrating the cisplatin dose-dependent ssDNA induction in CRL4-proficient cells, the conformation-specific anti-IdU antibody also revealed that the CUL4A/B depletion results in an increase of ssDNA foci in HeLa cells even without any exogenous genotoxic insult (Figures 5A and 5B). This response is expected from the loss of CUL4A/B-dependent licensing regulation and the notion that ssDNA intermediates provide the initial signal for S-phase checkpoint activation under conditions of uncontrolled re-replication (Liu et al. 2007). Intriguingly, the amount of ssDNA was not or only marginally increased by treatment of these CUL4A/B-depleted cells with cisplatin. As a consequence, CUL4A/B-depleted cells treated with cisplatin displayed significantly lower levels of ssDNA when compared to CUL4A/B-proficient controls exposed to the same cisplatin concentrations (Figures 5A and 5B). This effect was not due to changes in the efficiency of IdU incorporation, as the antibody yielded in all cases identical immunofluorescence signals after DNA denaturation, which converts all double-stranded to ssDNA conformations (Supplementary Figure S6).

As ssDNA stretches are immediately coated by RPA, the ssDNA foci co-localize with the immunofluorescence resulting from staining of the 32-kDa subunit of RPA (RPA2; Figure 5A and 5C). As expected, the immunofluorescence intensity of RPA2 foci increased upon cisplatin exposures in a dose-dependent manner. In CUL4A/B depleted cells, however, these RPA2 foci display significantly lower intensities when compared with CRL4-proficient controls treated with the same cisplatin concentrations. These results demonstrate that the CRL4 complex is indispensable for the generation of the ssDNA-RPA2 signaling platform required for activation of the S-phase checkpoint response.

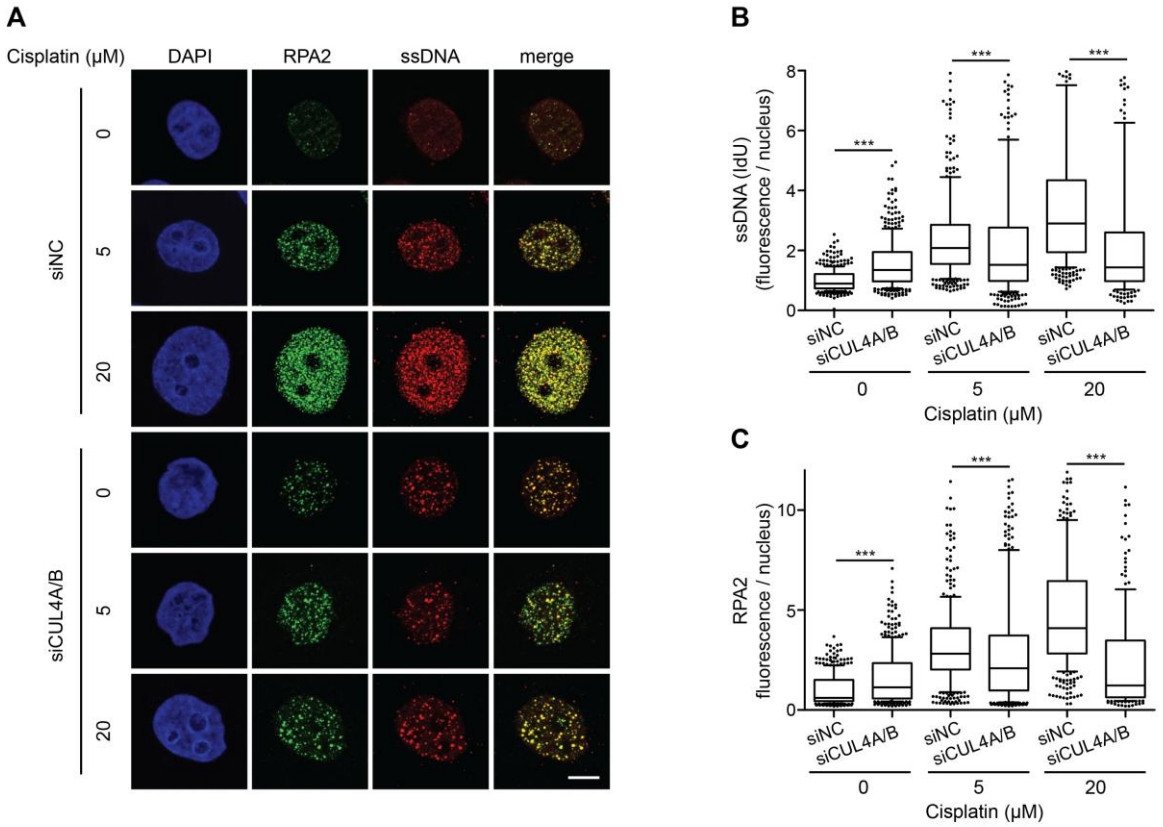

Figure 5. CRL4-depletion impairs recruitment of RPA upon cisplatin exposure
A) HeLa cells were transfected with siCUL4A/B, or with siNC, and labeled for 30 h with 5-iodo-2′-deoxyuridine (IdU) before genotoxic treatment, which consisted of a 24-h exposure the indicated cisplatin concentration. For the detection of ssDNA, the cells were fixed and stained with anti-IdU antibodies under native conditions. Concomitantly, the cells were stained for RPA foci using anti-RPA2 antibodies. DAPI was used to visualize the nuclei. **B)** Quantification of mean nuclear fluorescence intensities reflecting ssDNA (N > 200 nuclei from 2-4 experiments). Horizontal lines represent median values, boxes and whiskers show the 10-90th percentiles. The statistical analysis was carried out by 1-way ANOVA according to Kruskal-Wallis. Asterisks (***P < 0.0001) indicate significant difference between CUL4A/B-depleted cells and non-coding controls. **C)** Quantification of mean nuclear fluorescence intensities reflecting RPA foci (N > 200 nuclei from 2-4 experiments). Asterisks indicate significant difference between CUL4A/B-depleted cells and non-coding controls. Scale bar: 10 µm.

CUL4A/B depletion reduces RPA and H2AX phosphorylation upon ICL induction

The ssDNA-RPA platform leads to recruitment of the ATR kinase that in turn phosphorylates *inter alia* the N-terminus of RPA2 and the C-terminus of histone H2AX. Phosphorylated RPA2 serves a binding motif for many downstream factors which mediate S-phase checkpoint response (Olson et al., 2006; Anantha et al., 2007, Lin & Dutta, 2007,

Zou & Elledge, 2003). The ATR-dependent phosphorylation of RPA2 on serine 33 (generating pS33) and the ATR-dependent phosphorylation of H2AX (generating γH2AX), as well as the phosphorylation of RPA2 on serines 4 and 8 through a downstream protein kinase (generating pS4/8) were assayed in immunofluorescence microscopy experiments by probing HeLa cells with phospho-specific antibodies (Figure 6A). The quantification of nuclear immunofluorescence signals under the different assay conditions demonstrated the dose-dependent rise of pS33, pS4/8 and γH2AX upon cisplatin treatments at concentrations of 5 and 20 μM. However, this phosphorylation was markedly reduced for the direct ATR targets pS33 (Figure 6B) and γH2AX (Figure 6C) in CUL4A/B-depleted cells compared to CRL4-proficient controls. A significant reduction in CUL4A/B-depleted cells was also observed for the formation of pS4/8, but only at the higher cisplatin concentration (Figure 6D). These reduced phosphorylation levels indicate an overall suppression of checkpoint activation upon CUL4A/B depletion.

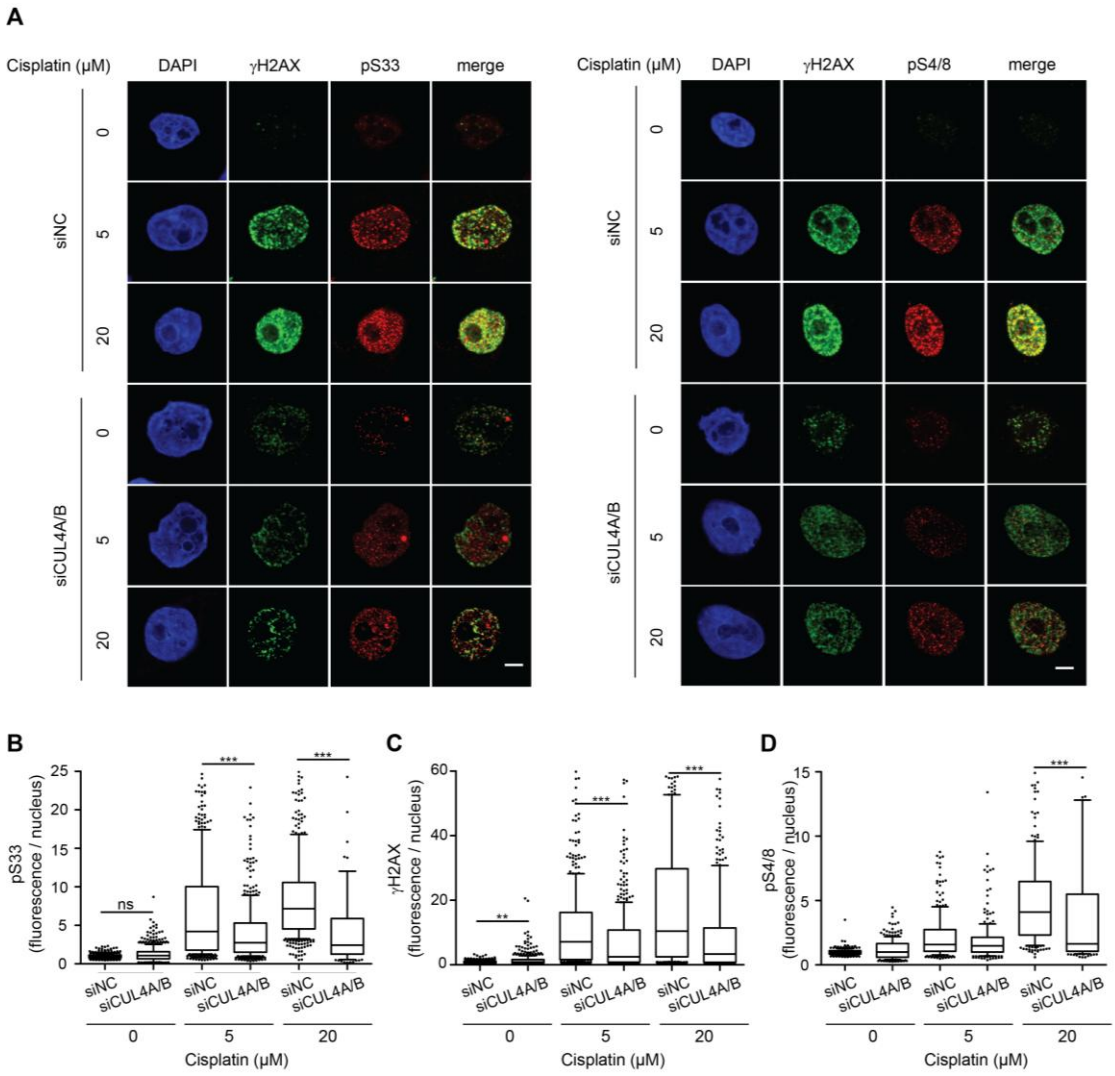

Figure 6. Reduced H2AX and RPA phosphorylation upon cisplatin exposure

A) HeLa cells were transfected with siCUL4A/B, or with siNC, and subjected to a 24-h challenge with the indicated cisplatin concentrations. For the detection of γH2AX, pS33 and pS4/S8, the cells were fixed and stained with the respective phospho-specific antibodies. Concomitantly, DAPI was used to visualize the nuclei. **B)** Quantification of mean nuclear fluorescence intensity of pS33 foci. Horizontal lines represent medians, boxes and whiskers the 10-90th percentiles. Asterisks indicate significant difference between CUL4A/B-depleted cells and non-coding controls (N > 200 nuclei from 2-4 experiments; ***P < 0.0001, 1-way ANOVA according to Kruskal-Wallis). **C)** Quantification of mean nuclear fluorescence intensity of γH2AX foci. **D)** Quantification of mean nuclear fluorescence of pS33 foci (**P < 0.005). Scale bar: 10 μm.

To demonstrate the general relevance of the above-described findings, we also assessed the appearance of ssDNA and consequent RPA phosphorylation using MMC, at a concentration of 1 µM, as another crosslinking agent (Figure 7A), and using Skov3 as another cancer cell line (Figure 7B). The quantification of nuclear immunofluorescence signals in both HeLa and Skov3 cells confirmed that the siRNA-mediated CUL4A/B depletion counteracts partially the ICL-dependent display of ssDNA and pS33 upon exposure to the crosslinking agent.

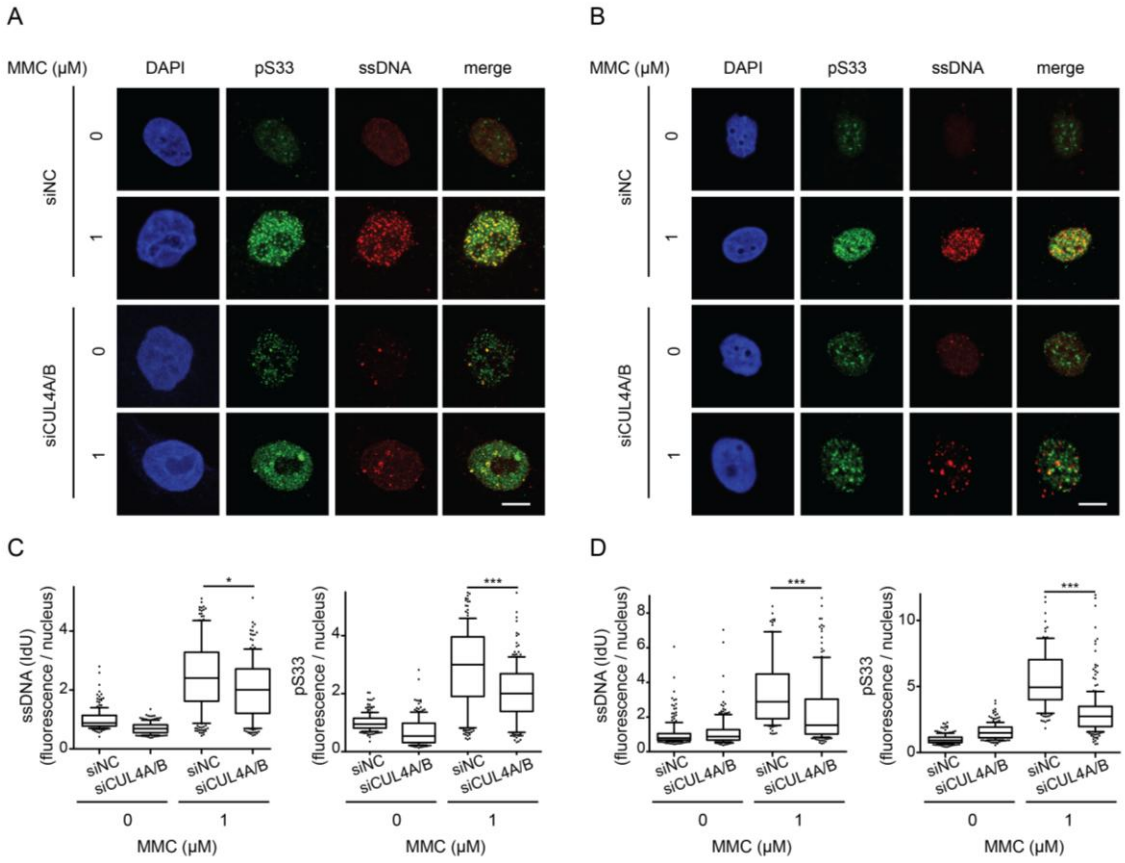

Figure 7. Reduced RPA phosphorylation upon MMC exposure
A) HeLa cells were transfected with siCUL4A/B, or with siNC, and subjected to a 24-h challenge with 1 µM MMC. The appearance of ssDNA and phosphorylated RPA2 in the form of pS33 was monitored by immunofluorescence. Concomitantly, DAPI was used to visualize the nuclei. **B)** Skov3 cells were transfected with siCUL4A/B, or with siNC, and subjected to the 24-h challenge with 1 µM MMC. The appearance of ssDNA and pS33 was monitored by immunofluorescence. **C)** Quantification of mean nuclear fluorescence intensity representing ssDNA and pS33 foci in HeLa cells. Horizontal lines represent medians, boxes and whiskers the 10-90th percentiles. Asterisks indicate significant difference between CUL4A/B-depleted cells and non-coding controls (N = 200 nuclei from 2-4 experiments; *P < 0.05, ***P < 0.0001, 1-way ANOVA according to Kruskal-Wallis). **D)** Quantification of mean nuclear fluorescence intensity representing ssDNA and pS33 foci in Skov3 cells (N = 200 nuclei from 2-4 experiments).

Biochemical analysis of RPA phosphorylation

The effect of CUL4A/B depletions on the cisplatin-induced phosphorylation of RPA2 (yielding pS33 and pS4/8) was confirmed biochemically by immunoblot analysis of whole-cell lysates. A damage-induced RPA2 phosphorylation was observed upon incubation of HeLa cells with 5 µM (Figure 8A) and 20 µM cisplatin (Figure 8B). In both cases, however, the degree of ATR-dependent pS33 formation was significantly reduced in CUL4A/B-depleted cells compared to CRL4-proficient controls transfected with non-coding RNA. This result was confirmed using a second siRNA sequence for CUL4A and CUL4B (Supplementary Figure S7A and S7B). A trend of reduced phosphorylation was also detected by examining pS4/8. Decreased pS33 and pS4/8 levels in CUL4A/B-deficient cells, compared to CRL4-proficient controls, were also found upon MMC treatment of HeLa and in Skov3 cells (Supplementary Figure S7C). Although these assays were carried out with phosphoprotein-specific antibodies, we wanted to ensure that the observed signals result from phosphorylation of RPA2 and not from a hypothetical ubiquitination by CRL4 ligase. Phosphatase treatment of lysates from cisplatin-treated cells clearly diminished the pS33 signal, thus confirming the detection of phosphorylated RPA2 (Supplementary Figure S7D).

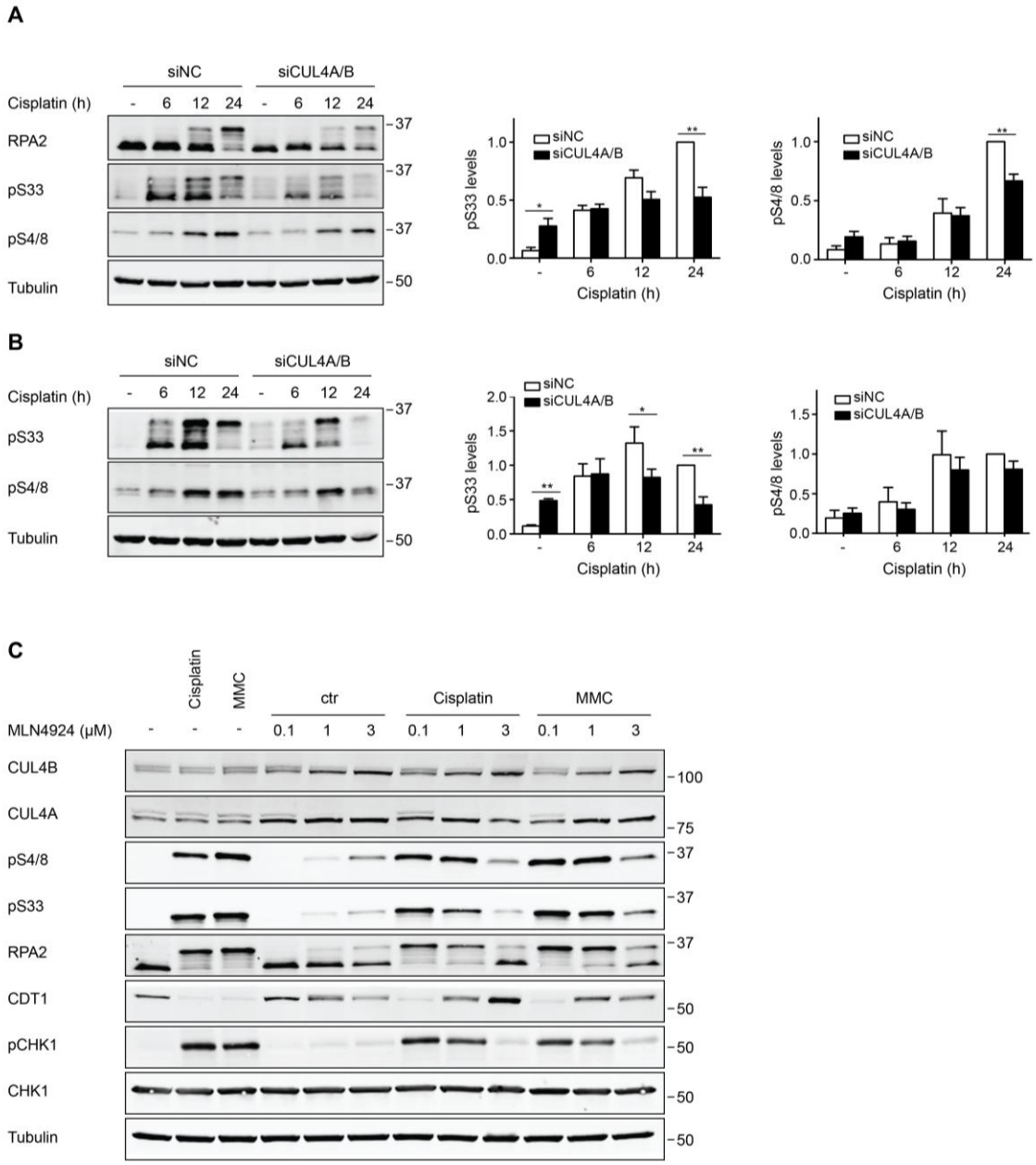

Figure 8. Immunoblotting analyses after treatment with crosslinking agents

A) HeLa cells were transfected with siCUL4A/B, or with siNC, incubated with 5 μM cisplatin and analyzed following the indicated incubation periods. Whole cell lysates were probed with antibodies against RPA2, pS33 and pS4/8. Tubulin served as the loading control. The graphs represent quantifications of pS33 and pS4/8 levels, normalized to tubulin, from 3-5 experiments. All values are shown relative to the respective phosphoprotein observed in siNC-transfected cells after a 24-cisplatin treatment. Asterisks indicate significant difference between CUL4A/B-depleted cells and non-coding controls (*$P < 0.05$, **$P < 0.005$). **B)** Same experiments as in panel A, except that HeLa cells were challenged with 20 μM cisplatin. **C)** HeLa cells were treated simultaneously with an ICL-inducing agent and with MLN4924 as indicated. The cisplatin and MMC concentrations were 5 μM and 1 μM, respectively. After 24 h, the cells were analyzed to determine CUL4A/B modifications, RPA2, CDT1 and CHK1, and the phosphorylation of RPA2 (pS4/8 and pS33) and CHK1 (pCHK1). Tubulin served as the loading controls. Scale bar: 10 μm.

MLN4924 recapitulates the effects of CUL4A/B depletion

Our initial result based on siRNA-mediated depletions of the scaffold proteins CUL4A and CUL4B indicated that the cytotoxic effect of the neddylation inhibitor MLN4924 is largely mediated by inactivation of the CRL4 ligase (Figure 1B). Therefore, we examined whether MLN4924 would reiterate the effect of CUL4A/B depletions on cell cycle checkpoint following cisplatin and MMC exposure (Figure 8C). Efficient CRL4 inhibition is confirmed by the disappearance of the slower migrating CUL4A and CUL4B bands representing the neddyated, active forms of these cullins, upon incubation of HeLa cells with MLN4924 at 1 μM or higher. The inhibitor alone only weakly activates the DNA damage response, reflected by slight increases in pS4/8, pS33 and pCHK1, whereas cisplatin and MMC induce a pronounced phosphorylation of RPA2 and CHK1, accompanied by nearly complete degradation of CDT1. This activation of the DNA damage response, involving enhanced pS4/8, pS33 and pCHK1 as well as reduced CDT1 upon cisplatin and MMC treatment, was progressively suppressed in the presence of increasing MLN4924 concentrations. We concluded that CRL4 inhibition or depletion of its subunits has the same potentiating effect on cisplatin sensitivity.

Discussion

Cisplatin is highly cytotoxic because the ICLs generated by this drug block transcription and DNA replication (Kelland, 2007). The processing of ICLs during DNA replication requires proteins of the FA pathway, but the mechanism of checkpoint induction by cisplatin or other crosslinking agents is still controversial. One previous study indicated that the FA pathway members FANCM/FAAP24 are able to initiate a checkpoint response to ICLs without generation of ssDNA intermediates (Huang et al., 2010). However, many other studies documented the formation of persistent stretches of ssDNA upon ICL induction (Higgs et al., 2015; Huang et al., 2010; Murina et al., 2014; Unno et al., 2014; Zellweger et al., 2015). Our own analysis revealed that the increase in ssDNA levels observed after cisplatin treatment depends on the FA pathway member FANCD2 (Figure 4), whose interactors are known to form ssDNA by nucleolytic DNA resection (Yamamoto et al., 2011; Klein Douwel et al., 2014; Pizzolato et al., 2015; Lachaud et al., 2016). In turn, the ICL-induced ssDNA acts as an initiating signal for S-phase checkpoint responses by recruitment of RPA and subsequent activation of the ATR protein kinase. We further

observed that cancer cells lacking CLR4 ubiquitin ligase activity (after depletion of the CUL4A/B cullin scaffold) are impaired in this ability to mount the ssDNA-RPA-initiated signaling response upon replication stress caused by ICLs (Figures 5-7). By suppressing the ssDNA-RPA checkpoint-signaling platform, this CLR4 deficiency potentiates the cytotoxic effect of cisplatin and MMC in the tested cells (Figure 1).

CRL4 complexes represent a family of ubiquitin ligases that regulate a variety of biological processes and are formed by assembly of one of two closely related scaffold proteins (CUL4A or CUL4B) with the adaptor protein DDB1, which associates with substrate receptors, and the RING finger protein RBX1 mediating the association with ubiquitin-delivering enzymes. The two paralogs CUL4A and CUL4B share high sequence similarity and have redundant functions (Hannah and Zhou, 2015). Notably, these two CUL4 paralogs are overexpressed in many human carcinomas and provide negative prognostic markers for survival (Jia et al., 2017 and references therein). Core CRL4 complexes, of which CUL4A/B constitutes the scaffold, recruit via DDB1 one of a variety of substrate receptors that target specific proteins for ubiquitination (Fischer et al., 2011a; Jackson and Xiong, 2009). For example, the $CRL4^{CDT2}$ ubiquitin ligase promotes degradation of the replication licensing factor CDT1 after replication origin firing to ensure that DNA is replicated only once per cell cycle (Jin et al., 2006; Lovejoy et al., 2006). Exposure to DNA-damaging agents also induces rapid CDT1 proteolysis through CRL4-mediated ubiquitination (Higa et al., 2003; Hu et al., 2004; Roukos et al., 2011; Stathopoulou et al., 2012), whereas ectopic CDT1 expression promotes DNA re-replication (Arias and Walter, 2006; Liontos et al., 2007). Accordingly, CRL4-deficient cells display higher constitutive levels of CDT1 and the ensuing re-replication has been shown to activate DDR signaling (Lin & Dutta, 2007; Liu et al., 2007; Pan et al., 2013). This high CDT1 level is maintained in CRL4-deficient cells after cisplatin treatment, such that re-replication occurs even at a concentration of this crosslinking agent that abrogates DNA synthesis in CRL4-proficient cells (Figures 2 and 3).

Uncontrolled origin firing and DNA re-replication constitutes on its own a highly genotoxic reaction causing fork breakage and DNA fragmentation (Alexander & Orr-Weaver 2016, Neelsen et al. 2013). Surprisingly, the higher ssDNA levels seen in CRL4-deficient cells are not further increased by exposure to cisplatin and, in fact, the extent of cisplatin-induced ssDNA remains significantly lower in CRL4-deficient cells compared to CRL4-proficient counterparts (Figure 5). This observation indicates that re-replication

resulting from CDT1 stabilization dampens the ICL-induced formation of ssDNA, thus limiting the assembly of ssDNA-RPA signaling complexes and activation of the ATR checkpoint kinase. As a consequence, the ATR-dependent phosphorylation of RPA2 (at position Ser33) and downstream effectors like H2AX is significantly suppressed in cisplatin-exposed cells lacking CRL4 compared to CRL4-proficient controls (Figures 6 and 7). This reduced checkpoint response provides a mechanistic basis for the ability of CRL inhibitors to potentiate the cytotoxicity of cisplatin or other crosslinking agents.

A possible scenario to explain the link between re-replication and the suppressed ICL response is that ssDNA stretches generated by ICL-inducing agents become themselves a template for re-replication rounds, such that most of this ssDNA is readily reconverted to double helical products. By this process, origin firing and re-replication near ICL sites would be able to mask ssDNA as the key signal for checkpoint activation upon ICL induction. Re-replication has been shown to lead to the accumulation of DNA double strand breaks arising from fork collisions (Alexander & Orr-Weaver 2016) or, alternatively, from DNA gaps in the template strand (Neelsen et al. 2013). In the tested HeLa cells, however, DNA double strand breaks caused by CUL4A/B depletion, if formed, remained largely undetected as demonstrated by the poor ATM activation (Supplementary Figure S4) and reflected by a minor phosphorylation of the Ser4/8 sites targeted by the ATM kinase (Figure 6D). Thus, at least a subset of cancer cells are unable to respond properly to this interactive effect of ICLs and re-replication, making them particularly vulnerable to combinations of crosslinking agents and CRL4 inhibitors like MLN4924. The future challenge is to develop selective CRL4 inhibitors to avoid side effects due to the unnecessary blockage of other cullin-type ubiquitin ligases. Also, it is necessary to discover and validate cancer biomarkers that allow for the identification of cancer subsets that are susceptible to the combined treatment strategy of a CRL inhibitor with cisplatin.

Material and methods

Cell lines and treatment

HeLa and SKOV3 cells (American Type Culture Collection) were cultured in low-glucose Dulbecco's modified Eagle medium (DMEM) and Roswell Park Memorial Institute (RPMI) 1640 medium, respectively, supplemented with 10% (vol/vol) fetal calf serum and 100 U/ml penicillin-streptomycin (all cell culture materials were from Gibco). Cells were incubated at 37°C in a humidified atmosphere under 5% CO_2. The cisplatin (Sigma) solutions were prepared freshly each time in DMEM. MMC (Sigma) was dissolved in a 1.5-mM stock solution in PBS and MLN4924 (ApexBio) in a 50-mM stock solution in DMSO. Working solutions were prepared from these stocks in DMEM to reach the indicated final concentrations. Cells were treated with these ICL-inducing agents 3 days after siRNA transfections, except in the viability assays where the drugs were applied 2 days after transfections.

siRNA transfection

Transfections were performed with Lipofectamine RNAiMAX (Invitrogen) according to the manufacturer's protocol. The siRNA concentrations were 24 nM for siCUL4A (5-UUCGAAGGACAUCAUGGUUCA-3) and siCUL4B (5'-CAC CGU CUC UAG CUU UCU AA-3') and 8 nM for siDDB1 (5'-UUUAUUAUCGCGAUCUAGUGG-3').

Viability assay

Resazurin was purchased from Alfa Aesar and proliferative activity measured according to the manufacturer's instruction. In brief, 2000 cells per well were seeded into a 96-well plate and 24 h thereafter treated with indicated doses of drugs. After 2 days, resazurin was added to the cells and fluorescence measured after 3 h (LS55 luminescence Spectrometer; Perking Elmer). The proliferative activity was expressed as percentage of treated versus untreated cells and IC_{50}'s were calculated using GraphPad Prism.

Colony formation assay

Cells were treated with increasing doses of cisplatin for 2 h. After the incubation, cells were washed twice with PBS and further incubated in fresh media without drug for 10 days.

Colonies were fixed and stained with 0.25% crystal violet solved in 80% ethanol. Colonies composed of at least 50 cells were counted and surviving fraction was calculated and normalized to untreated control.

LDH release

Cell death was measured using the LDH Cytotoxicity Assay Kit (Pierce). Briefly, 48 h after siRNA transfection, 5000 cells per well were seeded into a 96-well plate. After 24 h, cells were treated with increasing doses of cisplatin for 2 days and released LDH was measured in the supernatant according to the manufacturer's instruction. LDH release was calculated as ratio of released LDH in relation to the maximal LDH activity for each condition and LDH activity expressed as percentage of treated versus untreated cells. IC_{50}'s were calculated using GraphPad Prism.

Immunoblotting

Cells were treated as indicated, washed once with PBS and lysed in RIPA buffer (50 mM Tris-HCl pH 7.0, 1% NP-40, 0.5% sodium deoxycholate, 0.1% SDS, 150 mM NaCl, 2 mM EDTA) complemented with 1 mM N-ethylmaleimide (NEM), 1 mM phenylmethylsulfonyl fluoride, PhosStop (Roche) and Complete protease inhibitor cocktail (Roche) for 10 min on ice. After sonication for 5 cycles (30 sec on, 30 sec off) at 4°C (Biorupture Plus; Diagenode), protein concentration was determined by BCA protein assay (Pierce) according to manufacturer's instruction. Lämmli buffer was added and boiled for 5 min at 98°C. 10 µg of protein was separated on 4-20 % Criterion TGX stain-free precast gels (Bio-Rad) and transferred to nitrocellulose membrane using a Turbo transfer device (Bio-Rad). Membranes were incubated with primary antibodies over night at 4°C followed by incubation with fluorescence labelled secondary antibodies for 30 min. Membranes were developed using Odyssey CLx Imaging System and quantification of protein expression was performed using the Image Studio Lite Software (Li-Core Biosciences).

Cell cycle analysis

Replicative cells were labelled for 3 h with 5-ethynyl-2´-deoxyuridine (EdU, Sigma) and fixed in 1% paraformaldehyde for 10 min. Coupling of the Alexa Fluor 488 azide was performed using Click-iT EdU Flow Cytometry Assay Kits (Invitrogen) according to the manufacturer's instruction. DNA content was quantified by DAPI (4',6-Diamidino-2-

Phenylindole, Dihydrochloride; Life Technologies) staining. Mitotic cells were stained for phospho histone 3 (pSer10) (pH3) for 2 hrs, followed by 1 h secondary antibody incubation using anti-mouse Alexa 647. 10'000 and 50'000 cells per samples were acquired for cell EdU-488 and pH3, respectively with a Fortessa LSR ll flow cytometer and data analyzed using FlowJo.

Immunofluorescence

Cells were grown on glass coverslips in 12-well plates and treated as indicated 3 days after siRNA transfection. After indicated time points, cells were washed with PBS and pre-extraction buffer (25 mM HEPES pH 7.5, 50 mM NaCl, 1 mM EDTA, 3 mM $MgCl_2$, 300 mM sucrose, 0.5 % Triton X-100) was added for 2 min. Cells were fixed with 4% paraformaldehyde in PBS for 10 min and permeabilized with PBS containing 0.2 % Triton X-100 and 3% BSA for 10 min. Coverslips were then washed with 1% BSA in PBS and incubated with primary antibodies diluted in 1% BSA in PBS. Secondary antibodies, diluted in 1% BSA in PBS containing DAPI (4',6-Diamidino-2-Phenylindole, Dihydrochloride; Life Technologies) were added for 30 min at 37°C after washing 3x for 10 min with 1% BSA in PBS. To detect ssDNA, cells were labelled with 25 µM IdU (5-Iodo-2′-deoxyuridine, Sigma) 30 h prior to the treatment. ssDNA was detected by an anti-BrdU antibody under non-denaturating conditions. To quantify total incorporated IdU, DNA was denaturated with 2 M HCl in 0.5 Tween20 for 40 min and washed twice with 0.1 M Na-borate buffer pH 9.0 prior to antibody staining (Huang et al., 2010). Images of immunostained cells were taken with an SP8 confocal microscope (Leica) and analysed with the ImageJ software.

Quantitative reverse transcriptase PCR (qRT-PCR)

To determine the knock-down efficiency, mRNA was extracted three days after siRNA transfection using RNeasy Mini Kit (Qiagen) according to manufacturer's instructions. cDNAn was synthesized from 500 ng mRNA with iScript cDNA synthesis kit from Bio-Rad. Gene specific primers were designed with NCBI Primer-BLAST (Ye et al., 2012) and GAPDH served as internal control. Quantitative PCR was performed using KAPA SYBR Fast qPCR Master Mix (2x) Kit (KAPA Biosystems) according to manufacturer's instructions. The amplification conditions for the Biorad CFX (Bio-Rad) consisted of an initial step of 3 min at 95°C followed by 40 cycles of 3 sec 95°C, 40 sec 60°C. The delta-

delta ct method was used to determine the relative mRNA expression levels between siRNA transfected samples and control samples transfected with non-coding siRNA (Schmittgen and Livak, 2008).

***In vitro* protein dephosphorylation**

HeLa cells were harvested 3 days after siRNA transfection and lysed for 30 min on ice under mild lysis conditions (1% NP-40, 0.5% SDS, complete protease inhibitor cocktail - EDTA free (Roche) followed by sonication for 10 cycles (30 sec on, 30 sec off) at 4°C (Biorupture Plus; Diagenode). Cell lysates were then diluted in CIP buffer (100 mM NaCl, 50 mM Tris-HCl pH 8.0, 10 mM $MgCl_2$, 1 mM DTT, 1x complete protease inhibitor, EDTA free) and complemented with 2 U/µg protein calf intestinal alkaline phosphatase (CIP) (Sigma), and /or 1x phosStop (Roche) and/or 1 mM N-ethylmaleimide (NEM) (known inhibitor of deubiquitinases) (Kapuria et al., 2010). Reactions were incubated for 2 h at 37 °C, then boiled in Lämmli buffer for 5 min and subjected for Western blot analysis as described above.

References

Abbas, T., and Dutta, A. (2011). CRL4 Cdt2: Master coordinator of cell cycle progression and genome stability. Cell Cycle 10, 241–249.

Alexander, J.L., and Orr-Weaver, T.L. (2016). Replication fork instability and the consequences of fork collisions from rereplication. Genes Dev. 30, 2241–2252.

Anantha, R.W., Vassin, V.M., and Borowiec, J.A. (2007). Sequential and Synergistic Modification of Human RPA Stimulates Chromosomal DNA Repair. J. Biol. Chem. 282, 35910–35923.

Arias, E.E., and Walter, J.C. (2006). PCNA functions as a molecular platform to trigger Cdt1 destruction and prevent re-replication. Nat. Cell Biol. 8, 84–90.

Blank, J.L., Liu, X.J., Cosmopoulos, K., Bouck, D.C., Garcia, K., Bernard, H., Tayber, O., Hather, G., Liu, R., Narayanan, U., et al. (2013). Novel DNA Damage Checkpoints Mediating Cell Death Induced by the NEDD8-Activating Enzyme Inhibitor MLN4924. Cancer Res. 73, 225–234.

Brown, J.S., and Jackson, S.P. (2015). Ubiquitylation, neddylation and the DNA damage response. Open Biol. 5, 150018–150018.

Bulatov, E., and Ciulli, A. (2015). Targeting Cullin–RING E3 ubiquitin ligases for drug discovery: structure, assembly and small-molecule modulation. Biochem. J. 467, 365–386.

Byun, T.S. (2005). Functional uncoupling of MCM helicase and DNA polymerase activities activates the ATR-dependent checkpoint. Genes Dev. 19, 1040–1052.

Cavadini, S., Fischer, E.S., Bunker, R.D., Potenza, A., Lingaraju, G.M., Goldie, K.N., Mohamed, W.I., Faty, M., Petzold, G., Beckwith, R.E.J., et al. (2016). Cullin–RING ubiquitin E3 ligase regulation by the COP9 signalosome. Nature 531, 598–603.

Clauson, C., Schärer, O.D., and Niedernhofer, L. (2013). Advances in understanding the complex mechanisms of DNA interstrand cross-link repair. Cold Spring Harb. Perspect. Biol. 5, a012732.

Dantuma, N.P., and van Attikum, H. (2015). Spatiotemporal regulation of posttranslational modifications in the DNA damage response. EMBO J.

Deans, A.J., and West, S.C. (2011). DNA interstrand crosslink repair and cancer. Nat. Rev. Cancer 11, 467–480.

Dobbelstein, M., and Sørensen, C.S. (2015). Exploiting replicative stress to treat cancer. Nat. Rev. Drug Discov. 14, 405–423.

Duda, D.M., Borg, L.A., Scott, D.C., Hunt, H.W., Hammel, M., and Schulman, B.A. (2008). Structural insights into NEDD8 activation of cullin-RING ligases: conformational control of conjugation. Cell 134, 995–1006.

Fischer, E.S., Scrima, A., Böhm, K., Matsumoto, S., Lingaraju, G.M., Faty, M., Yasuda, T., Cavadini, S., Wakasugi, M., Hanaoka, F., et al. (2011). The molecular basis of CRL4 DDB2/CSA ubiquitin ligase architecture, targeting, and activation. Cell 147, 1024–1039.

Garcia, K., Blank, J.L., Bouck, D.C., Liu, X.J., Sappal, D.S., Hather, G., Cosmopoulos, K., Thomas, M.P., Kuranda, M., Pickard, M.D., et al. (2014). Nedd8-Activating Enzyme Inhibitor MLN4924 Provides Synergy with Mitomycin C through Interactions with ATR, BRCA1/BRCA2, and Chromatin Dynamics Pathways. Mol. Cancer Ther. 13, 1625–1635.

Hannah, J., and Zhou, P. (2015). Distinct and overlapping functions of the cullin E3 ligase scaffolding proteins CUL4A and CUL4B. Gene 573, 33–45.

Huang, M., Kim, J.M., Shiotani, B., Yang, K., Zou, L., and D'Andrea, A.D. (2010). The FANCM/FAAP24 Complex Is Required for the DNA Interstrand Crosslink-Induced Checkpoint Response. Mol. Cell 39, 259–268.

Huh, J., and Piwnica-Worms, H. (2013). CRL4CDT2 Targets CHK1 for PCNA-Independent Destruction. Mol. Cell. Biol. 33, 213–226.

Jackson, S., and Xiong, Y. (2009). CRL4s: the CUL4-RING E3 ubiquitin ligases. Trends Biochem. Sci. 34, 562–570.

Jazaeri, A.A., Shibata, E., Park, J., Bryant, J.L., Conaway, M.R., Modesitt, S.C., Smith, P.G., Milhollen, M.A., Berger, A.J., and Dutta, A. (2013). Overcoming platinum resistance in preclinical models of ovarian cancer using the neddylation inhibitor MLN4924. Mol. Cancer Ther. 12, 1958–1967.

Jia, L., Yan, F., Cao, W., Chen, Z., Zheng, H., Li, H., Pan, Y., Narula, N., Ren, X., Li, H., et al. (2017). Dysregulation of CUL4A and CUL4B Ubiquitin Ligases in Lung Cancer. J. Biol. Chem. 292, 2966–2978,.

Jin, J., Arias, E.E., Chen, J., Harper, J.W., and Walter, J.C. (2006). A Family of Diverse Cul4-Ddb1-Interacting Proteins Includes Cdt2, which Is Required for S Phase Destruction of the Replication Factor Cdt1. Mol. Cell 23, 709–721.

Kee, Y., Huang, M., Chang, S., Moreau, L.A., Park, E., Smith, P.G., and D'Andrea, A.D. (2012). Inhibition of the Nedd8 system sensitizes cells to DNA interstrand cross-linking agents. Mol. Cancer Res. 10, 369–377.

Kelland, L. (2007). The resurgence of platinum-based cancer chemotherapy. Nat. Rev. Cancer 7, 573–584.

Kim, Y., and Kipreos, E.T. (2007). Cdt1 degradation to prevent DNA re-replication: conserved and non-conserved pathways. Cell Div. 2, 18.

Klein Douwel, D., Boonen, R.A.C.M., Long, D.T., Szypowska, A.A., Räschle, M., Walter, J.C., and Knipscheer, P. (2014). XPF-ERCC1 Acts in Unhooking DNA Interstrand Crosslinks in Cooperation with FANCD2 and FANCP/SLX4. Mol. Cell 54, 460–471.

Lachaud, C., Moreno, A., Marchesi, F., Toth, R., Blow, J.J., and Rouse, J. (2016). Ubiquitinated Fancd2 recruits Fan1 to stalled replication forks to prevent genome instability. Science 351, 846–849.

Lin, J.J., and Dutta, A. (2007). ATR Pathway Is the Primary Pathway for Activating G2/M Checkpoint Induction After Re-replication. J. Biol. Chem. 282, 30357–30362.

Lin, J.J., Milhollen, M.A., Smith, P.G., Narayanan, U., and Dutta, A. (2010). NEDD8-Targeting Drug MLN4924 Elicits DNA Rereplication by Stabilizing Cdt1 in S Phase, Triggering Checkpoint Activation, Apoptosis, and Senescence in Cancer Cells. Cancer Res. 70, 10310–10320.

Liontos, M., Koutsami, M., Sideridou, M., Evangelou, K., Kletsas, D., Levy, B., Kotsinas, A., Nahum, O., Zoumpourlis, V., Kouloukoussa, M., et al. (2007). Deregulated Overexpression of hCdt1 and hCdc6 Promotes Malignant Behavior. Cancer Res. 67, 10899–10909.

Liu, E., Lee, A.Y.-L., Chiba, T., Olson, E., Sun, P., and Wu, X. (2007). The ATR-mediated S phase checkpoint prevents rereplication in mammalian cells when licensing control is disrupted. J. Cell Biol. 179, 643–657.

Lopez-Martinez, D., Liang, C.-C., and Cohn, M.A. (2016). Cellular response to DNA interstrand crosslinks: the Fanconi anemia pathway. Cell. Mol. Life Sci. 73, 3097–3114.

Lovejoy, C.A., Lock, K., Yenamandra, A., and Cortez, D. (2006). DDB1 Maintains Genome Integrity through Regulation of Cdt1. Mol. Cell. Biol. 26, 7977–7990.

Manthey, K.C., Glanzer, J.G., Dimitrova, D.D., and Oakley, G.G. (2010). Hyperphosphorylation of replication protein A in cisplatin-resistant and -sensitive head and neck squamous cell carcinoma cell lines. Head Neck NA-NA.

Maréchal, A., and Zou, L. (2015). RPA-coated single-stranded DNA as a platform for post-translational modifications in the DNA damage response. Cell Res. 25, 9–23.

Milhollen, M.A., Narayanan, U., Soucy, T.A., Veiby, P.O., Smith, P.G., and Amidon, B. (2011). Inhibition of NEDD8-Activating Enzyme Induces Rereplication and Apoptosis in Human Tumor Cells Consistent with Deregulating CDT1 Turnover. Cancer Res. 71, 3042–3051.

Nawrocki, S.T., Kelly, K.R., Smith, P.G., Espitia, C.M., Possemato, A., Beausoleil, S.A., Milhollen, M., Blakemore, S., Thomas, M., Berger, A., et al. (2013). Disrupting protein NEDDylation with MLN4924 is a novel strategy to target cisplatin resistance in ovarian cancer. Clin. Cancer Res. 19, 3577–3590.

Neelsen, K.J., Zanini, I.M.Y., Mijic, S., Herrador, R., Zellweger, R., Ray Chaudhuri, A., Creavin, K.D., Blow, J.J., and Lopes, M. (2013). Deregulated origin licensing leads to

chromosomal breaks by rereplication of a gapped DNA template. Genes Dev. 27, 2537–2542.

Olson, E., Nievera, C.J., Klimovich, V., Fanning, E., and Wu, X. (2006). RPA2 Is a Direct Downstream Target for ATR to Regulate the S-phase Checkpoint. J. Biol. Chem. 281, 39517–39533.

Pan, W.-W., Zhou, J.-J., Yu, C., Xu, Y., Guo, L.-J., Zhang, H.-Y., Zhou, D., Song, F.-Z., and Fan, H.-Y. (2013). Ubiquitin E3 Ligase CRL4 CDT2/DCAF2 as a potential chemotherapeutic target for ovarian surface epithelial cancer. J. Biol. Chem. 288, 29680–29691.

Pizzolato, J., Mukherjee, S., Schärer, O.D., and Jiricny, J. (2015). FANCD2-associated Nuclease 1, but Not Exonuclease 1 or Flap Endonuclease 1, Is Able to Unhook DNA Interstrand Cross-links in Vitro. J. Biol. Chem. 290, 22602–22611.

Siddik, Z.H. (2003). Cisplatin: mode of cytotoxic action and molecular basis of resistance. Oncogene 22, 7265–7279.

Soucy, T.A., Smith, P.G., Milhollen, M.A., Berger, A.J., Gavin, J.M., Adhikari, S., Brownell, J.E., Burke, K.E., Cardin, D.P., Critchley, S., et al. (2009). An inhibitor of NEDD8-activating enzyme as a new approach to treat cancer. Nature 458, 732–736.

Yamamoto, K.N., Kobayashi, S., Tsuda, M., Kurumizaka, H., Takata, M., Kono, K., Jiricny, J., Takeda, S., and Hirota, K. (2011). Involvement of SLX4 in interstrand cross-link repair is regulated by the Fanconi anemia pathway. Proc. Natl. Acad. Sci. 108, 6492–6496.

Zou, L., and Elledge, S.J. (2003). Sensing DNA Damage Through ATRIP Recognition of RPA-ssDNA Complexes. Science 300, 1542–1548.

Supplementary Material

CRL4 ubiquitin ligase promotes Fanconi anemia pathway-induced single-stranded DNA signaling at interstrand crosslinks

Tamara Codilupi, Doreen Taube and Hanspeter Naegeli

Institute of Pharmacology and Toxicology, University of Zurich-Vetsuisse,
Winterthurerstrasse 260, 8057 Zurich

Corresponding author: Hanspeter Naegeli (naegelih@vetpharm.uzh.ch)

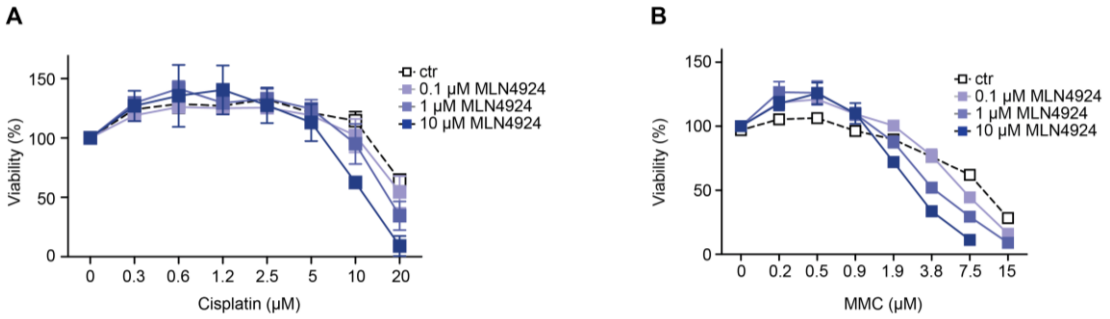

Figure S1. CRL inhibition potentiates ICL cytotoxicity in Skov3 cells
Skov3 cells were incubated for 48 h with increasing concentrations of **A)** cisplatin or **B)** mitomycin C (MMC) in combination with the indicated concentrations of MLN4924. Cell viability is expressed as the percentage of control values obtained in the absence of cisplatin (N =3 experiments, error bars show s.e.m.).

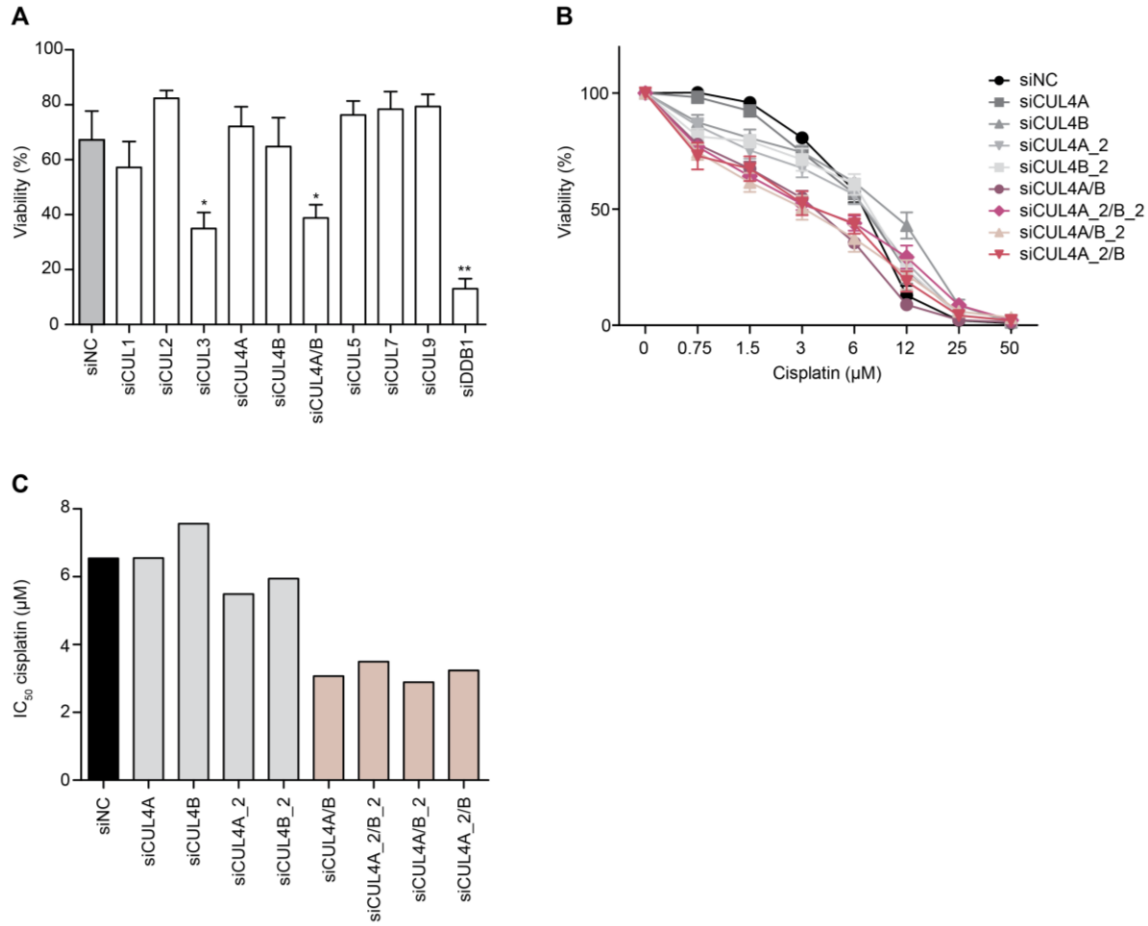

Figure S2. Screen for cullin targets mediated hypersensitivity to cisplatin
A) HeLa cells were transfected with siRNA to down regulate the indicated cullins or DDB1. Control reactions contained cells transfected with non-coding RNA (siNC). The cells were incubated with 5 µM cisplatin and cell viability is expressed as the percentage of control values obtained in the absence of cisplatin (N = 3-5; error bars show s.e.m.). Asterisks indicate significantly lower viability in depleted cells relative to non-coding controls (*P < 0.05 and **P <

0.005, unpaired two-tailed t-test). **B)** Two different siRNAs for CUL4A and CUL4B were used either alone or in combination to inhibit the CRL4 complex in HeLa cells. Transfected cells were incubated with the indicated concentrations of cisplatin and viability testeded after 48 hours by Alamar blue assay; error bars show s.e.m. **C)** IC_{50} values of cisplatin calculated from panel B.

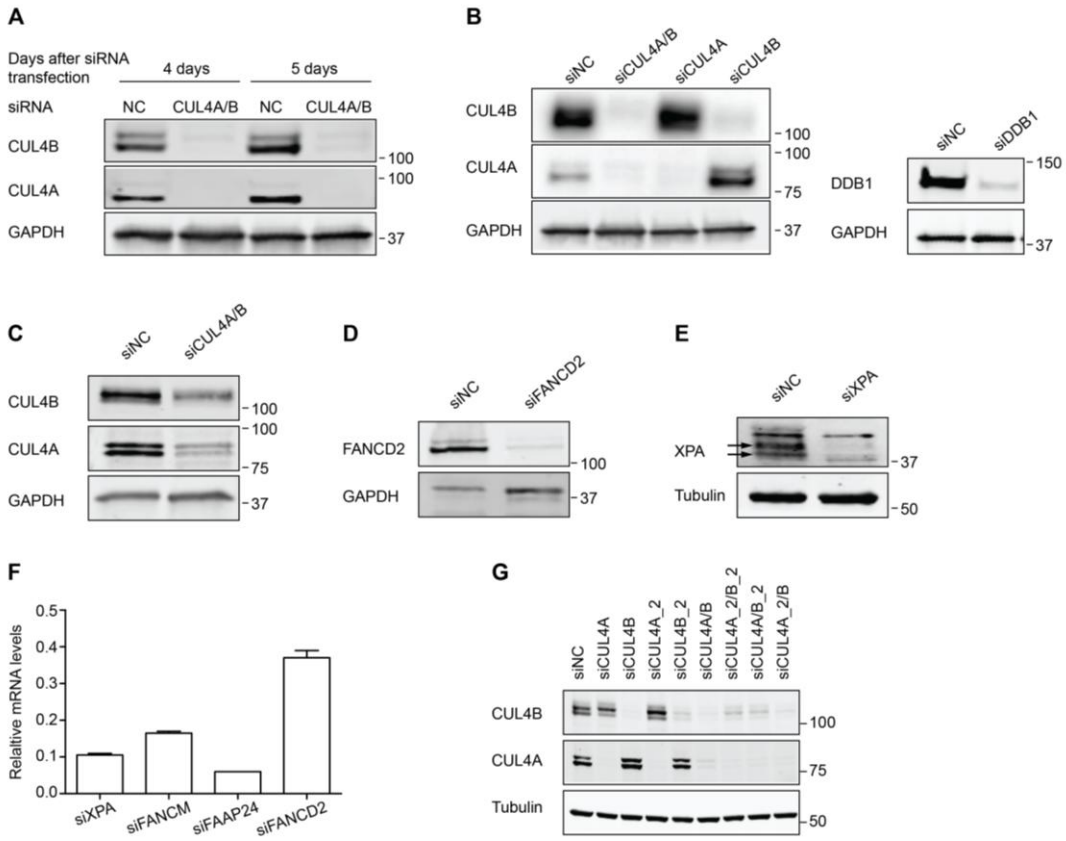

Figure S3. Protein down regulation after siRNA transfections

A) Immunoblots demonstrating the depletion of CUL4A and CUL4B at the indicated times after siRNA transfections. GAPDH was used as the loading control. **B)** CUL4A/B and DDB1 levels in HeLa cells 3 days after transfection with the indicated siRNA reagents. **C)** CUL4A/B levels in Skov3 cells 4 days after transfection with the indicated siRNA reagents. **D)** FANCD2 levels in HeLa cells 4 days after transfection with the indicated siRNA reagents. **E)** Levels of XPA (migrating as a double band) in HeLa cells 4 days after transfection with the indicated siRNA reagents. **F)** Residual XPA, FANCM, FAAP25 and FANCD2 mRNA levels (compared to siNC controls) quantified by qRT-PCR 3 days after siRNA transfection of HeLa cells. GAPDH was used as internal standard. **G)** Knock down levels CUL4A and CUL4B three days after the indicated siRNA transfections.

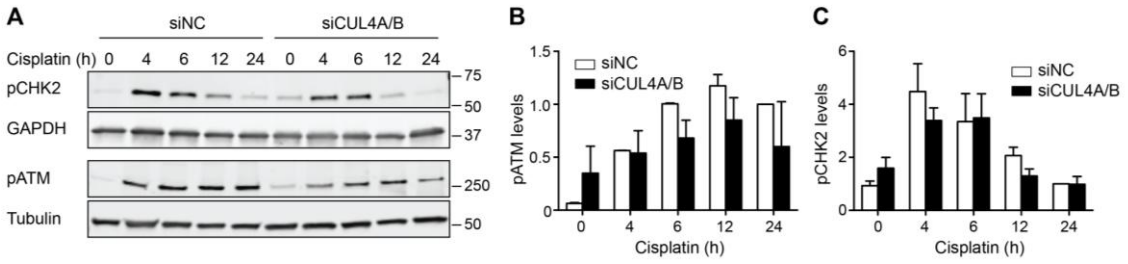

Figure S4. Poor activation of the ATM-CHK2 pathway

A) Representative immunoblot showing changes of phosphorylated ATM (pATM) and phosphorylated CHK2 (pCHK2) relative to tubulin used as the loading control. HeLa cells were depleted of CUL4A/B as indicated and incubated with 20 µM cisplatin for different time periods. **B)** Quantification of pATM levels normalized to tubulin in HeLa cells challenged with 20 µM cisplatin. Values are expressed relative to the pATM levels in the 24 h-treated control cells (N = 3); none of the differences were statistically significant (unpaired two-tailed t-test). **C)** Quantification of pCHK2 levels normalized to tubulin in HeLa cells challenged with 20 µM cisplatin. Values are expressed relative to the pCHK2 levels in the 24 h-treated control cells (N = 3-5); none of the differences were statistically significant.

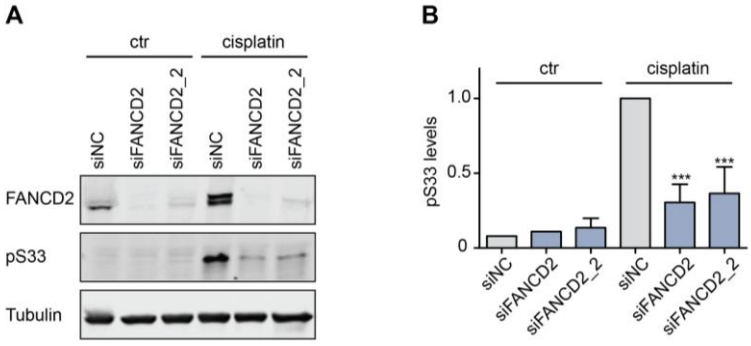

Figure S5. FANCD2 depletion impairs RPA2 phosphorylation

A) FANCD2 was depleted in HeLa cells using two different siRNAs, siFANCD2 and siFANCD2_2 and exposed to 5 µM cisplatin for 24 h. Whole cell lysates were probed in immunoblots with the phospho-specific antibody against pS33. Tubulin served as the loading control. **B)** Quantification of pS33 levels normalized to tubulin. Values are expressed relative to cisplatin-exposed control cells (siNC) (N = 3; ***P < 0.0005, unpaired two-tailed t-test).

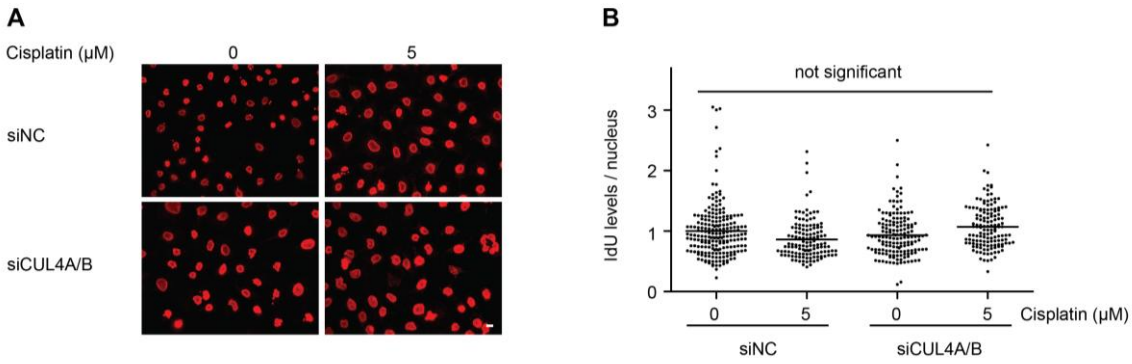

Figure S6. Immunofluorescence control with ssDNA-specific antibody

A) Representative images demonstrating that differences in fluorescence intensity are not due to changes in the efficiency of IdU incorporation, as the antibody yielded identical immunofluorescence signals after DNA denaturation, which converts all double-stranded to ssDNA conformations. HeLa cells were transfected with the indicated siRNA and labeled for 30 h with IdU before genotoxic treatment, which consisted of a 24-h exposure to cisplatin. Control cells were mock-treated. For the detection of ssDNA, the cells were fixed and stained with anti-IdU antibodies after denaturation. **B)** Quantification of mean nuclear fluorescence obtained after DNA denaturation (N = 200 nuclei). Horizontal lines represent median values. The statistical analysis carried out by 1-way ANOVA according to Kruskal-Wallis revealed no significant differences between treatments.

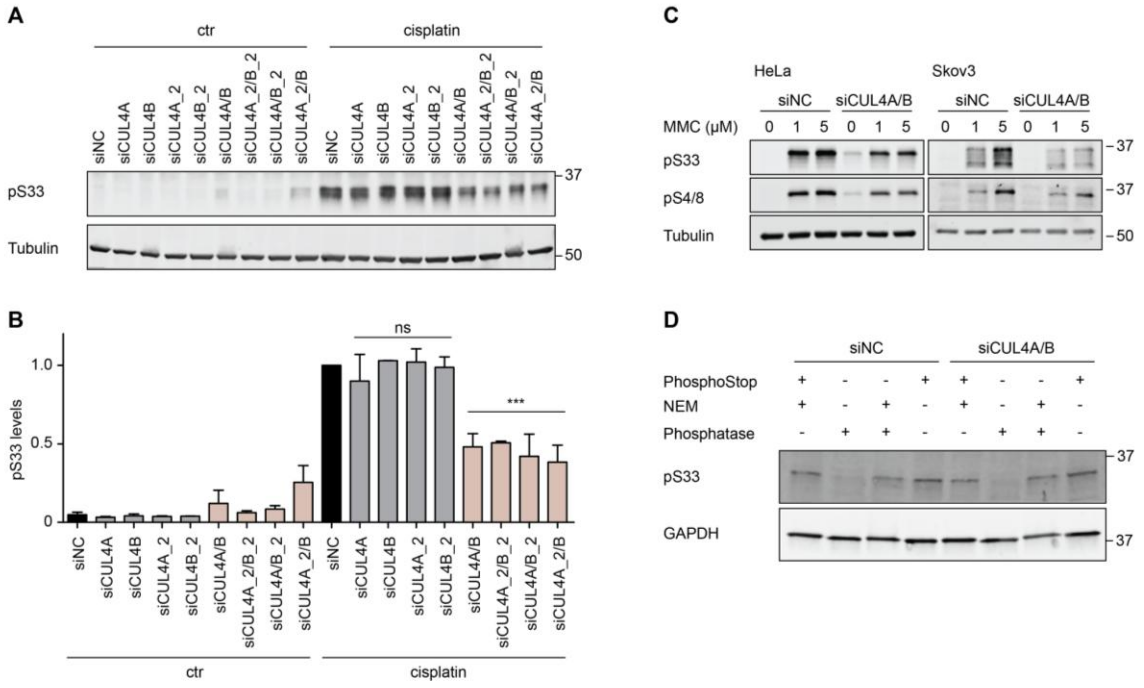

Figure S7. Impaired RPA phosphorylation in CRL4-deficient cells

A) HeLa cells were depleted for CUL4A and CUL4B using two distinct siRNA sequences for each protein, siCUL4A, siCUL4A_2, siCUL4B, siCUL4B_2, either alone or in combination. Transfected cells were exposed to 5 μM cisplatin for 24 h. Whole cell lysates were probed in immunoblots with the phospho-specific antibody pS33. Tubulin serves as the loading control. **B)** Quantification of pS33 levels normalized to tubulin. Values are expressed relative to pS33 levels of control cells (siNC) exposed to 5 μM cisplatin (N = 3); asterisks indicate significant lower levels of pS33 in CUL4A/B co-depleted cells relative to non-coding controls, whereas single depleted cells show no significant differences relative to siNC controls (***P < 0.0005, unpaired two-tailed t-test). **C)** HeLa or Skov3 cells were transfected with siCUL4A/B, or with siNC, and incubated for 24 h with 1 or 5 μM MMC. Whole cell lysates were probed in immunoblots with phospho-specific antibodies against pS33 and pS4/8. Tubulin served as the loading control. **D)** Control immunoblot demonstrating the susceptibility of pS33 to dephosphorylation by phosphatase treatment. PhosphoStop, phosphatase inhibitor. NEM, N-ethylmaleimide.

Supplementary Table 1. List of antibodies with working dilutions

antibody	source	company	Catalog No.	dilutions WB	IF	FC
alpha-Tubulin	mouse	Sigma	T5168	1:10'000		
pATM (pS1981)	rabbit	Abcam	81292	1:10,000		
pATR (pS428)	rabbit	Santa Cruz	109912	1:100		
BrdU (IdU)	mouse	BD Biosciences	347580		1:200	
CDT1	rabbit	Cell Signaling	8064	1:1000		
Chk1 (D-7)	mouse	Santa Cruz	377231	1:200		
pChk1 (pS345) (133D3)	rabbit	Cell Signaling	2348P	1:1000		
pChk2 (pThr68)	rabbit	Cell Signaling	2661P	1:1000		
CUL4A	rabbit	Thermo Scientific	PA5-17101	1:1000		
CUL4B	rabbit	Sigma	HPA011880	1:200		
DDB1	mouse	BD Biosciences	612488	1:1000		
FANCD2	rabbit	Abcam	108928	1:5000		
GAPDH	mouse	Abcam	9484	1:40'000		
pHistone H2A.X (pS139)	mouse	Millipore	05-636		1:1000	
pHistone H3 (pS10) (K.872.3)	mouse	Thermo Scientific	MA5-15220			1:100
RPA2 / RPA2	rat	Cell Signaling	2208	1:1000	1:200	
pRPA2 (pS33)	rabbit	Novus Biologicals	NB100-544	1:5000	1:1000	
pRPA2 (pS4/S8)	rabbit	Abcam	87277	1:1000	1:500	
XPA (FL273)	rabbit	Santa Cruz	853	1:100		

Supplementary Table 2. List of siRNA sequences.

Target	Sequence (5' - 3')	Source
non-coding (NC)	AAUUCUCCGAACGUGUCACGU	Qiagen
CUL1	AACGTAGTTATCAGCGATTCA	Qiagen
CUL2	CGGCACAATGCCCTTATTCAA	Qiagen
CUL3	AACAACTTTCTTCAAACGCTA	Qiagen
CUL4A	UUCGAAGGACAUCAUGGUUCA	Microsynth
CUL4A_2	AGCGATCGTAATCAATCCTGA	Qiagen
CUL4B	CACCGUCUCUAGCUUUCUAA	Qiagen
CUL4B_2	TTGGAGCCGTTAGGAAGATTA	Qiagen
CUL5	TACGAGCAGTAAACTTGCCAA	Qiagen
CUL7	AACCCAAGAGUUUGAUUAUAAAA	Microsynth
CUL9	AACCACAUCCUCUGAAGAACACU	Microsynth
DDB1	UUUAUUAUCGCGAUCUAGUGG	Qiagen
FANCM	AAGCUCAUAAAGCUCUCGGAA	Microsynth
FANCD2	UUGGAGGAGAUUGAUGGUCUA	Microsynth
FANCD2_2	CGGCTTCTCGGAAGTAATTTA	Qiagen
FAAP24	CCGGAUGAGUGAACAAUACUU	Microsynth
XPA	GCUACUGGAGGCAUGGCUA	Microsynth

Supplementary Table 3. List of primer sequences.

Target	Sequence (5' - 3')
FANCM_Fw	ACCAGGTAGTGATATAAAGGCTGT
FANCM_Rev	CTCTCCCTCGATTATGCCTTGT
FAAP24_Fw	GGATGGCTTGACACCAGACT
FAAP24_Rev	ACTGGGCTCTTTGGTTTGCT
FANCD2_Fw	TTCCGAGAGCTGGACATTGA
FANCD2_Rev	TGGCAATAGGAGGTGTCAGC
XPA_Fw	GGCGAGTATCGAGCGGAAG
XPA_Rev	TGAAGCCTCCTCCTGTGTCA

Quantitative reverse transcriptase-PCR (qRT-PCR)

To determine the knock down efficiency, mRNA was extracted 3 days after siRNA transfection using the RNeasy Mini Kit (Qiagen) according to the manufacturer's instructions. Therafter, cDNA was synthesized from 500 ng mRNA with the iScript cDNA synthesis kit from Bio-Rad. Gene specific primers were designed using the NCBI Primer-BLAST (Ye et al., 2012) and GAPDH served as the internal control. Quantitative PCR was performed using the KAPA SYBR Fast qPCR Master Mix (2x) kit (KAPA Biosystems) according to the manufacturer's instructions. The amplification conditions in the Bio-Rad CFX instrument consisted of an initial step of 3 min at 95°C followed by 40 cycles of 3 sec at 95°C and 40 sec at 60°C. The delta-delta ct method was used to determine relative mRNA expression levels between siRNA-transfected samples and control samples transfected with non-coding siRNA (Schmittgen and Livak, 2008).

In vitro protein dephosphorylation

HeLa cells were harvested 3 days after siRNA transfections and lysed for 30 min on ice under mild lysis conditions [1% NP-40 (wt/wt), 0.5% SDS (wt/wt), complete protease inhibitor cocktail - EDTA-free (Roche)] followed by sonication for 10 cycles (30 sec on, 30 sec off) at 4°C (Biorupture Plus, Diagenode). Cell lysates were then diluted in CIP buffer (100 mM NaCl, 50 mM Tris-HCl, pH 8.0, 10 mM $MgCl_2$, 1 mM DTT, complete protease inhibitor cocktail - EDTA-free) and complemented with calf intestinal alkaline phosphatase (2 U/µg of protein , Sigma), and / or phosStop (Roche) and / or 1 mM N-ethylmaleimide (NEM) (inhibitor of deubiquitinases) (Kapuria et al., 2010). Reactions

were incubated for 2 h at 37°C, boiled in Lämmli buffer for 5 min and subjected to Western blot analysis.

References

Schmittgen, T.D., and Livak, K.J. (2008). Analyzing real-time PCR data by the comparative CT method. Nat. Protoc. 3, 1101–1108.

Ye, J., Coulouris, G., Zaretskaya, I., Cutcutache, I., Rozen, S., and Madden, T.L. (2012). Primer-BLAST: a tool to design target-specific primers for polymerase chain reaction. BMC Bioinformatics 13, 134.

3.2 The CHD1 remodeler promotes XPC to TFllH handoffs on nucleosomes during DNA repair of UV lesions

*Peter Rüthemann‡, Chiara Balbo Pogliano‡, Tamara Codilupi, Zuzana Garajovà and Hanspeter Naegeli**

Institute of Pharmacology and Toxicology, University of Zurich-Vetsuisse, Winterthurerstrasse 260, 8057 Zurich, Switzerland

*Corresponding author: naegelih@vetpharm.uzh.ch

‡These authors contributed equally to this work as first authors

Running title: CHD1 promotes XPC to TFIIH handoffs

Manuscript in revision.

This chapter describes the function of the chromatin remodeler CHD1 in the recognition step of UV-lesions during GG-NER. I contributed to the design and execution of the experiments.

Abstract

Ultraviolet (UV) light induces mutagenic cyclobutane pyrimidine dimers (CPDs) embedded in chromatin, where the DNA helix is wrapped around histone octamers forming nucleosomes. How global-genome nucleotide excision repair (GG-NER) processes CPDs despite this chromatin arrangement is poorly understood. A role for the chromatin remodeler known as chromodomain helicase DNA-binding 1 (CHD1) in the DNA damage response is indicated by its increased chromatin association upon UV exposure. Immunoprecipitations of chromatin fragments revealed that CHD1 co-localizes in part with GG-NER factors. Chromatin fractionations showed that the recruitment of CHD1 occurs to UV lesions in histone-assembled DNA of nucleosomes and that this UV-dependent CHD1 relocation requires the xeroderma pigmentosum group C (XPC) sensor. In situ immunofluorescence analyses further disclosed that CHD1 facilitates the substrate handover from XPC to the downstream transcription factor IIH (TFIIH). Accordingly, CHD1 stimulates CPD excision and protects from UV-induced cytotoxicity. The finding that a CHD1-driven handoff between sequential GG-NER factors takes place on the histone octamers of nucleosomes suggests that chromatin provides a recognition scaffold enabling the detection of a subset of CPDs.

Keywords: Chromatin remodeling / DNA damage / Nucleosomes / Skin cancer / UV light

Introduction

Genomic DNA is susceptible to damage caused by a plethora of endogenous or environmental genotoxic agents. In particular, bulky base lesions induced by ultraviolet (UV) light and the consequent accumulation of mutations are the major cause of skin cancer (Mouret *et al*, 2011; Marteijn *et al*, 2014; DiGiovanna & Kraemer, 2012). UV irradiation of DNA gives rise to cyclobutane pyrimidine dimers (CPDs) and 6-4 photoproducts (6-4PPs) in a ratio of ~3:1 (Kobayashi *et al*, 2001). The quantitatively predominant CPDs are distributed evenly in chromatin and arise abundantly in nucleosome cores where the DNA is wrapped around histone octamers (Smerdon & Conconi, 1999; Zavala *et al*, 2014; Han *et al*, 2016). Nucleotide excision repair (NER) is the versatile process that removes these UV lesions as well as other bulky base adducts elicited by chemical carcinogens or oxygen radicals. Depending on their genomic location, bulky lesions are sensed by two alternative mechanisms. In the template strand of transcribed genes, detection of DNA damage occurs when the elongating RNA polymerase II encounters obstructing lesions (Hanawalt & Spivak, 2008; Vermeulen & Fousteri, 2013). Conversely, global-genome NER (GG-NER) detects bulky DNA adducts anywhere in the genome independently of transcription (Sancar, 1996; Hoeijmakers, 2009; Schärer, 2013). Genetic defects in the latter pathway result in the cancer-prone syndrome xeroderma pigmentosum (XP) with patients being classified into complementation groups (XP-A through XP-G) reflecting mutations in distinct repair genes (Friedberg *et al*, 2006).

The GG-NER reaction relies on a trimeric complex consisting of XPC, RAD23B (a human homolog of yeast RAD23) and centrin 2 to initially sense the presence of bulky lesions in the DNA double helix (Sugasawa *et al*, 1998; Araki *et al*, 2001; Volker *et al*, 2001). The DNA-binding function of this initiator complex resides entirely with the XPC subunit that, for the recognition of CPDs, is additionally supported by UV-damaged DNA-binding (UV-DDB) protein, also known as DDB1-DDB2 heterodimer (Hwang *et al*, 1999; Wakasugi *et al*, 2001; Rapic-Otrin, 2002; Fitch *et al*, 2003). The XPC subunit mediates recruitment of the transcription factor IIH (TFIIH) complex, which contains the XPD helicase that scans DNA for damage verification and unwinds the double helix by 20-25 nucleotides around the lesion (Evans *et al*, 1997; Riedl *et al*, 2003; Compe & Egly, 2016). The transiently unwound state is then stabilized by XPA in conjunction with replication protein A (RPA) (Li *et al*, 2015), until the endonucleases XPG and XPF/ERCC1 (a heterodimer of XPF and excision repair cross-complementing 1) incise the damaged strand

on each side of the unwound duplex to remove damaged bases as part of an excised oligonucleotide (Araújo *et al*, 2000; Reardon & Sancar, 2003; Staresincic *et al*, 2009). The remaining single-stranded gap is filled by DNA synthesis and closed by DNA ligation (Ogi *et al*, 2010; Moser *et al*, 2007). To allow for repair despite compaction of the DNA substrate in chromatin, this multi-step process involves the temporary release of histones from damaged DNA (Adam *et al*, 2016) but how these chromatin rearrangements take place is not yet understood.

Members of distinct families of ATP-dependent remodelers have been implicated in relaxing histone-DNA interactions to prime chromatin for GG-NER activity (Czaja *et al*, 2012; Peterson & Almouzni, 2013). A pioneer study in yeast indicated that switch/sucrose non-fermenting (SWI/SNF) stimulates GG-NER activity in transcriptionally silent loci (Gong *et al*, 2006). In higher eukaryotes, UV-DDB has been shown to recruit at least three chromatin remodelers, i.e., brahma-related gene 1 (BRG1, a catalytic subunit of SWI/SNF) (Zhang *et al*, 2009; Zhao *et al*, 2009), amplified in liver cancer 1 (ALC1) (Pines *et al*, 2012) and inositol requiring 80 (INO80) (Jiang *et al*, 2010). In a further study, however, INO80 was not required for chromatin remodeling before initiating GG-NER activity, but for the restoration of nucleosome repeats after DNA repair (Sarkar *et al*, 2010). In addition, the mammalian SWI/SNF subunit SNF5 (for sucrose non-fermenting 5) interacts with XPC protein and its deletion causes UV hypersensitivity (Klochendler-Yeivin *et al*, 2006; Ray *et al*, 2009), although these results were challenged by another study where no effect of SNF5 on UV sensitivity was detected (McKenna *et al*, 2008). The above reports all suggest that chromatin remodelers facilitate GG-NER activity although the underlying mechanisms are lacking (Aydin *et al*, 2014). The basic conundrum remains whether chromatin relaxation precedes DNA lesion detection or vice versa (Rubbi & Milner, 2003). It is also not known if remodelers are recruited to unfold nucleosomes for the access of GG-NER factors to DNA, or rather promote the assembly of repair complexes, or their release from DNA, after chromatin relaxation by other mechanisms. In addition, previous reports on BRG1 and SNF5 show that chromatin remodelers may assist the GG-NER reaction by activating cell cycle checkpoints (Ray *et al*, 2009; Zhang *et al*, 2013) or that their depletion may lead to apoptosis, which attenuates GG-NER activity (Gong *et al*, 2008).

Chromodomain helicase DNA-binding 1 (CHD1) supports chromatin plasticity crucial for the pluripotency of embryonic stem cells, for transcriptional reprogramming and for homologous recombination (Park *et al*, 2014; Gaspar-Maia *et al*, 2009; Piatti *et al*, 2015;

Kari *et al*, 2016). The genome-wide range of these known CHD1 functions prompted us to test whether this same remodeler is also involved in chromatin dynamics required for GG-NER activity. We found that, in UV-damaged chromatin, CHD1 stimulates the handover between XPC protein and the TFIIH complex at DNA lesion sites. To facilitate this substrate handover, XPC protein recruits CHD1 directly to nucleosome cores indicating that the XPC subunit is able to form lesion recognition intermediates with a subset of damage positioned around histone octamers. The main implication of this unexpected mechanism is that, rather than always representing a barrier impeding the accessibility to damaged DNA, nucleosomes play a scaffolding role in priming specific lesions for the GG-NER reaction.

Results

CHD1 co-localizes in chromatin with GG-NER factors

We tested whether CHD1 translocates to the chromatin of human cells upon exposure to UV-C light. For that purpose, HeLa cells were UV-irradiated or mock-treated and collected after different incubation times. For the detection of chromatin recruitments, the cells were lysed in the presence of 0.3 M NaCl to extract, into the supernatant, free proteins that are not associated with chromatin or only loosely bound to chromatin. The remaining pellet contains chromatin-bound proteins (Fei *et al*, 2011). After measuring protein concentrations in each fraction, 25 µg of free proteins and 15 µg of chromatin-bound proteins were separated by gel electrophoresis and analyzed by immunoblotting. The validity of this approach to monitor UV-dependent redistributions is demonstrated by the strong relocation to chromatin of DDB2 observed 1 h after irradiation (Fig 1A), in line with the expected association of this recognition subunit with UV lesions (Otrin *et al*, 1997; Yeh *et al*, 2012). The immunoblot of Fig. 1A also reproduces the well-described degradation of DDB2 in response to UV exposure (Rapic-Otrin, 2002), which is apparent after the 3- and 6-h incubation periods. In addition, the UV treatment led to a modest increase of CHD1 in the fraction of chromatin-bound proteins over the normal presence of this remodeler in the chromatin of unchallenged cells. The immunoblot quantifications using histone H3 as the internal standard revealed that the level of CHD1 in chromatin is increased by ~40% at 1 h after UV irradiation compared to unirradiated controls (Fig 1B).

To test whether this CHD1 recruited to chromatin upon UV radiation co-localizes with GG-NER factors, we transiently transfected HEK293 cells with a construct that drives

overexpression of the DDB2 subunit of the UV-DDB heterodimer fused to the FLAG peptide. HEK293 cells were used for this experiment because of their permissivity to DNA transfections. The purpose of this approach was to exploit the tight binding of DDB2 protein to UV-damaged DNA and, concomitantly, its transient interactions with the core GG-NER factors XPC and XPA (Sugasawa *et al*, 2005; Wakasugi *et al*, 2009). These two factors, in turn, associate with each other and with the TFIIH complex comprising the XPD helicase (Nocentini *et al*, 1997; Yokoi *et al*, 2000; Uchida *et al*, 2002; Bunick *et al*, 2006). The DDB2-FLAG fusion protein was, therefore, used as a molecular bait to isolate short chromatin fragments containing UV lesions and GG-NER factors and to test whether CHD1 co-localizes with these nucleoprotein complexes.

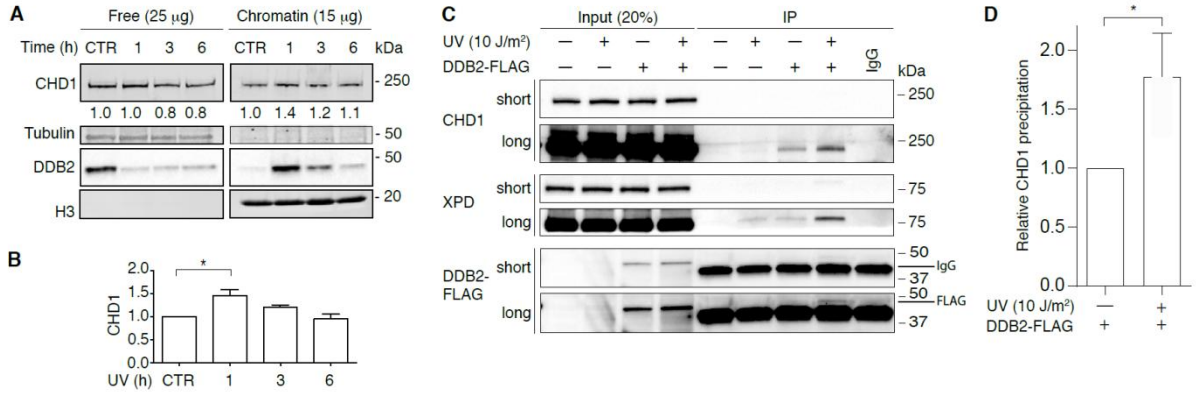

Figure 1 - CHD1 co-localizes in chromatin with GG-NER proteins.

A Chromatin recruitment of DDB2 and CHD1. The chromatin of HeLa cells was salt-extracted at different times after exposure to UV-C light (10 J/m^2). Free proteins in the supernatant (25 µg per sample) and chromatin-bound proteins in the pellet (15 µg per sample) were analyzed by gel electrophoresis and immunoblotting. CHD1 (197 kDa) migrates to a position just below the 250-kDa marker; tubulin and histone H3 were loading controls for the free and chromatin-associated fraction, respectively. CTR, mock-treated control cells. Numbers indicate the relative quantity of free CHD1 (normalized to tubulin) and chromatin-bound CHD1 (normalized to H3), whereby the respective CHD1 levels in unirradiated cells are set to 1.

B Quantification of chromatin-bound CHD1 normalized to H3 (n = 5 independent experiments). The CHD1 level in the chromatin of unirradiated cells is set to 1.

C Co-localization of CHD1 with GG-NER factors in the chromatin of UV-irradiated cells. HEK293 cells were transfected with a vector for expression of FLAG-tagged DDB2 and treated with UV light (10 J/m^2). After a 1-h incubation, the chromatin was salt-extracted and, following fragmentation by MNase digestion, dissolved by sonication. The resulting chromatin fragments were precipitated with anti-FLAG antibodies, thus exploiting the FLAG tag to isolate nucleoprotein complexes containing DDB2. Input chromatin fractions and immunoprecipitated nucleoprotein complexes were analyzed by blotting with antibodies

against CHD1, DDB2 and XPD (short and long exposures are shown). IgG, immunoglobulin G heavy chains interfering with the detection of DDB2-FLAG.

D Quantified CHD1 levels co-localizing in fragmented chromatin with NER factors, normalized to the amount of CHD1 in the respective input fractions (n = 3 independent experiments).

Data information: In B and D, data are presented as mean ± SEM. *P ≤ 0.05 (one-sample t-test with a hypothetical value of 1).

After pre-extraction with 0.3 M NaCl, chromatin was dissected by digestion with saturating amounts of micrococcal nuclease (MNase), which cleaves DNA preferentially in linker segments spacing the nucleosome cores (Fig EV1). Finally, the fragmented chromatin was solubilized by sonication before carrying out precipitations taking advantage of anti-FLAG antibodies (Fig 1C). This immunoprecipitation of short chromatin fragments from UV-irradiated cells resulted in the co-fractionation of both CHD1 and XPD (a core NER subunit). Much less DDB2, CHD1 and XPD was immunoprecipitated from the chromatin of cells that were not subjected to UV radiation or not previously transfected with the DDB2-FLAG-expressing construct. The quantification of CHD1 levels in immunoprecipitated complexes, using CHD1 in the respective input fractions as the reference, highlights its redistribution in response to UV radiation (Fig 1D). Collectively, the UV-dependent CHD1 recruitment to chromatin (Fig 1A) and its co-localization with short chromatin fragments containing GG-NER factors (Fig 1C) led to the hypothesis that CHD1 may contribute to GG-NER activity.

CHD1 is recruited to UV-damaged nucleosome cores

The observed redistribution of CHD1 protein to chromatin sites containing GG-NER factors prompted us to use U2OS and HeLa cells to delineate the exact positions to which CHD1 moves after UV radiation. As above, free proteins that are not or only loosely associated with chromatin were removed by salt (0.3 M NaCl) extraction and the remaining chromatin was dissected by incubation with MNase. At a saturating level of this nuclease, the genome is totally converted to short DNA segments of 147-base pairs (Fig 2A). The size of these residual fragments corresponds to the DNA length of nucleosome cores protected from MNase digestion by interactions with histone octamers. Thus,

saturating MNase digestions reduce the entire chromatin to nucleosome cores by eliminating all internucleosomal linker DNA segments.

Analysis of defined proportions of the different fractions from U2OS cells showed that most CHD1 is actually found in the unbound state as free protein extracted with buffer containing 0.3 M NaCl (Fig 2B, top panel). The subsequent MNase digestion of pre-extracted chromatin generates a soluble supernatant of proteins released from chromatin that also includes some dissociated nucleosome cores containing *inter alia* histone H3 but no CHD1 protein (Fig 2B, middle panel). However, the vast majority of nucleosome cores remains in a condensed and, hence, insoluble form even after digestion with saturating MNase concentrations (Fig EV1). We observed that a proportion of CHD1 protein is immobilized in this nucleosome core-enriched fraction upon UV irradiation (Fig 2B, bottom panel). This UV-dependent recruitment of CHD1 to nucleosome cores is observed around 1 h after UV irradiation but, subsequently, CHD1 disappears from this chromatin localization within 6 h after UV treatment (Fig 2C). A transient recruitment of CHD1 to nucleosome cores, *i.e.*, to the insoluble fraction of MNase-digested chromatin is also observed in HeLa cells (Fig 2D). This UV-dependent CHD1 recruitment is less pronounced in HeLa than in U2OS cells but follows similar kinetics with an increased occupancy of nucleosome cores detected at 1 h following UV irradiation, but not at the later time points after the UV pulse.

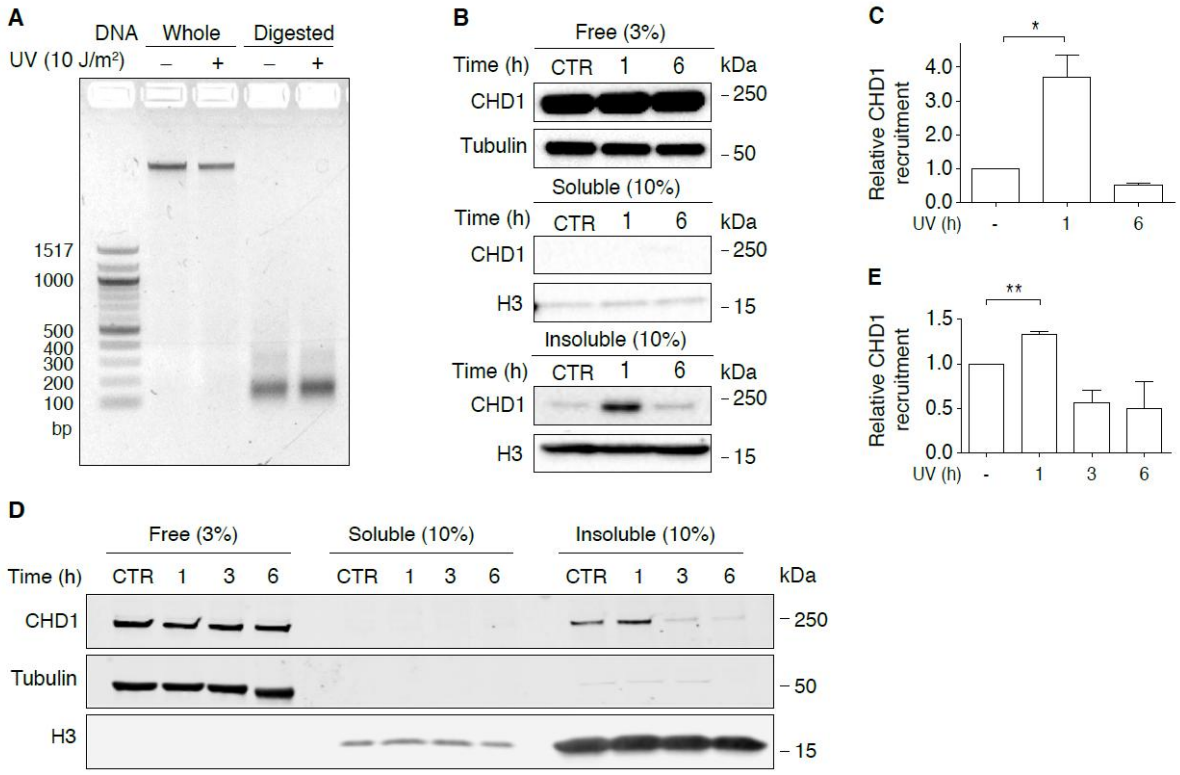

Figure 1 - CHD1 is recruited to nucleosome cores upon UV irradiation.

A The chromatin of U2OS cells, untreated or UV-irradiated (10 J/m^2), was fragmented by MNase digestion (4 U/µl). A subsequent agarose gel analysis demonstrates the complete breakdown of internucleosomal linker DNA segments resulting in residual chromatin containing exclusively nucleosome core fragments of 147 base pairs. Whole, undigested chromatin. Digested, MNase-fragmented chromatin.

B Upon UV irradiation, CHD1 is transiently recruited to nucleosome cores. The chromatin of U2OS cells (harvested 1 or 6 h after the UV pulse) was salt-extracted and MNase-digested (4 U/µl) to generate, as shown in the three panels from top down, a fraction of free (or loosely chromatin-bound) proteins, a fraction of MNase-solubilized chromatin proteins and a fraction of condensed and, hence, insoluble nucleosome cores. CTR, unirradiated control. Histone H3 and tubulin serve as the loading standards. The proportion of each fraction loaded onto the gel (3% or 10%) is indicated in parenthesis.

C Quantification of CHD1 recruitment to the insoluble fraction of nucleosome cores of U2OS cells, normalized to the H3 level, following 1 and 6 h after UV irradiation (n = 4 independent experiments). The amount of CHD1 in the nucleosome core fraction of control cells was set to 1.

D Same experiment as in panel B using HeLa cells. The UV-dependent recruitment of CHD1 to the insoluble fraction of nucleosome cores is confirmed but less pronounced than in U2OS cells. The chromatin was analyzed at 1, 3 and 6 h after the UV pulse.

E Quantification of CHD1 recruitment to the insoluble fraction of nucleosome cores of HeLa cells, normalized to the H3 level, following 1, 3 and 6 h after UV irradiation (n = 3 independent experiments). The amount of CHD1 in the nucleosome core fraction of control cells was set to 1.

Data information: In C and E, data are presented as mean ± SEM. *P ≤ 0.05, **P ≤ 0.01 (one-sample t-test with a hypothetical value of 1).

XPC-dependent recruitment of CHD1 to nucleosomes

Next, different GG-NER factors were depleted in HeLa cells by transfection with short interfering RNA (siRNA) to understand the mechanism by which CHD1 is relocated to nucleosome cores. The efficiency of each siRNA-mediated down regulation is demonstrated by immunoblotting (Fig EV2). These depletion experiments revealed that the UV-dependent recruitment of CHD1 to nucleosome cores, observed 1 h after UV irradiation, was essentially abolished by depletion of XPC protein (Fig 3A). Consistent with this dependence on the XPC subunit, we confirmed as previously reported (Fei *et al*, 2011) that XPC protein itself effectively binds this same nucleosome core fraction around 1 h after the UV challenge (Fig 3B). Depletion of DDB2, an accessory subunit that is active in the GG-NER pathway upstream of XPC, does not detectably reduce the UV-dependent relocation of CHD1 protein to this MNase-insoluble fraction of nucleosome cores. Similarly, depletion of XPA, a core subunit acting in the GG-NER pathway downstream of XPC, does not influence the UV-dependent relocation of CHD1 to nucleosome cores (Fig 3C).

The above results indicated that XPC protein mediates the recruitment of CHD1 to UV lesions, implying that XPC and CHD1 interact transiently in UV-irradiated cells. To test this prediction, HeLa cells were UV-exposed and, 1 h later, their chromatin was collected, MNase-fragmented and solubilized by sonication as described for the experiments of Fig 1C. In this case, however, immunoprecipitations were carried out with anti-XPC antibodies and control reactions were performed by omitting these antibodies (Fig 3D). The input chromatin samples brought to light the known constitutive association of XPC protein with chromatin even in unchallenged cells and also its expected ubiquitination after UV irradiation (Sugasawa *et al*, 2005). To avoid unspecific binding, the immunoprecipitation buffer was adapted to contain 1% (vol/vol) of the Triton X-100 detergent and, therefore, the proportion of antibody-precipitated XPC protein was low. Nevertheless, this XPC immunoprecipitation resulted in the co-isolation of CHD1 from the chromatin. The amount of co-immunoprecipitated CHD1 was higher after UV irradiation, reflecting an extra UV-dependent recruitment to chromatin not only of XPC but also of CHD1 and lending support to the conclusion that XPC protein is responsible for the co-localization of CHD1 with GG-NER sites.

Next, we tested if other NER factors influence this XPC-CHD1 interaction. Immunoprecipitations with anti-XPC antibodies were carried out after siRNA transfections to down regulate the expression of DDB2, XPD or XPA. In these experiments the amount of co-isolated CHD1 relative to the immunoprecipitated XPC protein was slightly reduced after down regulation of DDB2 and XPA, but none of these changes were statistically significant (Fig 3E). We conclude that, although DDB2 and XPA are not absolutely needed for the recruitment of CHD1 to chromatin (as shown in Fig 3A and Fig 3C), the stringent condition used for the XPC immunoprecipitation reveals that these factors may stabilize XPC-CHD1 interactions.

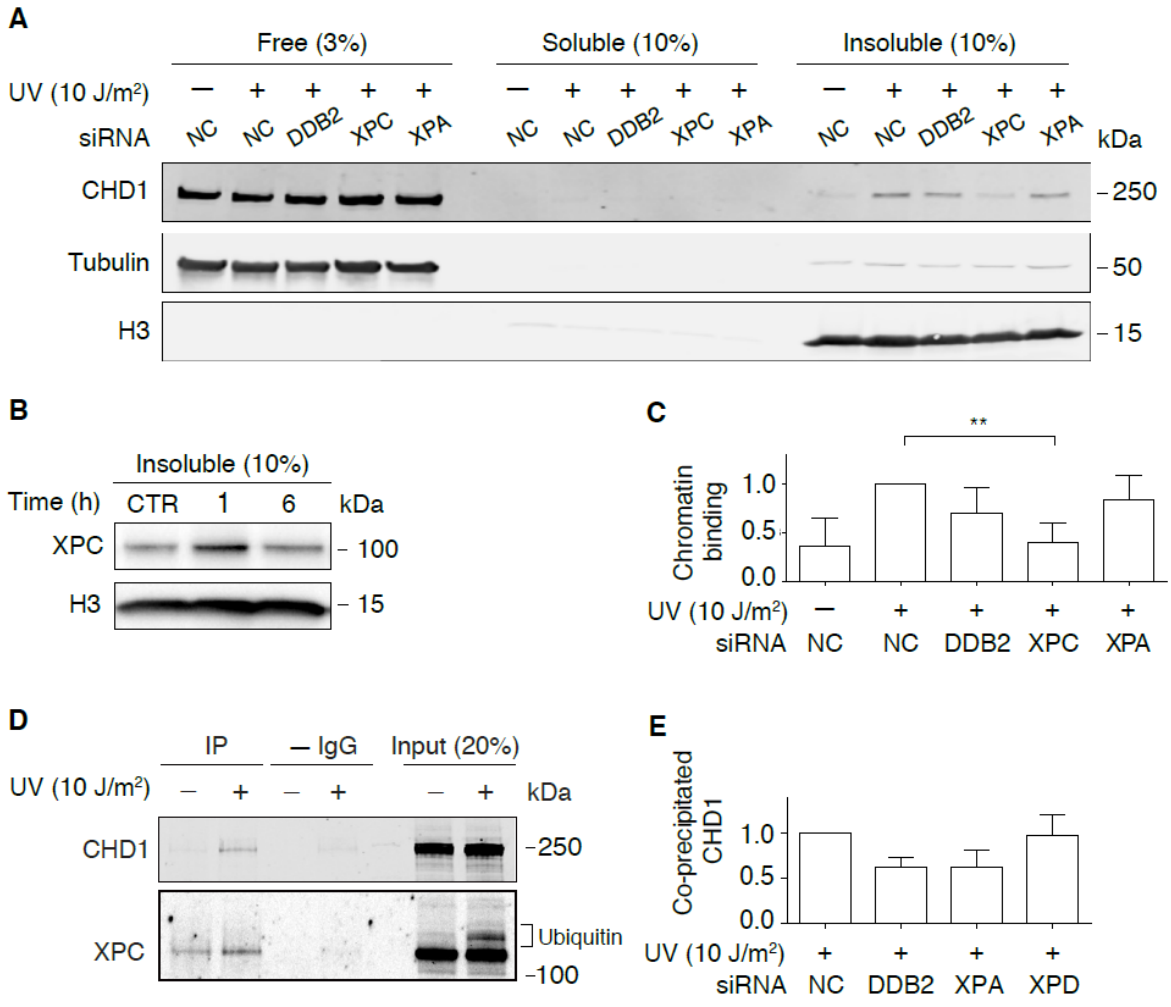

Figure 2 - CHD1 is recruited to nucleosome cores by the XPC initiator.

A XPC-dependent recruitment of CHD1 to nucleosome cores. HeLa cells were siRNA-transfected as indicated two days before irradiation with UV (10 J/m^2), or before mock treatment, and incubated for another 1 h. Chromatin was salt-extracted and MNase-digested to generate, from left to right, a fraction of free (or loosely chromatin-bound) proteins, a fraction

of solubilized chromatin proteins and the insoluble fraction of nucleosome cores. NC, non-coding RNA. Histone H3 and tubulin serve as loading standards.

B Transient association of XPC protein with the insoluble fraction of nucleosome cores of HeLa cells in response to UV irradiation (10 J/m^2). CTR, mock-treated cells.

C Quantification of CHD1 recruitment to the insoluble fraction of nucleosome cores normalized to the level of CHD1 in control reactions with non-coding RNA (n = 4 independent experiments). The asterisks indicate a significantly lower chromatin binding of CHD1 upon XPC depletion.

D Co-immunoprecipitation of XPC and CHD1. HeLa cells were left unchallenged or UV-treated. Following a 1-h incubation, the chromatin was salt-extracted and, after MNase fragmentation, dissolved by sonication. Immunoprecipitation was carried out with anti-XPC antibodies. Input fractions and immunoprecipitated (IP) complexes were analyzed by blotting with antibodies against XPC and CHD1; –IgG, control pull-down reactions without antibodies. Appendix Fig S3 displays a longer exposure of the same immunblot showing the low background association of CHD1 with XPC in unchallenged cells.

E HeLa cells were transfected with the indicated siRNA sequences two days before UV irradiation. Following a 1-h incubation, the irradiated cells were processed for immunoprecipitation with anti-XPC antibodies as in Fig 3D. After immunoblotting, the level of co-immunoprecipitated CHD1 was quantified and normalized to the amount of immunoprecipitated XPC in each individual sample (n = 3 independent experiments). For a representative blot see Fig S4.

Data information: In C and E, data are presented as mean ± SEM. **P ≤ 0.01 (one-sample t-test with a hypothetical value of 1).

CHD1 stimulates XPC displacement and recruitment of downstream GG-NER factors

Due to their larger nuclear surface area in culture, U2OS cells are more amenable than HeLa cells to immunofluorescence analyses. U2OS cells were depleted of CHD1 using siRNA to test by immunofluorescence the impact of this chromatin remodeler on the GG-NER pathway. This down regulation reduced the level of CHD1 protein by ~80% within two days after transfection with siRNA (Fig 4A). However, such a substantial reduction of CHD1 protein did not affect the cell division cycle of unchallenged cells (Fig S1) and did not trigger any apoptotic responses leading to activation of caspase 3 (Fig S2). In view of its established role in transcription (Simic *et al*, 2003; Smolle *et al*, 2012; Park *et al*, 2014), it could have been expected that the down regulation of CHD1 may interfere with DNA damage processing by diminishing the expression of repair proteins. However, Fig 4A shows that the CHD1 depletion does not reduce the cellular level of GG-NER factors like XPB, XPC or DDB2 measured two days after transfection with siRNA. On the contrary, we consistently observed that cells respond to CHD1 depletion with a constitutively

increased level of XPC protein (see quantification in Fig 4B). The high molecular weight forms of XPC in the immunoblot of Fig 4A (representing ubiquitinated XPC protein) also indicate that the CHD1 down regulation does not detectably interfere with the UV-dependent ubiquitination reaction. Reflecting the overall higher XPC level, the amount of ubiquitinated XPC is increased in CHD1-depleted cells. The CHD1 deficiency similarly does not impair the well-described proteasomal degradation of DDB2 in response to UV irradiation (Fig 4A and Fig 4B). The observed up regulation of XPC under conditions of a CHD1 deficiency already takes place at the mRNA level as indicated by quantitative reverse-transcription PCR measurements (Fig 4C).

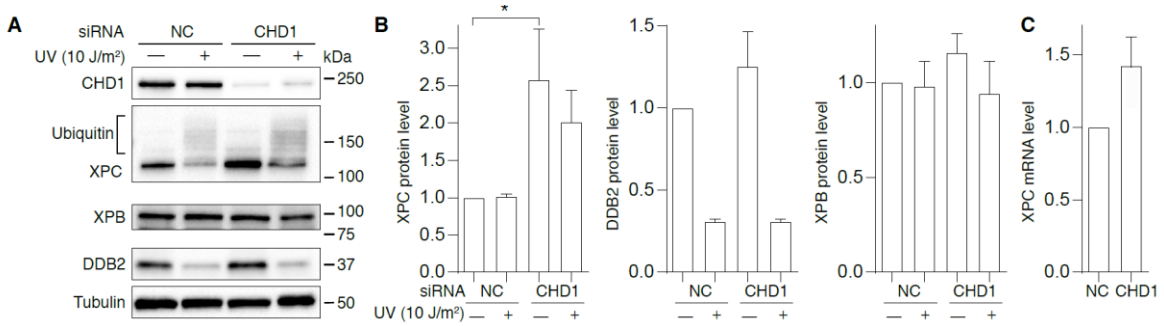

Figure 3 - Depletion of CHD1 by siRNA treatment.

A Effect of CHD1 on NER protein levels. U2OS cells were transfected with non-coding control RNA (NC) or siRNA against the CHD1 transcript and tested after two days. Cells were harvested for analysis 1 h after UV exposure (10 J/m^2) or mock treatment. Immunoblots of whole cell lysates were carried out with the indicated antibodies. The higher molecular weight forms of XPC protein reflect its ubiquitination by the CRL4^{DDB2} ligase (Sugasawa *et al*, 2005). Similarly, the ubiquitin-dependent degradation of DDB2 is a well-described response to UV irradiation. Tubulin served as the loading control.

B Quantification of XPC, DDB2 and XPB protein levels determined by immunoblotting two days after transfection with siRNA (*n* = 3-6 independent experiments). The UV-irradiated samples were analyzed 1 h after treatment and the XPC amount in control cells was set to 1.

C Increased level of mRNA coding for XPC due to CHD1 depletion two days after transfection with siRNA (*n* = 3 independent experiments).

Data information: In B, C, data are presented as mean ± SEM. *P ≤ 0.05 (one-sample t-test with a hypothetical value of 1).

In situ immunofluorescence is recognized as a straightforward tool to monitor the assembly and disassembly of GG-NER complexes in living human cells (Volker *et al*, 2001; Fitch *et al*, 2003). Here, this methodology was used to examine the effect of CHD1

depletion on the recruitment of GG-NER factors to UV lesions. For that purpose, U2OS cells were irradiated with UV-C light through the 5-µm pores of filters to generate local spots of damage containing CPDs. Following 1 or 3 h of incubation, the formaldehyde-fixed cells were permeabilized and stained with antibodies against CPDs and different GG-NER proteins. These immunofluorescence studies revealed a differential effect of CHD1 depletion on distinct factors. Upon CHD1 down regulation, the level of the initial damage sensor XPC on spots of CPDs is increased relatively to controls (Fig 5A). This increased accumulation of XPC is statistically significant at 1 h after UV irradiation and the same response is detected by immunofluorescence analyses of HeLa cells (Fig EV3). This prolonged binding of XPC to lesion sites is not observed upon depletion of the downstream NER factors XPD and XPA (Fig. EV4) and, hence, represents a specific reaction to the lack of CHD1.

To quantify protein redistributions, the fluorescence intensity at damaged spots was divided by the background fluorescence measured in each nucleus outside the lesion spots. This procedure ensures that the data demonstrate a truly increased accumulation of XPC protein at lesion sites rather than simply reflecting the higher overall level of this factor following CHD1 depletion. In contrast to the increased accumulation observed for XPC as the pathway initiator, the redistribution of downstream NER factors, assessed 1 h after UV irradiation, is reduced upon CHD1 depletion. A diminished recruitment to UV lesions following CHD1 depletion is observed for the TFIIH subunits XPD (Fig 5B), XPB (Fig 5C) or p62 (Fig 5D), and also for XPA protein (Fig 5E). This differential effect on factor recruitment to UV lesion sites indicates that CHD1 stimulates the coordinated transition from the XPC complex (as the initiator of the GG-NER pathway) to the follow-up effector TFIIH and, consequently, to further downstream factors like XPA. In the absence of CHD1, XPC persists on UV lesion sites without being able to hand over the damage to the TFIIH complex. The fact that this prolonged binding of XPC to lesion sites, caused by the lack of CHD1, is not reproduced by depletions of XPD or XPA (Fig EV4) argues against the possibility that this observation represents solely an indirect effect of downstream factors not being recruited efficiently.

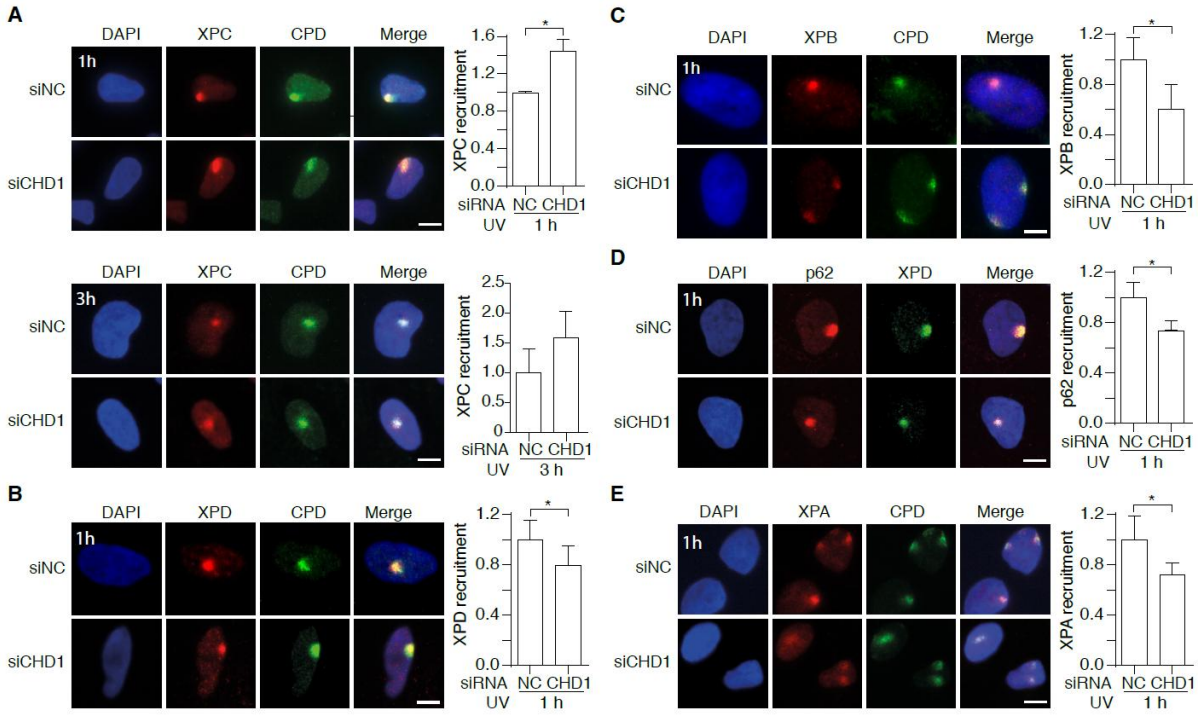

Figure 4 - CHD1 promotes the XPC to TFIIH handoff.

A Accumulation of XPC protein. Representative immunofluorescence images of U2OS cells UV-irradiated through micropore filters (dose applied to the filter surface: 100 J/m^2) to generate local spots of DNA damage. Immunostaining was carried out after 1 or 3 h with antibodies against CPDs and XPC protein. Cells were pretreated with siRNA targeting the CHD1 transcript (siCHD1) or with non-coding control RNA (siNC). DAPI (4',6-diamidino-2-phenylindole) was used to stain nuclear DNA. Scale bar: 10 µm. The recruitment of NER subunits was quantified by measuring spot intensities followed by normalization to the nuclear background (n = 6, 100 cells for each experiment). Control values were set to 1.

B Reduced recruitment to UV lesion spots of XPD, a subunit of the TFIIH complex, upon CHD1 depletion. Cells were analyzed 1 h after the UV pulse. The panel shows a representative immunofluorescence image and the quantification over 3 independent experiments with at least 100 cells per experiment.

C Representative image and quantification (n = 3, at least 100 cells per experiment) demonstrating the reduced recruitment to UV lesion spots of XPB (another TFIIH subunit) upon CHD1 depletion. Cells were analyzed 1 h after the UV pulse.

D Representative image and quantification (n = 6, 100 cells per experiment) demonstrating the reduced recruitment to UV lesion spots of p62 (yet another TFIIH subunit) upon CHD1 depletion. Cells were analyzed 1 h after the UV pulse. XPD was used to mark the UV spots, because it was not possible to stain p62 and CPDs simultaneously.

E Representative image and quantification (n = 6, 100 cells per experiment) demonstrating the reduced XPA recruitment to UV lesion spots upon CHD1 depletion. Cells were analyzed 1 h after the UV pulse.

Data information: In A-E, data are presented as mean ± SEM. *P ≤ 0.05, **P < 0.01 (unpaired, two-tailed t-test).

CHD1 stimulates CPD excision and reduces UV cytotoxicity

Functional consequences of a CHD1 down regulation (see Fig EV2 for the efficiency of protein depletion) were tested by monitoring the formation and excision of UV lesions in HeLa cells. The lack of CHD1 induced by siRNA treatment does not influence the MNase digestion pattern of chromatin (Fig 6A), indicating that the overall nucleosome assembly is unchanged. Consistent with this maintained chromatin configuration, the initial damage formation (frequency of CPDs and 6-4PPs) following UV irradiation is not affected by the lack of CHD1 (Fig 6B). However, the excision of CPDs is significantly slowed down upon CHD1 depletion in comparison to the respective excision in control cells transfected with non-coding RNA. After 24 h of repair incubation, nearly 70% of the initial CPDs were excised in control cells but only 45-55% of CPDs were repaired in CHD1-depleted cells. This same inhibitory effect of CHD1 depletion was induced by three different siRNA sequences directed against the CHD1 transcript (Fig 6C). In a side-by-side comparison, this reduction of CPD excision after down regulation of CHD1 relative to non-coding RNA controls was similar to that observed upon depletion of the chromatin remodeler ALC1 as previously reported (Pines *et al*, 2012) (Fig EV5). In contrast, the CHD1 depletion had no effect on the repair of 6-4PPs, which are removed from the genome with faster kinetics than CPDs (Fig 6D).

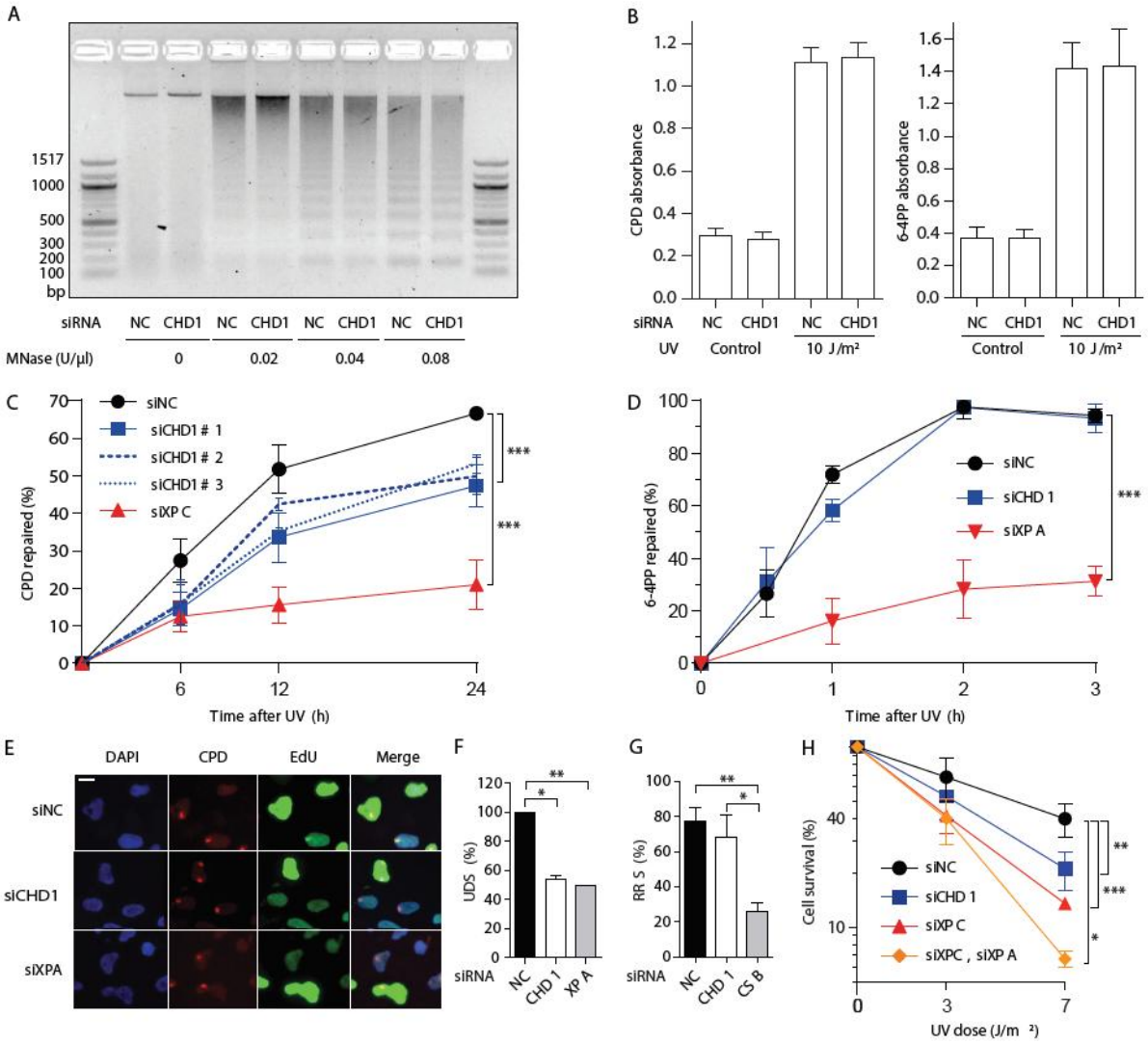

Figure 5 - CHD1 stimulates CPD repair.

A MNase digestion of the chromatin of CHD1-depleted HeLa cells in comparison to control cells transfected with non-coding RNA (NC). Isolated chromatin was incubated with the indicated nuclease concentrations.

B Initial damage formation following UV irradiation (10 J/m^2). HeLa cells were transfected with siCHD1 or siNC. Immunoassay absorbance values, providing a measure of UV lesions, were not affected by CHD1 depletions (n = 6, each experiment with 4 replicates).

C Excision of CPDs in HeLa cells treated with siRNA targeting CHD1 (three different sequences) or XPC, compared to transfections with siNC (n = 6, each experiment with 4 replicates). The UV dose was 10 J/m^2.

D Excision of 6-4PPs upon treatment with siRNA targeting CHD1 or XPA, in comparison to siNC (n = 3, each experiment with 4 replicates). The UV dose was 10 J/m^2.

E U2OS cells were pre-treated with siRNA as indicated and UV-irradiated through micropore filters two days later (dose applied to the filter surface: 100 J/m^2). EdU was added after a 2-h recovery to allow for 6-4PP excision, and fluorescence reflecting repair synthesis was measured after another 1-h incubation. Lesion spots were identified by staining with antibodies against CPDs. EdU incorporation was detected by copper-mediated reaction with

the Alexa 488 fluorophore. DAPI was used to visualize nuclear DNA. S-phase cells displaying an overall bright nuclear EdU signal were excluded from quantifications.

F Quantification of EdU incorporation reflecting repair synthesis (UDS, unscheduled DNA synthesis) in the damage spots of CHD1- or XPA-depleted U2OS cells normalized to control cells. S-phase cells were excluded from these evaluations (n = 3 with at least 100 cells per experiment).

G Recovery of RNA synthesis (RSS) assessed by monitoring the nuclear incorporation of EU during 16 h after UV irradiation (10 J/m^2) of U2OS cells. Cells were depleted of CHD1 or CSB as indicated (n = 3, 100 cells per experiment). RNA synthesis values, reported as the percentage of unirradiated control cells, show that only the depletion of CSB impairs TC-NER activity.

H HeLa cells transfected with the indicated siRNA sequences were UV-irradiated or mock-treated. Colony survival was quantified 7 days later and expressed as the percentage of controls in a logarithmic scale (n = 3, each experiment with four replicates).

Data information: In B, C, D and F-H, data are presented as mean ± SEM. *P ≤ 0.05, **P < 0.01, ***P < 0.001 (unpaired, two-tailed t-test).

To confirm the role of CHD1 in stimulating CPD excision, we monitored the rates of DNA repair patch synthesis. Spots of UV damage were generated in the nuclei of U2OS cells and, for the measurement of repair synthesis elicited specifically by CPDs, these cells were first incubated for 2 h to allow for the removal of 6-4PPs and then supplemented with the nucleoside analog 5-ethynyl-2′-deoxyuridine (EdU) (Nakazawa *et al*, 2010) for another 1-h period. The fluorescence in CPD spots, due to EdU incorporation, revealed that like an XPA deficiency the depletion of CHD1 causes lower levels of DNA repair patch synthesis compared to controls (Fig 6E). The quantification of EdU signals within spots of DNA damage confirmed that DNA repair synthesis takes place in CHD1-depleted cells at a significantly lower rate than in control cells (Fig 6F). Thus, both CPD excision and unscheduled DNA synthesis are reduced in cells depleted of CHD1, indicating that this remodeler is required for efficient processing of CPDs by the GG-NER reaction.

Conversely, transcription-coupled NER (TC-NER) can be monitored by comparing transcription rates after DNA damage. UV radiation causes a decrease of RNA synthesis, which recovers readily in normal cells due to TC-NER activity (Nakazawa *et al*, 2010; Aydin *et al*, 2014). We globally irradiated U2OS cells, incubated them for 16 h in the presence of 5-ethynyl uridine (EU) and, thereafter, the EU-linked fluorescence reflecting RNA synthesis was measured across cell nuclei. As expected, the recovery of RNA synthesis was delayed in cells depleted of Cockayne syndrome group B (CSB) protein required for the TC-NER reaction. In contrast, the CHD1 depletion did not interfere with this recovery of RNA synthesis (Fig 6G) indicating that, although CHD1 regulates GG-

NER activity, it is not involved in the TC-NER pathway. Finally, HeLa cell colony assays demonstrate that the reduced rate of CPD repair observed upon CHD1 depletion correlates with significantly lower survival following UV irradiation (Fig 6H).

Discussion

The GG-NER system needs to process bulky base lesions in condensed chromatin, where genomic DNA is organized in nucleosomes thought to act as physical barriers to damage recognition and repair (Thoma, 2005; Bell *et al*, 2011; Rodriguez *et al*, 2015; Adam *et al*, 2016; Dabin *et al*, 2016). Being the fundamental repeat unit of chromatin, each nucleosome consists of a core particle containing 147 base pairs of DNA wrapped in superhelical turns ~1.7 times around an octamer of two each of the histone proteins H2A, H2B, H3 and H4. These nucleosome cores are spaced by linker DNA segments of variable lengths (generally 10-70 base pairs) and further interactions with histone H1 promote higher levels of chromatin condensation (Grigoryev, 2012). Within the 147 base pairs of nucleosome core DNA, CPDs arise with a periodicity pattern of 10.3-nucleotide intervals and are preferentially introduced at sites farthest from the surface of the histone octamer (Gale *et al*, 1987).

The modulation of chromatin structure by ATP-dependent remodelers has been identified as one important mechanism that promotes accessibility of the GG-NER complex to damaged DNA (Ura *et al*, 2001; Gong *et al*, 2006; Klochendler-Yeivin *et al*, 2006; Ray *et al*, 2009; Zhang *et al*, 2009; Zhao *et al*, 2009; Jiang *et al*, 2010; Pines *et al*, 2012). Our present study identifies the chromatin remodeler CHD1 as an accessory GG-NER factor that facilitates the repair of a subset of CPD lesions located within nucleosome cores. We discovered (i) that a fraction of the cellular CHD1 is recruited to chromatin upon UV irradiation (Fig 1A), (ii) that this extra CHD1 in the chromatin of UV-irradiated cells co-localizes with GG-NER factors (Fig 1C), (iii) that the recruitment of CHD1 to UV damage occurs in a nucleosome core-enriched fraction (Fig 2), (iv) that this UV-dependent CHD1 recruitment to nucleosome cores relies on a prior lesion demarcation by XPC protein (Fig 3), (v) that CHD1 stimulates the XPC to TFIIH handoff at damaged sites (Fig 5) and, therefore, (vi) that the lack of CHD1 slows down the excision of CPDs and enhances the cytotoxicity of UV light (Fig 6). The inhibitory effect of a CHD1 depletion on the repair of CPDs, formed everywhere in the genome, but not on the excision of 6-

4PPs, induced predominantly in linker segments of euchromatin (Gale & Smerdon, 1990; Han *et al*, 2016; Mitchell *et al*, 1990), supports the notion that chromatin remodeling by CHD1 is required to ensure the access of GG-NER factors to DNA damage located within nucleosome cores. Additionally, the measurement of RNA synthesis following UV radiation confirmed that, unlike CSB as an example of TC-NER factor, CHD1 is not involved in the TC-NER subpathway (Fig 6G).

Whether CHD1 displaces nucleosomes while facilitating the known interactions between XPC and TFIIH (Yokoi *et al*, 2000; Uchida *et al*, 2002) during the GG-NER process is not known. However, it is of interest to note that such a role has been postulated for CHD1 during transcription initiation. In fact, CHD1 associates with the chromatin template just downstream of transcription start sites at an early stage of transcription (Skene *et al*, 2014). CHD1 is thereby recruited to the promoter-proximal nucleosomes of active genes and thought to evict this nucleosome to allow for promoter escape by RNA polymerase II. Skene *et al* (2014) showed that, in the absence of CHD1 activity, RNA polymerase II remains sequestered on these promoter-proximal nucleosomes. Our observation that, like RNA polymerase II during transcription initiation, also XPC protein remains sequestered at its binding sites in the absence of CHD1, suggests a similar remodeling activity of CHD1 during initiation of the GG-NER process. A plausible scenario is that the function of CHD1 in stimulating the XPC to TFIIH handoff on nucleosomes is facilitated by eviction of the targeted nucleosome.

Although CHD1 co-localizes in chromatin with DDB2 (Fig 1C), it might be surprising that its recruitment to nucleosomes depends on XPC but apparently not on the accessory DDB2 subunit (Fig 3). Indeed, previous biochemical studies suggested that XPC protein loses the ability to interact with DNA once the substrate is wrapped around histone octamers in nucleosomes (Yasuda *et al*, 2005), suggesting that preceding DDB2-induced rearrangements are indispensable before the DNA substrate becomes accessible to the XPC complex (Scrima *et al*, 2008; Osakabe *et al*, 2015). It is important in this regard to point out that CPDs are the predominant UV lesions within nucleosome cores (Mitchell *et al*, 1990; Gale & Smerdon, 1990; Han *et al*, 2016) and that, when tested in binding assays with naked DNA substrates, the XPC complex is unable to sense the presence of CPDs (Sugasawa, 2001; Hey *et al*, 2002). If not embedded in chromatin, CPDs appear as non-distorting lesions that preserve Watson-Crick hydrogen bonding (Kim *et al*, 1995; Jing *et al*, 1998; McAteer *et al*, 1998) and remain, therefore, invisible to the DNA damage-sensing

domains of XPC protein. However, a recent crystal structure of nucleosome cores containing CPD lesions revealed that, unlike their configuration in naked DNA, the two affected pyrimidines do not form proper Watson-Crick hydrogen bonds with the opposite purines and that hydrogen bonds are actually destabilized at one pyrimidine of the CPD lesion (Horikoshi *et al*, 2016). This substantial local distortion and base pair destabilization detected on nucleosome cores may render the lesions more conducive to recognition by XPC, such that a subset of CPDs in the nucleosome landscape of chromatin becomes amenable to the GG-NER process even in the absence of DDB2 protein. This scenario may explain our previously reported finding that XPC protein binds to UV lesions in nucleosome core particles but not to UV lesions in internucleosomal linkers in the absence of DDB2 (Fei *et al*, 2011). In any case, a local distortion of CPDs induced by wrapping around histone octamers may account for the finding of Fig 3 that the XPC-dependent recruitment of CHD1 to nucleosomes could occur without assistance from the DDB2 subunit. An alternative explanation for this finding is that even trace amounts of DDB2 remaining in the cells after siRNA-mediated depletion might still be sufficient to load XPC complexes onto these more conducive CPDs located on nucleosome cores.

To summarize, we identified CHD1 as an XPC-associated remodeler facilitating GG-NER activity in chromatin. Our findings suggest a scenario by which CHD1 is required for the effective handover of CPD lesions from the XPC initiator to the TFIIH effector when the target lesions are wrapped around the histone octamer of nucleosomes. These findings imply that nucleosomes are not simply an impediment to initiation of the GG-NER pathway but act as a structural scaffold that, in the presence of CHD1, facilitates the repair of a subset of CPD lesions.

Material and Methods

Cell lines. HeLa and HEK293 cells (American Type Culture Collection) were grown in Dulbecco's modified Eagle's medium (low-glucose DMEM; ThermoFisher), U2OS cells (ATCC, cell type certified by STR profiling) in high-glucose DMEM (Sigma) supplemented with 10% (vol/vol) fetal calf serum (FCS, Gibco), 100 U ml^{-1} penicillin and 100 µg ml^{-1} streptomycin.

RNA transfections. The following RNAi sequences were used: CHD1#1 (5'-CAUCAAGCCUCAUCUAAUAtt-3') from Ambion; CHD1#2 and CHD1#3 (5'-

AUGCAGAAAUUAGGCGGUUUAtt-3' and 5'-AAGAUUCCGAUGACUCAUCAAtt-3') from Qiagen (CHD1 sequence #1 is used unless otherwise stated); DDB2 (5'-AGGGAUCAAGCAGUUAUUUGA-3') from Qiagen; XPA (5'-GCUACUGGAGGCAUGGCUAtt-3') from Qiagen; XPC (5'-UAGCAAAUGGCUUCUAUCGAA-3') from Microsynth and CSB (5'-GAAGCAAGGUUGUAAUAAAtt-3') from Microsynth. The non-coding control RNA was from Qiagen. Cells were transfected in 10-cm dishes with siRNA (10 or 16 nM) following the manufacturer's protocol for the Lipofectamine RNAiMAX (Invitrogen) reagent, and allowed to incubate for 48 h before starting the experiments.

Determination of mRNA. For gene expression analysis, total RNA from U2OS cells was isolated using an RNase isolation kit (Qiagen) according to the manufacturer's protocol. DNA was removed by DNase I (Qiagen) digestion. RNA concentration was determined in a NanoDrop instrument (Thermo Scientific). One µg RNA from each sample and 3 µg/µl random primers (Invitrogen) were subjected to reverse transcription (Roche) according to manufacturer's protocol. Fifty ng cDNA, 0.5 µl of FAM-tagged XPC primers (Life Technology) and 0.5 µl of VIC-tagged GAPDH primers (Life Technology) were applied to qRT-PCR according to manufacturer's protocol (Life Technology, TaqMan Fast Universal PCR Master Mix). The relative gene expression levels are presented as $2^{-\Delta\Delta CT}$ and normalized to the sample treated with noncoding siRNA.

Antibodies. The following antibodies, listed according to supplier, were used at the indicated dilutions. Abcam: mouse anti-DDB2 (ab51017, 1:50 for immunofluorescence, 1:200 for immunoblotting), mouse anti-XPC (ab6264, 1:1,000 for immunoblotting), mouse anti-p62 (ab55199, 1:300 for immunofluorescence). Cell Signaling: rabbit anti-caspase 3 (9501S, 1:1,000 for immunoblotting). Cosmo Bio: mouse anti-CPD [NMDND001, 1:1,000 for immunofluorescence, 1:5,000 for enzyme-linked immunosorbent assay (ELISA)], mouse anti-6-4PP (NMDND002, 1:1,000 for ELISA). Invitrogen: Alexa Fluor 488 and 594 goat anti-mouse IgG (1:400 for immunofluorescence). Protein-Tech: rabbit anti-CHD1 (20576-1-AP, 1:100 for immunoblotting). Santa-Cruz: mouse anti-CHD1 (sc-271626, 1:500 for immunoblotting), goat anti-H3 (sc-8654, 1:10'000 for immunoblotting), rabbit anti-XPB (sc-293, 1:100 for immunofluorescence), rabbit anti-XPA (sc-853, 1:100 for immunoblotting). Sigma: mouse anti-α-tubulin (T5168, 1:10,000 for immunoblotting),

mouse anti-FLAG M2 (F3165, 1:1,000 for immunoprecipitation), rabbit anti-XPC (X1129, 1:100 for immunofluorescence and immunoprecipitation), peroxidase anti-mouse IgG (1:20,000), peroxidase anti-rabbit IgG (1:20,000).

UV irradiation. Exposure to UV-C light was carried out in culture dishes at the indicated doses with a germicidal lamp (wavelength 254 nm) after washing the cells with phosphate-buffered saline (PBS) and removal of residual buffer. Local damage was generated by irradiation with 100 J/m^2 through a 5-μm polycarbonate filter (Whatman). After UV irradiation, the cells were incubated for the indicated times with fresh culture medium.

Immunoblotting. Cells were treated as indicated, washed with Puck's EDTA (137.0 mM NaCl, 5.4 mM KCl, 5.6 mM glucose, 4.2 mM $NaHCO_3$, 0.7 mM EDTA) and lysed in 100 μl of 1% Triton buffer [150 mM KCl, 25 mM Tris-HCl, pH 7.5, 5 mM $MgCl_2$, 2 mM β-mercaptoethanol, 5% (vol/vol) glycerol, 1 mM N-ethylmaleimide and 1% (vol/vol) Triton X-100] supplemented with protease inhibitor cocktail (Roche). Protein concentrations were measured by the bicinchoninic acid assay (Pierce). A Laemmli buffer stock [final concentration: 63 mM Tris-HCL, pH 6.8, 10% (vol/vol) glycerol, 2% (wt/vol) sodium dodecyl sulfate (SDS), 0.0005% (wt/vol) bromophenol blue] was added and the samples were heated to 95°C for 5 min. Fifty μg of sample proteins were separated in 4-20% Criterion TGX Stain-Free precast gels (BioRad) for 22 min at 300 V and transferred to PVDF membranes using the Turbo transfer device (BioRad, 7 min at 5 A). The signals resulting from antibody incubations were analyzed and quantified with the Chemidoc MP Imaging System (Bio-Rad).

Cell lysis and chromatin digestion. Chromatin was fragmented as described (Fei *et al*, 2011). Protein synthesis was inhibited by the addition of cycloheximide (100 μg ml^{-1}; Sigma) for 30 min prior to UV irradiation. Cells were irradiated with the indicated UV-C doses and lysed on ice with NP-40 buffer [25 mM Tris-HCl, pH 8.0, 300 mM NaCl, 1 mM EDTA, 10% (vol/vol) glycerol, 1% (vol/vol) NP-40, 0.25 mM phenylmethylsulfonyl fluoride and EDTA-free protease inhibitor cocktail (Roche)] (Sugasawa *et al*, 2005). Lysis was carried out for 30 min on a turning wheel. Free proteins not bound to chromatin were recovered in the supernatant after centrifugation (10 min at 15'000 g). The remaining chromatin pellet was resuspended in CS buffer [20 mM Tris-HCl, pH 7.5, 100 mM KCl, 2

mM $MgCl_2$, 1 mM $CaCl_2$, 0.3 M sucrose and 0.1 % (vol/vol) Triton X-100] (Kapetanaki *et al*, 2006). This mixture was supplemented with 10-fold reaction buffer [500 mM Tris-HCl, pH 7.9, 50 mM $CaCl_2$, 0.1 mg/ml bovine serum albumin (New England Biolabs). MNase (0.4 U/µl; New England Biolabs) was added and digestion carried out for 20 min at 37°C. The solubilized constituents were separated from the insoluble pellet by centrifugation (10 min, 15'000 g) after adding EDTA (5 mM final concentration) to stop the reaction.

MNase profiling. U2OS cells were irradiated with UV-C (10 J/m^2) and lysed on ice 1 h later with NP-40 buffer; the chromatin pellet was resuspended in CS buffer and the mixture was supplemented with 10-fold reaction buffer as outlined above. MNase was added in different concentrations, the digestion carried out for 5 min at 37°C and the reaction stopped with 5 mM EDTA. The DNA was extracted from each digested sample (50 µl) by adding 150 µl TE buffer [10 mM Tris-HCl, pH 8.0, 1 mM EDTA] and 200 µl neutral phenol (ThermoFisher). After shaking for 15 min and centrifugation (5 min at 6,000 g), the phenol was discarded and the aqueous phase was washed twice with 200 µl chloroform. The DNA was precipitated with ethanol in the presence of 100 mM sodium acetate, dried and resuspended in TE buffer. DNA concentrations were determined in the NanoDrop device.

Pull-down of chromatin-associated GG-NER complexes. HEK293 cells were transiently transfected at 80% confluency with plasmid DDB2-p3XFLAG-14-N3 (10 µg) according to the manufacturer's protocol for the FuGENE® HD reagent (Roche), and UV-irradiated 24 h later. Following another 30 min, the cells were lysed on ice in NP-40 buffer, the remaining pellet was resuspended in CS buffer and the mixture was supplemented with 10-fold reaction buffer. The MNase digestion (4 U/µl) was carried out for 20 min at 37°C. The residual insoluble chromatin was recovered by centrifugation (10 min, 16'000 g) and resuspended by sonication on an ice-water bath (3 cycles of 30 s with 30-s intervals) in CS buffer. Subsequently, nucleoprotein complexes bound to the DDB2-FLAG prey were purified using 40 µl of anti-FLAG M2 Affinity Gel (Sigma) in the presence of IP buffer [150 mM NaCl, 50 mM Tris-HCl, pH 7.5, 5 mM $MgCl_2$, 1% (vol/vol) NP-40, 2 mM β-mercaptoethanol, 5% (vol/vol) glycerol and all protease inhibitors]. Beads were incubated overnight at 4 °C with the sonicated mixture, washed once with TNET [50 mM Tris-HCl, pH 7.4, 150 mM NaCl, 5 mM EDTA, 0.5% (vol/vol) Triton X-100 and protease inhibitors]

and once with TBS (50 mM Tris-HCl, pH 7.4, 150 mM NaCl and protease inhibitors). The beads were heated to 95°C for 5 min in 10 µl TBS complemented with 5.0 µl of Laemmli buffer stock. The samples were separated on a 10% (wt/vol) denaturing polyacrylamide gel and transferred to PVDF membranes. Proteins were subsequently detected by immunoblotting.

Pull down of XPC protein. After washing on ice with PBS, 10 µl of slurry Protein G sepharose (GE Healthcare) for each sample were washed twice with PBS and then incubated for 45 min at 4°C on a turning wheel with 4 µl anti-XPC antibodies. After centrifugation (1 min, 100 g), the protein G sepharose was suspended in 100 µl buffer A [0.5 M Tris-HCl, pH 8.0, 20% (vol/vol) glycerol, 300 mM NaCl, 2% (vol/vol) Triton X-100, 2 mM EDTA, 0,25 mM phenylmethylsulfonyl fluoride and ETDA-free protease inhibitor cocktail (Roche)], added to 100 µg of fragmented and sonicated chromatin, and incubated for 3 h at 4°C on a turning wheel. The beads were washed twice by centrifugation (2 min, 100 g) in HNTG buffer [20 mM HEPES, pH 7.5, 150 mM NaCl, 0.1% (vol/vol) Triton X-100 and 10% (vol/vol) glycerol] and the samples were analysed by polyacrylamide gel electrophoresis and immunoblotting.

Immunofluorescence microscopy. Cells were grown on 12-mm glass coverslips (Thermo Scientific) to 80% confluency and irradiated through filters to induce local spots of UV damage. After the indicated repair times, cells were processed with pre-extraction buffer [25 mM HEPES, pH 7.5, 50 mM NaCl, 1 mM EDTA, 3 mM $MgCl_2$, 300 mM sucrose and 0.5% (vol/vol) Triton X-100] added for 2.5 min at 4°C. Next, cells were fixed with 4% (wt/vol) paraformaldehyde for 15 min and permeabilized for 20 min with PBS containing 0.1% (vol/vol) Tween 20. For the detection of CPDs and 6-4 PPs, the DNA was denaturated for 8 min with 0.07 M NaOH in PBS. Following a 30-min blocking step with PBS containing 20% (vol/vol) FCS, primary antibodies were diluted in PBS containing 5% (vol/vol) FCS and applied for 1 h at 37°C. Washing with PBS-0.1% Tween 20 was followed by incubation with secondary antibodies and DAPI (0.2 µg ml^{-1}), diluted in PBS containing 5% FCS, for 1 h at 37°C. Images were taken with a bright field microscope (Leica, 63x oil Plan-Apochromat, 1.4 numerical aperture oil immersion lens) and analysed using the Image J software. The fluorescence of 100 nuclei was examined and the

accumulation of proteins at UV lesion sites is expressed as the ratio of fluorescence signal intensity in damaged spots relative to the signal intensity of the surrounding nuclear area.

Unscheduled DNA synthesis and RNA synthesis. The synthesis of DNA repair patches was measured by a fluorescence-based method (Nakazawa *et al*, 2010). U2OS cells were seeded on 12-mm coverslips and locally UV-irradiated. After 2 h, the culture medium was supplemented with 10 mM EdU (Invitrogen) followed by another 1 h of incubation. Cells were washed with PBS, preextracted for 2.5 min, fixed with 4% (wt/vol) paraformaldehyde for 15 min and permeabilized for 20 min. Antibodies against CPDs were applied as described above. Incorporated EdU was coupled to Alexa Fluor 488 using the Click-it kit as instructed by the manufacturer (Invitrogen). Images were obtained by microscopy with the Leica instrument and analysed using the Image J software. For quantifications, EdU incorporation was measured in 100 cells by determining fluorescence intensity in the UV-damaged areas (marked by CPD staining) divided by the background nuclear intensity. S-phase cells displaying high EdU fluorescence across their entire nucleus were excluded. For the measurement of RNA synthesis, cells were UV-irradiated globally (10 J/m^2) and incubated for 16 h in culture medium supplemented with 100 μM EU (Thermo Scientific). Thereafter, cells were washed, pre-extracted, fixed and permeabilized as outlined above. EU incorporation was analyzed in 100 cells per treatment by determining fluorescence intensity of the whole nucleus divided by the background slide intensity.

Quantification of UV lesions. Formation and removal of UV lesions was detected by ELISA as described (Fei et al, 2011). Briefly, whole-genome DNA was extracted using the DNeasy kit (Qiagen) and denatured by heating to 99ºC for 10 min, followed by a 15-min incubation on ice. A volume of 50 μl per well of denatured DNA (at a concentration of 4 μg/ml for 6-4PP detection, 200 ng/ml for CPD detection) was distributed into a 96-well microtiter plate (Greiner) coated with protamine sulfate (Sigma) and dried overnight at 37ºC. The DNA-coated plates were washed five times with PBST [0.05% (vol/vol) Tween-20 in PBS] and blocked with 2% (vol/vol) FBS in PBS at 37 ºC for 60 min. The antibodies against either 6-4PPs (64M-2) or CPDs (TDM-2) were applied for 30 min (at 37ºC). Primary antibodies bound to DNA were recognized by biotin-labelled $F(ab´)_2$ fragments of anti-mouse IgG (1:2,000; Invitrogen) added for 30 min at 37ºC. After washing the plates, 100 μl of a peroxidase-streptavidin conjugate (1:10.000; Invitrogen) was distributed into

each well. The reaction was started by adding 0.5 mg/ml o-phenylenediamine, 0.007% (vol/vol) H_2O_2 and citrate-phosphate buffer (50 mM Na_2HPO_4, 24 mM citric acid, pH 5.0), stopped with 50 µl of 2 M H_2SO_4, and monitored by measuring the absorbance at 492 nm in a PLUS384 microplate spectrophotometer (Molecular Devices).

Colony forming assay. HeLa cells treated as indicated were seeded in different dilutions and left for 7 days at 37°C to allow for colony formation. The growing colonies were stained with 0.5% (w/v) crystal violet in 80% ethanol and counted.

Cell cycle analysis. HeLa cells were arrested in G1 by a 24-h treatment with mimosine (0.5 mM, Sigma). UV-exposed cells were allowed to recover for the indicated times and labelled with 10 µM EdU for 1 h prior to harvesting. Cells cycle profiles were analysed using the Life Technologies Click-iT Edu Alexa Fluor 488 Flow Cytometry Assay kit. Briefly, cells were fixed in 1% (wt/vol) PFA/PBS (Sigma) for 10 min and permeabilized in saponin buffer for 10 min; 200,000 cells were incubated with a mouse anti-γH2AX antibody (Millipore, 1:2000) for 1.5 h and with an Alexa Fluor 647 anti-mouse antibody (Invitrogen A31571, 1:50) for 30 min. EdU was coupled to Alexa Fluor 488 azide for 30 min. Cells were treated with 0.1 mg/ml RNase and DNA was stained with 1 µg/ml DAPI, followed by analysis in a CyAn ADP flow cytometer (Beckman Coulter). Results were analysed with Flow Jo 10 data analysis software (FLOWJO, LLC).

Statistics. GraphPad Prism 6 was used to perform unpaired, two-tailed *t*-tests as outlined in the figure legends. One-sample t test with a hypothetical value of 1.0 was applied for independent immunoblot assays. *P* values expressed as $*P < 0.05$, $**P < 0.01$ and $***P < 0.001$ were considered to indicate statistical significance.

Acknowledgements

This work was supported by the Swiss National Science Foundation (Grant 143669/1), the Velux Foundation (Project 753) and the Swiss Cancer League (2832-02-2011). We also acknowledge support by the Center of Clinical Studies.

Author contributions

P.R., C.B.P. T.C. and H.N. devised and planned the experiments, P.R., C.B.P., T.C. and Z.G. carried out the experiments and analyzed the data, P.R., C.B.P. and H.N. wrote the manuscript.

Conflict of interest

The authors declare that they have no conflict of interest.

References

Adam S, Dabin J, Chevallier O, Leroy O, Baldeyron C, Corpet A, Lomonte P, Renaud O, Almouzni G & Polo S (2016) Real-time tracking of parental histones reveals their contribution to chromatin integrity following DNA damage. Mol. Cell 64: 65–78

Araki M, Masutani C, Takemura M, Uchida A, Sugasawa K, Kondoh J, Ohkuma Y & Hanaoka F (2001) Centrosome protein centrin 2/caltractin 1 is part of the xeroderma pigmentosum group C complex that initiates global genome nucleotide excision repair. J. Biol. Chem. 276: 18665–18672

Araújo SJ, Tirode F, Coin F, Pospiech H, Syväoja JE, Stucki M, Hübscher U, Egly J-M & Wood RD (2000) Nucleotide excision repair of DNA with recombinant human proteins: definition of the minimal set of factors, active forms of TFIIH, and modulation by CAK. Genes Dev. 14: 349–359

Aydin ÖZ, Vermeulen W & Lans H (2014) ISWI chromatin remodeling complexes in the DNA damage response. Cell Cycle 13: 3016–3025

Bell O, Tiwari VK, Thomä NH & Schübeler D (2011) Determinants and dynamics of genome accessibility. Nat. Rev. Genet. 12: 554–564

Bunick CG, Miller MR, Fuller BE, Fanning E & Chazin WJ (2006) Biochemical and structural domain analysis of xeroderma pigmentosum complementation group C protein. Biochemistry 45: 14965–14979

Compe E & Egly J-M (2016) Nucleotide excision repair and transcriptional regulation: TFIIH and beyond. Annu. Rev. Biochem. 85: 265–290

Czaja W, Mao P & Smerdon MJ (2012) The emerging roles of ATP-dependent chromatin remodeling enzymes in nucleotide excision repair. Int. J. Mol. Sci. 13: 11954–11973

Dabin J, Fortuny A & Polo SE (2016) Epigenome maintenance in response to DNA damage. Mol. Cell 62: 712–727

DiGiovanna JJ & Kraemer KH (2012) Shining a light on xeroderma pigmentosum. J Investig Dermatol 132: 785–796

Fei J, Kaczmarek N, Luch A, Glas A, Carell T & Naegeli H (2011) Regulation of nucleotide excision repair by UV-DDB: prioritization of damage recognition to internucleosomal DNA. PLoS Biol. 9: e1001183

Fitch ME, Nakajima S, Yasui A & Ford JM (2003) In vivo recruitment of XPC to UV-induced cyclobutane pyrimidine dimers by the DDB2 gene product. J. Biol. Chem. 278: 46906–46910

Friedberg EC, Aguilera A, Gellert M, Hanawalt PC, Hays JB, Lehmann AR, Lindahl T, Lowndes N, Sarasin A & Wood RD (2006) DNA repair: From molecular mechanism to human disease. DNA Repair (Amst). 5: 986–996

Fuss JO & Tainer J a (2011) XPB and XPD helicases in TFIIH orchestrate DNA duplex opening and damage verification to coordinate repair with transcription and cell cycle via CAK kinase. DNA Repair (Amst). 10: 697–713

Gale JM, Nissen KA & Smerdon MJ (1987) UV-induced formation of pyrimidine dimers in nucleosome core DNA is strongly modulated with a period of 10.3 bases. Biochemistry 84: 6644–6648

Gale JM & Smerdon MJ (1990) UV induced (6-4) photoproducts are distributed differently than cyclobutane dimers in nucleosomes. Photochem. Photobiol. 51: 411–417

Gaspar-Maia A, Alajem A, Polesso F, Sridharan R, Mason MJ, Heidersbach A, Ramalho-Santos J, McManus MT, Plath K, Meshorer E & Ramalho-Santos M (2009) Chd1 regulates open chromatin and pluripotency of embryonic stem cells. Nature 460: 863–868

Gong F, Fahy D, Liu H, Wang W & Smerdon MJ (2008) Role of the mammalian SWI / SNF chromatin remodeling complex in the cellular response to UV damage. Cell Cycle 7: 1067–1074

Gong F, Fahy D & Smerdon MJ (2006) Rad4-Rad23 interaction with SWI/SNF links ATP-dependent chromatin remodeling with nucleotide excision repair. Nat. Struct. Mol. Biol. 13: 902–907

Grigoryev SA (2012) Nucleosome spacing and chromatin higher-order folding. Nucleus 3: 493–499

Han C, Srivastava AK, Cui T, Wang Q-E & Wani AA (2016) Differential DNA lesion formation and repair in heterochromatin and euchromatin. Carcinogenesis 37: 129–138

Hanawalt PC & Spivak G (2008) Transcription-coupled DNA repair: Two decades of progress and surprises. Nat. Rev. Mol. Cell Biol. 9: 958–970

Hey T, Lipps G, Sugasawa K, Iwai S, Hanaoka F & Krauss G (2002) The XPC−HR23B complex displays high affinity and specificity for damaged DNA in a true-equilibrium fluorescence assay. Biochemistry 41: 6583–6587

Hoeijmakers JHJ (2009) DNA damage, aging, and cancer. N. Engl. J. Med. 361: 1475–85

Horikoshi N, Tachiwana H, Kagawa W, Osakabe A, Matsumoto S, Iwai S, Sugasawa K & Kurumizaka H (2016) Crystal structure of the nucleosome containing ultraviolet light-induced cyclobutane pyrimidine dimer. Biochem. Biophys. Res. Commun. 471: 117–122

Hwang BJ, Ford JM, Hanawalt PC & Chu G (1999) Expression of the p48 xeroderma pigmentosum gene is p53-dependent and is involved in global genomic repair. Proc. Natl. Acad. Sci. 96: 424–428

Jiang Y, Wang X, Bao S, Guo R, Johnson DG, Shen X & Li L (2010) INO80 chromatin remodeling complex promotes the removal of UV lesions by the nucleotide excision repair pathway. Proc. Natl. Acad. Sci. 107: 2–7

Jing Y, Taylor JS & Kao JFL (1998) Thermodynamic and base-pairing studies of matched and mismatched DNA dodecamer duplexes containing cis-syn, (6-4) and dewar photoproducts of TT. Nucleic Acids Res. 26: 3845–3853

Kapetanaki MG, Guerrero-Santoro J, Bisi DC, Hsieh CL, Rapić-Otrin V & Levine AS (2006) The DDB1-CUL4ADDB2 ubiquitin ligase is deficient in xeroderma pigmentosum group E and targets histone H2A at UV-damaged DNA sites. Proc. Natl. Acad. Sci. U. S. A. 103: 2588–93

Kari V, Mansour WY, Raul SK, Baumgart SJ, Mund A, Grade M, Sirma H, Simon R, Will H, Dobbelstein M, Dikomey E & Johnsen SA (2016) Loss of CHD1 causes DNA repair defects and enhances prostate cancer therapeutic responsiveness. EMBO Rep. 487: e201642352

Kim JK, Soni SD, Arakali A V, Wallace JC & Alderfer JL (1995) Solution structure of a nucleic acid photoproduct of deoxyfluorouridylyl-(3'-5')-thymidine monophosphate (d-FpT) determined by NMR and restrained molecular dynamics: Structural comparison of two sequence isomer photoadducts (d-U5p5T and d-T5p5U). Nucleic Acids Res. 23: 1810–1815

Klochendler-Yeivin A, Picarsky E & Yaniv M (2006) Increased DNA damage sensitivity and apoptosis in cells lacking the Snf5 / Ini1 subunit of the SWI / SNF chromatin remodeling complex. Mol. Cell. Biol. 26: 2661–2674

Kobayashi N, Katsumi S, Imoto K, Nakagawa A, Miyagawa S, Furumura M & Mori T (2001) Quantitation and visualization of ultraviolet-induced DNA damage using specific antibodies: Application to pigment cell biology. Pigment Cell Res. 14: 94–102

Li C-L, Golebiowski FMM, Onishi Y, Samara NLL, Sugasawa K & Yang W (2015) Tripartite DNA lesion recognition and verification by XPC, TFIIH, and XPA in nucleotide excision repair. Mol. Cell 59: 1025–1034

Marteijn JA, Lans H, Vermeulen W & Hoeijmakers JHJ (2014) Understanding nucleotide excision repair and its roles in cancer and ageing. Nat. Rev. Mol. Cell Biol. 15: 465–481

Mathieu N, Kaczmarek N, Rüthemann P, Luch A & Naegeli H (2013) DNA quality control by a lesion sensor pocket of the xeroderma pigmentosum group D helicase subunit of TFIIH. Curr. Biol. 23: 204–212

McAteer K, Jing Y, Kao J, Taylor J-SS & Kennedy M. A (1998) Solution-state structure of a DNA dodecamer duplex containing a cis-syn thymine cyclobutane dimer, the major UV photoproduct of DNA. J. Mol. Biol. 282: 1013–1032

McKenna ES, Sansam CG, Cho Y-J, Greulich H, Evans JA, Thom CS, Moreau LA, Biegel JA, Pomeroy SL & Roberts CWM (2008) Loss of the epigenetic tumor suppressor SNF5 leads to cancer without genomic instability. Mol. Cell. Biol. 28: 6223–6233

Mitchell DL, Nguyen TD & Cleaver JE (1990) Nonrandom induction of pyrimidine-pyrimidone (6-4) photoproducts in ultraviolet-irradiated human chromatin. J. Biol. Chem. 265: 5353–5356

Moser J, Kool H, Giakzidis I, Caldecott K, Mullenders LHF & Fousteri MI (2007) Sealing of chromosomal DNA nicks during nucleotide excision repair requires XRCC1 and DNA ligase IIIα in a cell-cycle-specific manner. Mol. Cell 27: 311–323

Mouret S, Leccia M-T, Bourrain J-L, Douki T & Beani J-C (2011) Individual photosensitivity of human skin and UVA-induced pyrimidine dimers in DNA. J. Invest. Dermatol. 131: 1539–1546

Nakazawa Y, Yamashita S, Lehmann AR & Ogi T (2010) A semi-automated non-radioactive system for measuring recovery of RNA synthesis and unscheduled DNA synthesis using ethynyluracil derivatives. DNA Repair (Amst). 9: 506–516

Nocentini S, Coin F, Saijo M, Tanaka K & Egly JM (1997) DNA damage recognition by XPA protein promotes efficient recruitment of transcription factor II H. J. Biol. Chem. 272: 22991–22994

Ogi T, Limsirichaikul S, Overmeer RM, Volker M, Takenaka K, Cloney R, Nakazawa Y, Niimi A, Miki Y, Jaspers NG, Mullenders LHF, Yamashita S, Fousteri MI & Lehmann AR

(2010) Three DNA polymerases, recruited by different mechanisms, carry out NER repair synthesis in human cells. Mol. Cell 37: 714–727

Osakabe A, Tachiwana H, Kagawa W, Horikoshi N, Matsumoto S, Hasegawa M, Matsumoto N, Toga T, Yamamoto J, Hanaoka F, Thomä NH, Sugasawa K, Iwai S & Kurumizaka H (2015) Structural basis of pyrimidine-pyrimidone (6-4) photoproduct recognition by UV-DDB in the nucleosome. Sci. Rep. 5: 16330

Otrin VR, McLenigan M, Takao M, Levine AS & Protic M (1997) Translocation of a UV-damaged DNA binding protein into a tight association with chromatin after treatment of mammalian cells with UV light. J. Cell Sci. 110: 1159–1168

Park D, Shivram H & Iyer VRV (2014) Chd1 co-localizes with early transcription elongation factors independently of H3K36 methylation and releases stalled RNA polymerase II at introns. Epigenetics Chromatin 7: 1–11

Peterson CL & Almouzni G (2013) Nucleosome dynamics as modular systems that integrate DNA damage and repair. Cold Spring Harb. Perspect. Biol. 5: a012658

Piatti P, Lim CY, Nat R, Villunger A, Geley S, Shue YT, Soratroi C, Moser M & Lusser A (2015) Embryonic stem cell differentiation requires full length Chd1. Sci. Rep. 5: 8007

Pines A, Vrouwe MG, Marteijn J a, Typas D, Luijsterburg MS, Cansoy M, Hensbergen P, Deelder A, de Groot A, Matsumoto S, Sugasawa K, Thoma N, Vermeulen W, Vrieling H & Mullenders L (2012) PARP1 promotes nucleotide excision repair through DDB2 stabilization and recruitment of ALC1. J. Cell Biol. 199: 235–249

Rapic-Otrin V (2002) Sequential binding of UV DNA damage binding factor and degradation of the p48 subunit as early events after UV irradiation. Nucleic Acids Res. 30: 2588–2598

Ray A, Mir SN, Wani G, Zhao Q, Battu A, Zhu Q, Wang Q-E & Wani A a (2009) Human SNF5/INI1, a component of the human SWI/SNF chromatin remodeling complex, promotes nucleotide excision repair by influencing ATM recruitment and downstream H2AX phosphorylation. Mol. Cell. Biol. 29: 6206–6219

Reardon JT & Sancar A (2003) Recognition and repair of the cyclobutane thymine dimer, a major cause of skin cancers, by the human excision nuclease. Genes Dev. 17: 2539–2551

Riedl T, Hanaoka F & Egly J-MM (2003) The comings and goings of nucleotide excision repair factors on damaged DNA. EMBO J. 22: 5293–5303

Rodriguez Y, Hinz JM & Smerdon MJ (2015) Accessing DNA damage in chromatin: Preparing the chromatin landscape for base excision repair. DNA Repair (Amst). 32: 113–119

Rubbi CP & Milner J (2003) p53 is a chromatin accessibility factor for nucleotide excision repair of DNA damage. EMBO J. 22: 975–986

Sancar A (1996) DNA Excision Repair. Annu. Rev. Biochem. 65: 43–81

Sarkar S, Kiely R & McHugh PJ (2010) The Ino80 chromatin-remodeling complex restores chromatin structure during UV DNA damage repair. J. Cell Biol. 191: 1061–1068

Schärer OD (2013) Nucleotide excision repair in eukaryotes. Cold Spring Harb. Perspect. Biol. 5: 1–19

Scrima A, Koníčková R, Czyzewski BK, Kawasaki Y, Jeffrey PD, Groisman R, Nakatani Y, Iwai S, Pavletich NP & Thomä NH (2008) Structural basis of UV DNA-damage recognition by the DDB1-DDB2 complex. Cell 135: 1213–1223

Simic R, Lindstrom DL, Tran HG, Roinick KL, Costa PJ, Johnson AD, Hartzog GA & Arndt KM (2003) Chromatin remodeling protein Chd1 interacts with transcription elongation factors and localizes to transcribed genes. EMBO J. 22: 1846–1856

Skene PJ, Hernandez AE, Groudine M & Henikoff S (2014) The nucleosomal barrier to promoter escape by RNA polymerase ii is overcome by the chromatin remodeler Chd1. Elife 2014: e02042

Smerdon MJ & Conconi A (1999) Modulation of DNA damage and DNA repair in chromatin. Prog Nucleic Acid Res Mol Biol 62: 227–255

Smolle M, Venkatesh S, Gogol MM, Li H, Zhang Y, Florens L, Washburn MP & Workman JL (2012) Chromatin remodelers Isw1 and Chd1 maintain chromatin structure during transcription by preventing histone exchange. Nat. Struct. Mol. Biol. 19: 884–892

Staresincic L, Fagbemi AF, Enzlin JH, Gourdin AM, Wijgers N, Dunand-Sauthier I, Giglia-Mari G, Clarkson SG, Vermeulen W & Schärer OD (2009) Coordination of dual incision and repair synthesis in human nucleotide excision repair. EMBO J 28: 1111–1120

Sugasawa K (2001) A multistep damage recognition mechanism for global genomic nucleotide excision repair. Genes Dev. 15: 507–521

Sugasawa K, Ng JMY, Masutani C, Iwai S, van der Spek PJ, Eker APM, Hanaoka F, Bootsma D & Hoeijmakers JHJ (1998) Xeroderma pigmentosum group C protein complex is the initiator of global genome nucleotide excision repair. Mol. Cell 2: 223–232

Sugasawa K, Okuda Y, Saijo M, Nishi R, Matsuda N, Chu G, Mori T, Iwai S, Tanaka KK, Tanaka KK & Hanaoka F (2005) UV-induced ubiquitylation of XPC protein mediated by UV-DDB-ubiquitin ligase complex. Cell 121: 387–400

Thoma F (2005) Repair of UV lesions in nucleosomes – intrinsic properties and remodeling. DNA Repair (Amst). 4: 855–869

Uchida A, Sugasawa K, Masutani C, Dohmae N, Araki M, Yokoi M, Ohkuma Y & Hanaoka F (2002) The carboxy-terminal domain of the XPC protein plays a crucial role in nucleotide excision repair through interactions with transcription factor IIH. DNA Repair (Amst). 1: 449–461

Ura K, Araki M, Saeki H, Masutani C, Ito T, Iwai S, Mizukoshi T, Kaneda Y & Hanaoka F (2001) ATP-dependent chromatin remodeling facilitates nucleotide excision repair of UV-induced DNA lesions in synthetic dinucleosomes. EMBO J. 20: 2004–2014

Vermeulen W & Fousteri M (2013) Mammalian transcription-coupled excision repair. Cold Spring Harb. Perspect. Biol. 5: a012625–a012625

Volker M, Moné MJ, Karmakar P, van Hoffen A, Schul W, Vermeulen W, Hoeijmakers JHJ, van Driel R, van Zeeland AA & Mullenders LHF (2001) Sequential assembly of the nucleotide excision repair factors in vivo. Mol. Cell 8: 213–224

Wakasugi M, Kasashima H, Fukase Y, Imura M, Imai R, Yamada S, Cleaver JE & Matsunaga T (2009) Physical and functional interaction between DDB and XPA in nucleotide excision repair. Nucleic Acids Res. 37: 516–525

Wakasugi M, Shimizu M, Morioka H, Linn S, Nikaido O & Matsunaga T (2001) Damaged DNA-binding protein DDB stimulates the excision of cyclobutane pyrimidine dimers in vitro in concert with XPA and replication protein A. J. Biol. Chem. 276: 15434–15440

Yasuda T, Sugasawa K, Shimizu Y, Iwai S, Shiomi T & Hanaoka F (2005) Nucleosomal structure of undamaged DNA regions suppresses the non-specific DNA binding of the XPC complex. DNA Repair (Amst). 4: 389–395

Yeh JI, Levine AS, Du S, Chinte U, Ghodke H, Wang H, Shi H, Hsieh CL, Conway JF, Van Houten B & Rapic-Otrin V (2012) Damaged DNA induced UV-damaged DNA-binding Protein (UV-DDB) dimerization and its roles in chromatinized DNA repair. Proc. Natl. Acad. Sci. U. S. A. 109: 1–10

Yokoi M, Masutani C, Maekawa T, Sugasawa K, Ohkuma Y & Hanaoka F (2000) The xeroderma pigmentosum group C protein complex XPC-HR23B plays an important role in the recruitment of transcription factor IIH to damaged DNA. J. Biol. Chem. 275: 9870–9875

Zavala AG, Morris RT, Wyrick JJ & Smerdon MJ (2014) High-resolution characterization of CPD hotspot formation in human fibroblasts. Nucleic Acids Res. 42: 893–905

Zhang L, Chen H, Gong M, Gong F, Zhang Q, Jones K, Patel M & Gong F (2013) The chromatin remodeling protein BRG1 modulates BRCA1 response to UV irradiation by regulating ATR/ATM activation. Front. Oncol. 3: 1–9

Zhang L, Zhang Q, Jones K, Patel M & Gong F (2009) The chromatin remodeling factor BRG1 stimulates nucleotide excision repair by facilitating recruitment of XPC to sites of DNA damage. Cell Cycle 8: 3953–3959

Zhao Q, Wang Q-EE, Ray A, Wani G, Han C, Milum K & Wani AA (2009) Modulation of nucleotide excision repair by mammalian SWI/SNF chromatin-remodeling complex. J. Biol. Chem. 284: 30424–30432

Expanded view figures

The CHD1 remodeler promotes XPC to TFIIH handoffs on nucleosomes during DNA repair of UV lesions

Peter Rüthemann‡, Chiara Balbo Pogliano‡, Tamara Codilupi, Zuzana Garajovà and Hanspeter Naegeli

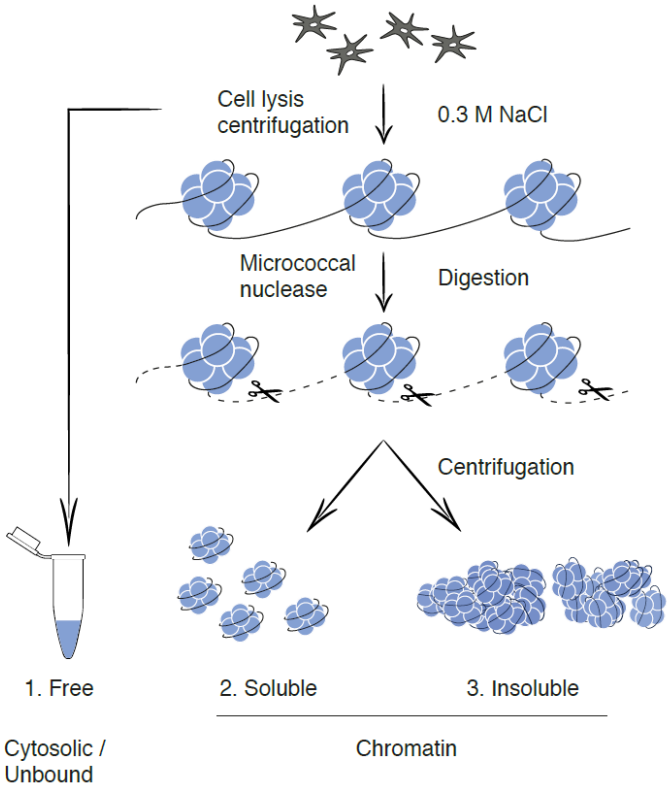

Figure EV1 - Chromatin fractionation.
Flow diagram illustrating the chromatin dissection after removal of unbound or loosely bound (free) proteins by salt extraction (0.3 M NaCl). MNase digestion removes linker DNA thus generating a supernatant of solubilized chromatin proteins and a remaining insoluble pellet strongly enriched in nucleosome cores.

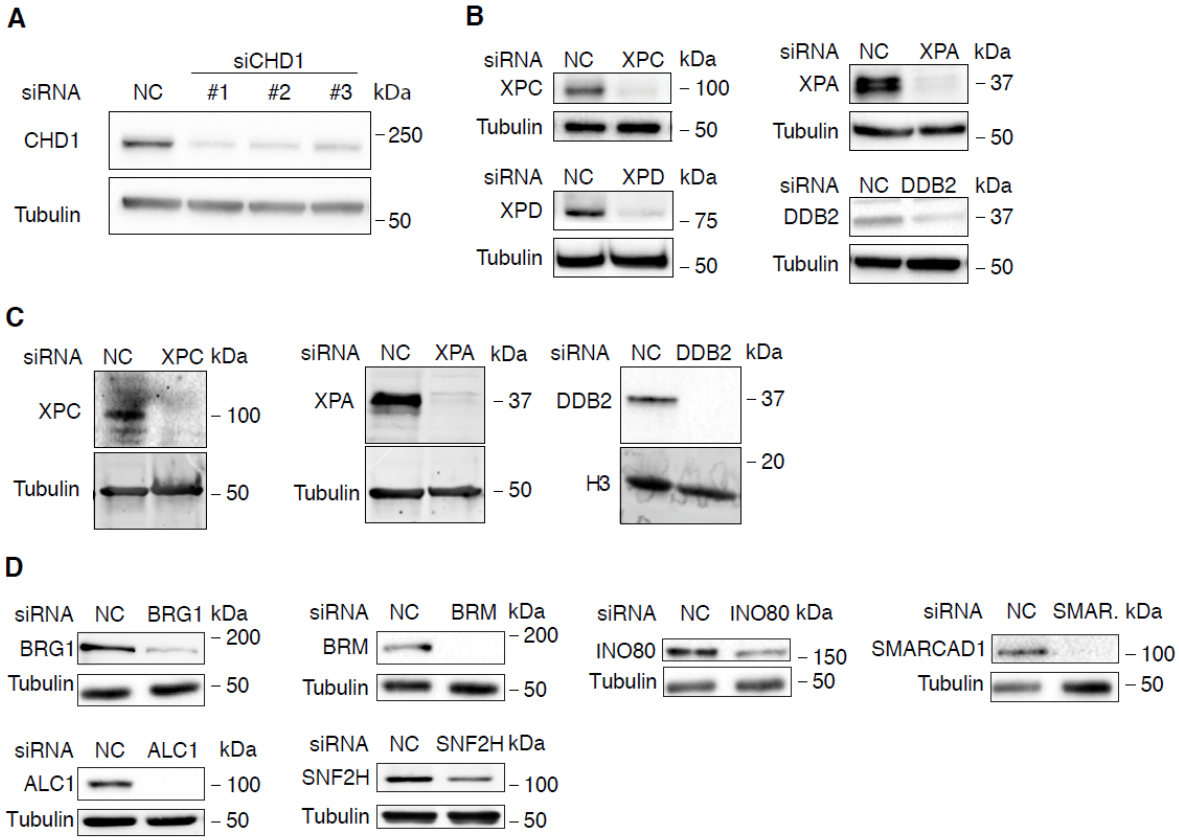

Figure EV2 - Efficiency of siRNA mediated protein depletion.

A Analysis of CHD1 protein levels after depletion with three different siRNA sequences (16 nM) directed against the CHD1 transcript. Immunoblots of HeLamnym,kfg cell lysates were carried out two days after transfection. Tubulin served as the loading control.

B Protein depletion achieved in U2OS cells two days after transfection with the indicated siRNA sequences (16 nm).

C Protein depletion achieved in HeLa cells two days after transfection with the indicated siRNA sequences (16 nm). Tubulin and histone H3 served as loading controls.

D Protein depletion achieved in HeLa cells two days after transfection with siRNA sequences (16 nM) against the indicated chromatin remodelers. Tubulin served as the loading control.

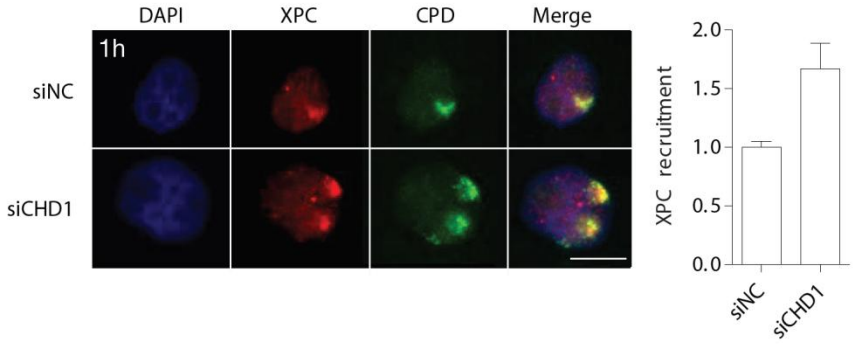

Figure EV3 - XPC accumulation in the chromatin of UV-irradiated HeLa cells.
Representative immunofluorescence images of HeLa cells that were UV-irradiated (dose applied to filters: 100 J/m^2) through micropore filters to generate local spots of DNA damage. Immunostaining was carried out after 1 h with antibodies against CPDs and XPC protein. Cells were pretreated two days earlier with siRNA targeting the CHD1 transcript (siCHD1) or with non-coding control RNA (siNC). DAPI was used to stain nuclear DNA. Scale bar: 10 µm. The recruitment of XPC protein was quantified by measuring spot intensities followed by normalization to the nuclear background. Control values were set to 1. Data information: Data are presented as mean ± SEM (n = 3, 100 cells for each experiment). **P ≤ 0.01 (unpaired, two-tailed t-test).

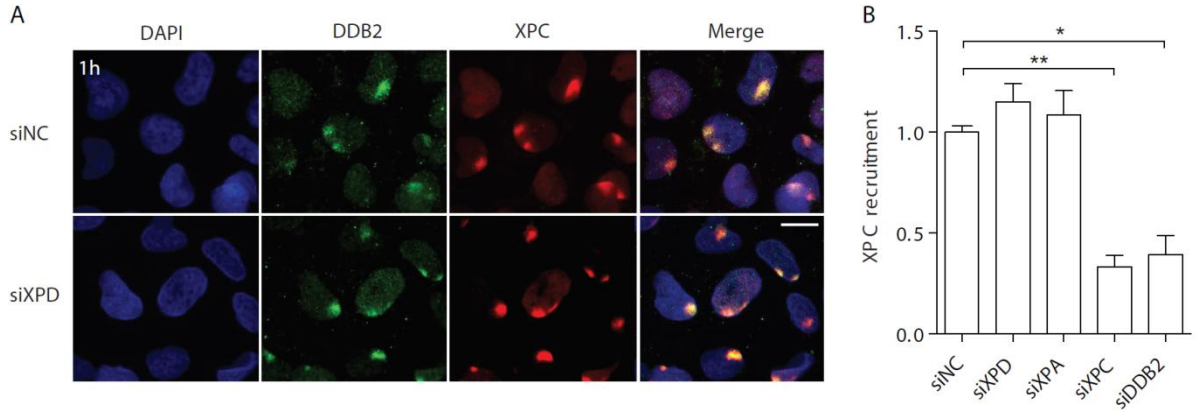

Figure EV4 - XPC recruitment to local spots of UV damage.

A Representative immunofluorescence images of U2OS cells that were UV-irradiated (dose applied to filters: 100 J/m^2) through micropore filters to generate local spots of DNA damage. Immunostaining was carried out after 1 h with antibodies against DDB2 (as a marker of UV lesions) and XPC proteins. Cells were pretreated two days earlier with siRNA targeting the XPD transcript (siXPD) or with non-coding control RNA (siNC). DAPI was used to stain nuclear DNA. Scale bar: 10 µm.

B The recruitment of XPC protein was quantified by measuring spot intensities followed by normalization to the nuclear background. Control values were set to 1. Cells were pretreated two days earlier with siRNA targeting the XPD, XPA, XPC or DDB2 transcripts, as indicated, or with non-coding control RNA (siNC).

Data information: In B, data are presented as mean ± SEM (*n* = 3, 100 cells for each experiment). **P ≤ 0.01 (unpaired, two-tailed t-test).

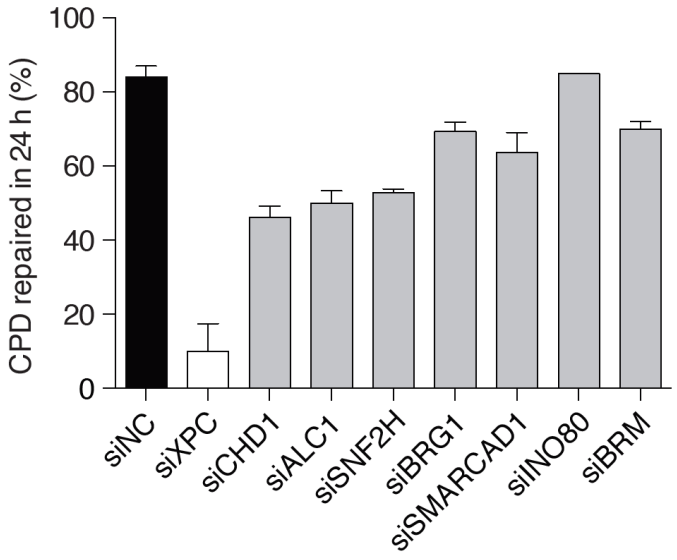

Figure EV5 - Comparison between chromatin remodelers.
Excision of CPDs in HeLa cells treated with siRNA (16 nM) targeting the indicated chromatin-remodeling factors, compared to transfection with siNC. The cells were UV-irradiated (10 J/m^2) two days after siRNA transfections and the proportion of excised CPDs was determined after a repair incubation of 24 h. The efficiency of protein down regulation is shown in the immunoblots of Figures EV2A and EV2D.
Data information: Data are presented as mean ± SEM (n = 5-7 independent experiments with 4 replicates). ****P ≤ 0.0001, ***P ≤ 0.001, *P ≤ 0.05 (unpaired, two-tailed t-test).

Appendix

The CHD1 remodeler promotes XPC to TFIIH handoffs on nucleosomes during DNA repair of UV lesions

Peter Rüthemann‡, Chiara Balbo Pogliano‡, Tamara Codilupi, Zuzana Garajovà and Hanspeter Naegeli

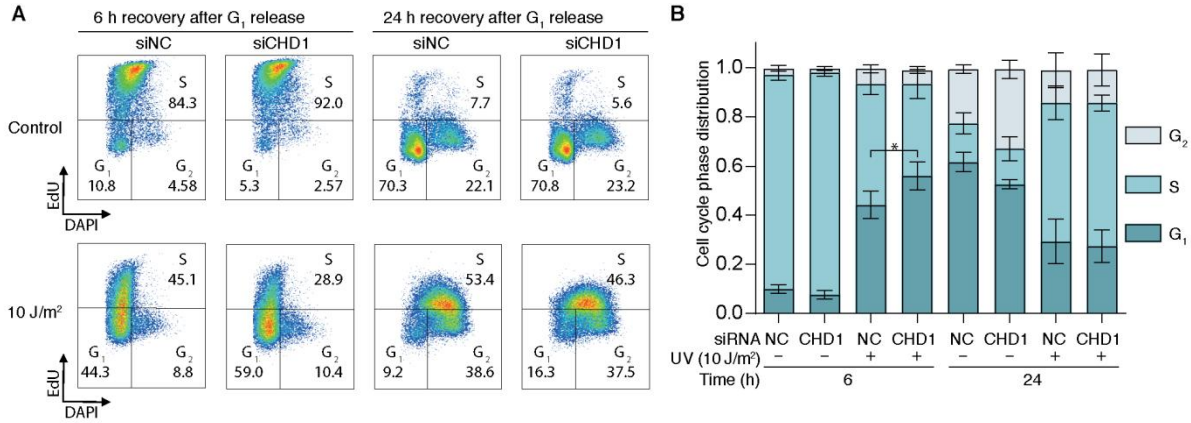

Appendix Figure S1 - Cell cycle arrest induced by UV irradiation

A HeLa cells were released from mimosine-induced G1 arrest 6 and 24 h before analysis. DNA replication was monitored by EdU incorporation. Cells were fixed, stained with DAPI and analyzed by flow cytometry.

B Quantification of cell cycle phases. The increased degree of G1-S arrest in cells depleted of CHD1 and subsequently UV-irradiated, is consistent with their reduced efficiency in repairing CPDs.

Data information: In B, data are presented as mean ± SEM (n = 3 independent experiments). *P ≤ 0.05 (unpaired, two-tailed t-test).

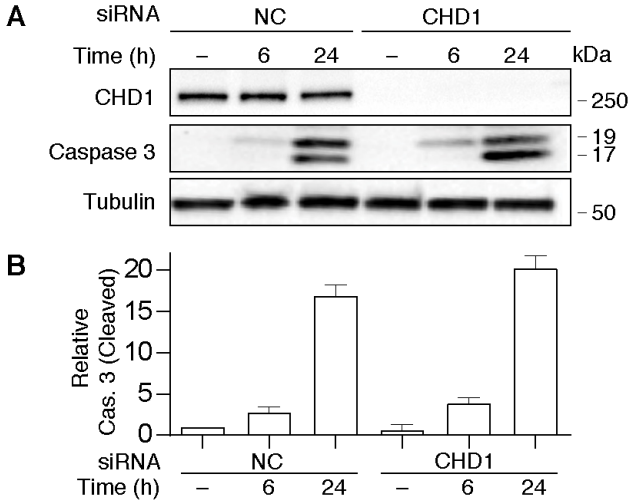

Appendix Figure S2 - Apoptotic response.

A Caspase 3 cleavage indicating that the depletion of CHD1 does not induce apoptosis in unchallenged U2OS cells. Caspase 3 cleavage is observed upon UV irradiation (10 J/m^2), particularly following 24 h-long incubations. The cleavage products migrate as polypeptides of 17 and 19 kDa. Tubulin served as the loading control.

B Quantification of immunoblots. Polypeptide fragments resulting from caspase 3 cleavage were normalized to their constitutive level in unchallenged cells. The slightly increased caspase 3 activation in UV-irradiated cells previously transfected with siRNA against CHD1, relative to non-coding (NC) RNA controls, is consistent with a role of CHD1 in repairing CPDs.

Data information: In B, data are presented as mean ± SEM (*n* = 3 independent experiments).

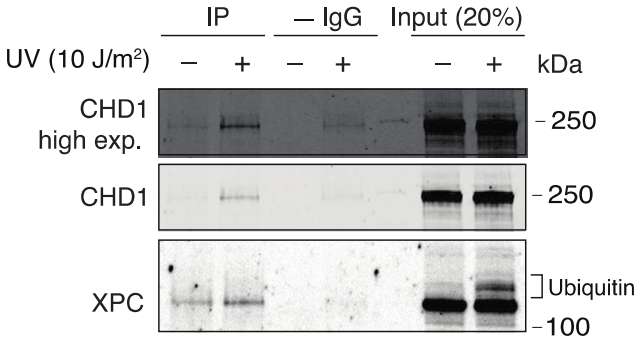

Appendix Figure S3 - Immunoprecipitation of XPC and CHD1 with anti-XPC antibodies.

Longer exposure of the immunoblot of Fig 3D revealing a low background association of CHD1 with XPC in unchallenged cells (first lane from the left). HeLa cells were mock-treated or UV-treated as indicated. Following a 1-h incubation, the chromatin was salt-extracted and, after MNase fragmentation, dissolved by sonication. Immunoprecipitation was carried out with anti-XPC antibodies. Input fractions and immunoprecipitated (IP) complexes were analyzed by blotting with antibodies against XPC and CHD1; –IgG, control pull-down reactions without antibodies.

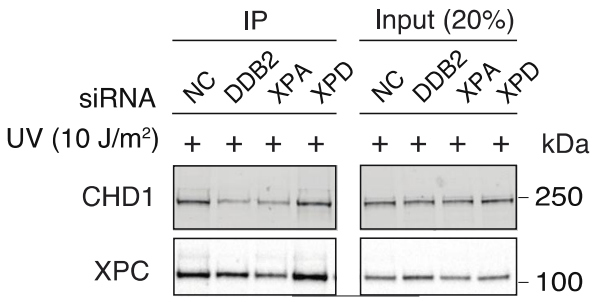

Appendix Figure S4 - Effect of GG-NER factors on XPC-CHD1 interactions.

HeLa cells were transfected with the indicated siRNA sequences two days before UV irradiation. Following a 1-h incubation, the irradiated cells were processed for immunoprecipitation with anti-XPC antibodies as in Fig 3D. After immunoblotting, the level of co-immunoprecipitated CHD1 was quantified and normalized to the corresponding amount of immunoprecipitated XPC in each individual sample. The protein depletions changed the efficiency of XPC immunoprecipitation, but quantifications did not reveal any significant difference in the degree by which CHD1 is co-immunoprecipitated with XPC protein using anti-XPC antibodies

4 Discussion

Posttranslational modifications including ubiquitination have emerged as key regulatory mechanisms in the cellular response to DNA damage (Brinkmann et al., 2015; Brown and Jackson, 2015). As a consequence, different approaches in cancer therapy attempt to target the ubiquitination system to improve cellular responsiveness toward therepeutic agents (Huang and Dixit, 2016). Cullin-RING E3 ubiquitin ligases (CRLs) build the largest family of ubiquitin ligases with numerous biological functions in cell signaling and DNA maintenance such as replication and repair. CRLs play not only an important role in cancer development and progression, but are also capable to modify the efficacy of chemotherapeutic drugs (Abbas and Dutta, 2011; Lee and Zhou, 2010; Terai et al., 2010). The activation of CRLs requires a neddylation reaction that can be blocked by the recently developed small molecule inhibitor MLN4924, which is currently under investigation in clinical trials against diverse malignancies (Shah et al., 2016; Soucy et al., 2009). In addition, preclinical studies demonstrated its ability to potentiate the cytotoxic effect of DNA crosslinking agents, suggesting a possible mechanisms to mitigate clinical drug resistances (Garcia et al., 2014; Kee et al., 2012; Tanaka et al., 2012). However, the role of each particular ubiquitin ligase and the mechanisms of this synergy are poorly understood. In my thesis, I aimed to elucidate in more detail how CRLs modulate the cellular response toward the DNA interstrand crosslinking agents cisplatin and mitomycin C (MMC). I could demonstrate that the effect of MLN4924 is in particular mediated via inhibition of CRL4. Inactivation of the CRL4 ubiquitin ligase complex by depletion of the cullin 4A and 4B (CUL4A/B) scaffold proteins potentiated the cytotoxic effect of cisplatin and MMC by suppressing the activation of the S-phase cell cycle checkpoint following ICLs. Specifically, my findings suggest that stabilization of CDT1 in CRL4-deficient cells induced aberrant DNA re-replication that masked the presence of ICL-induced single-stranded DNA (ssDNA). Consequently, cells lacking CRL4 are incapable to signal the presence of DNA damage and this deficiency ultimately triggers crosslink-induced cell death.

In an initial screen targeting individual CRLs by siRNA-mediated depletion of the cullin scaffolds, we identified CLR4 as an important factor in modulating cisplatin sensitivity in HeLa cells. The CRL4 complexes represent a broad family of ubiquitin ligases that are formed by assembly with different substrate receptors. The substrate

receptors are linked via the adaptor protein DDB1 to one of the two closely related scaffold proteins CUL4A and CUL4B. The two paralogs CUL4A and CUL4B share high sequence similarity and have mainly redundant functions by recruiting a widely overlapping set of substrate receptors (Cavadini et al., 2016; Fischer et al., 2011a; Hannah and Zhou, 2015; Jackson and Xiong, 2009). Importantly, only concomitant depletion of CUL4A and CUL4B or of the adaptor protein DDB1 sensitized HeLa cells toward cisplatin and MMC, whereas single knockdowns of only one cullin 4 had no effect regarding survival, confirming the redundancy of CUL4A and CUL4B.

Inhibition of the neddylation pathway by MLN4924 in HeLa cells "phenocopied" the effect of the CUL4A/B knockdown. This sensitizing effect of MLN4924 was clearly reduced in cells lacking CUL4A/B, indicating that MLN4924 exerts its function via inactivation of CRL4. It is possible that the remaining activity of MLN4924 in CRL4-deficient cells is mediated via inhibition of CRL3 as depletion of CUL3 had a similar effect than knockdown of CUL4A/B regarding cisplatin sensitivity. A synergistic effect of CUL3 depletion with cisplatin has been previously described (Jazaeri et al., 2013) in ovarian cancer cell lines. Similar to our findings, depletion of other cullins than CUL3 had either no effect or even slightly supported survival upon cisplatin. Of note, in this study only single depletions of CUL4A and CUL4B had been performed that did not affect cisplatin sensitivity, most probably due to their redundant functions.

The cytotoxic effect of cisplatin is mediated by its ability to covalently bind to the DNA, thereby generating DNA inter- and intrastrand crosslinks. Interstrand crosslinks (ICLs) display their toxicity by inhibiting transcription and DNA replication that ultimately triggers cell death (Kelland, 2007). The initial steps in ICL repair during DNA replication requires proteins of the Fanconi anemia (FA) pathway and the subsequent resolution of the damage involves the combined action of additional DNA damage-processing systems such as homologous recombination (HR), nucleotide excision repair (NER) and translesion synthesis (TLS). However, the mechanism of checkpoint activation by cisplatin is still controversial. It was previously shown that the FANCM/FAAP24 complex initiates the checkpoint response to ICLs without generation of ssDNA intermediates. The available data suggested a remodeling of the replication fork by FANCM/FAAP24 that leads to the recruitment of replication protein A (RPA) (Huang et al., 2010). On the other hand, many other studies reported the formation of persistent stretches of ICL induced ssDNA (Higgs et al., 2015; Murina et al., 2014; Unno et al., 2014; Zellweger et al., 2015). I found that the

increase in ssDNA levels observed after cisplatin treatment depends on FANCD2, which is an indispensable factor for the subsequent resection of the double strand break created after ICL incision to enable repair by HR (Unno et al., 2014). The ssDNA stretches resulting from this nucleolytic process act as an initiating signal for ICL-induced S-phase checkpoint responses by recruitment of RPA and subsequent activation of the ATR pathway. Although FANCD2 is recruited following assembly of the FA core complex, depletion of FANCM or FAAP24 had no effect on the formation of ssDNA. We cannot exclude that the remaining level of these proteins upon siRNA-mediated knockdown are sufficient for damage recognition and repair initiation. However, a plausible explanation is the involvement of UHRF1 (ubiquitin-like with PHD and RING finger domain 1), a recently discovered factor in ICL sensing that precedes FANCD2 recruitment and might act in parallel to the core FA pathway (Liang et al., 2015; Lopez-Martinez et al., 2016; Tian et al., 2015).

I further found that the CRL4 ubiquitin ligase activity is crucial for the formation of the ssDNA-RPA platform. Cells lacking CRL4 are unable to generate the full ssDNA-RPA2 initiated signaling response following ICL formation. CRL4 thereby potentiates the cytotoxic effect of cisplatin and MMC in the tested HeLa cells. The cisplatin-induced replication inhibition observed in CRL4-proficient HeLa cells was drastically abrogated in CRL4-deficient cells, which as a consequence also show a substantial increase of mitotic cells compared to CRL4-proficient controls. The activation of ATR by ssDNA-RPA and its function in the inhibition of replication have been extensively studied (Ben-Yehoyada et al., 2009; Brown, 2003; Olson et al., 2006; Zou and Elledge, 2003) and the chemosensitizing effect of ATR inhibition has been previously reported (Huntoon et al., 2013; Li et al., 2016a; Mohni et al., 2015).

The vast majority of damage induced by cisplatin are intrastrand crosslinks that are repaired by the NER pathway (Eastman, 1986; Fichtinger-Schepman et al., 1985; Hansson and Wood, 1989; Payne and Chu, 1994), whereby excision of the damage also results in ssDNA-RPA intermediates (Rubbi and Milner, 2001). Because $CRL4A^{DDB2}$ has an essential function in damage recognition during NER, I was wondering whether we suppress the excision of intrastrand crosslinks by depletion of CUL4A. However, I observed that the level of ssDNA is not reduced in cells depleted of XPA protein, a central player in the NER process. This results further support the finding that CRL4 functions in ICL repair. CRL4 has an essential role in DNA replication by regulating the turnover of the

replication licensing factor CDT1. After an origin has initiated replication, CDT1 is degraded by $CRL4^{CDT2}$ to prevent re-initiation of the same origin (Arias and Walter, 2006; Jin et al., 2006; Lovejoy et al., 2006). This mechanism ensures that DNA is replicated only once per cell cycle with the consequence that loss of licensing control leads to aberrant replication including re-replication that causes genome instability and drives tumorigenesis (Arentson et al., 2002; Neelsen et al., 2013). In addition to its function during normal replication, CDT1 proteolysis is an important mechanisms to arrest replication while DNA repair is in progress (Ballabeni et al., 2009; You and Masai, 2008). Hence, exposure to DNA-damaging agents induces rapid degradation of CDT1 through CRL4-mediated ubiquitination, thereby ensuring arrest of the cell cycle (Higa et al., 2003; Hu and Xiong, 2006; Roukos et al., 2011; Stathopoulou et al., 2012). It is known that ectopic expression of CDT1 promotes re-replication in human cells and subsequent activation of the DNA damage response (DDR) signaling (Arias and Walter, 2006; Jin et al., 2006; Lin and Dutta, 2007; Liontos et al., 2007; Pan et al., 2013). Accordingly, I observed higher constitutive levels of CDT1 in CRL4- deficient cells and partially re-replicated DNA is evident. Moreover, CRL4-deficient cells display a significant amount of ssDNA and strongly accumulate in G2/M phase of the cell cycle, providing evidence of severe replication stress caused by aberrant DNA synthesis. Uncontrolled origin firing and DNA re-replication is on its own highly deleterious due to resulting fork breakage and DNA fragmentation (Alexander and Orr-Weaver, 2016; Neelsen et al., 2013). In fact, depletion of DDB1, which results in a stronger inhibition of CRL4 complexes compared to the concomitant knockdown of its cullin scaffolds, induces massive cell death.

Exposure to cisplatin induces a rapid degradation of CDT1 in CRL4-proficientHeLa cells, whereas CRL4-deficient cells display stabilized CTD1 levels. Surprisingly, the initial higher levels of ssDNA in CRL4-deficient cells are not further increased by treatment with DNA-crosslinking agents. Indeed, cisplatin generates a significant amount of ssDNA in a dose-dependent manner in control cells but not in CRL4-deficient cells. Accordingly, the extent of RPA binding is reduced in CRL4-deficient cells compared to CRL4-proficient controls. Taken together, these findings suggest that ICL-induced ssDNA is masked by the uncontrolled re-replication as a result of CDT stabilization. The ssDNA-RPA complex and subsequent phosphorylation events of RPA2 (the middle subunit of RPA) play a central role in the DNA damage response by coordinating the recruitment and exchange of genome maintenance factors such as ATR that protect the replication fork (Maréchal and

Zou, 2015; Murphy et al., 2014; Zou and Elledge, 2003). In fact, I found a markedly reduced phosphorylation of ATR targets in CRL4-deficient cells upon exposure to ICL-agents. This includes a reduced phosphorylation of RPA2 (at position Ser33), CHK1 (at Ser345) and histone H2AX. These observation indicate that CRL4-dependent inhibition of the checkpoint response potentiate the cytotoxicity of ICLs by suppressing their repair. We observed the same checkpoint deficiency using the neddylation inhibitor MLN4924 in combination with cisplatin or MMC, demonstrating that suppression of the DDR via CDT1 stabilization represents a key mechanism in the synergistic effect of CRL-inhibition and ICLs. In fact, CDT1 stabilization has been identified by several groups as a central mechanism by which MLN4924 exerts its anti-tumor activity (Lin et al., 2010; Milhollen et al., 2011; Pan et al., 2013). Interestingly, Kee et al. (2012) further demonstrated the importance of the Nedd8-conjugation system in the activation of the DDR following exposure to various genotoxic agents. In particular, they observed highly reduced CHK1 and FANCD2 activation, both representing downstream targets of ATR, upon depletion of the UBE2M, which is an E2 conjugating-enzyme for Nedd8.

Re-replication as a mechanism to suppress the ICL response seems to be at first sight counterintuitive, especially as deregulated origin firing itself activates DDR following formation of ssDNA gaps. A possible explanation is that ssDNA stretches induced by ICLs become themselves a template for additional replication rounds, such that most of this ssDNA is readily reconverted to double stranded DNA. By this process, re-replication near ICL sites would be able to mask ssDNA as the key signal for checkpoint activation. Hence, in addition to the CDT1-induced over-replication, cells also display a defect in the suppressive function of the DDR system on DNA replication. In unchallenged CRL4-deficient cells, however, cell cycle checkpoints are efficiently activated. In fact, DNA synthesis is markedly reduced in those cells compared to control cells and CRL4 depletion further induces the accumulation in G2/M phase of the cell cycle. The ATR pathway is the major mechanism that counteracts re-replication when licensing control is disruption (Lin and Dutta, 2007; Liu et al., 2007; Zhu and Dutta, 2006). Thus, cells with intact ATR signaling might be able to evade cell death triggered by re-replication e.g. induced by CRL4 inhibition. The combination of CRL4 inhibitors like MLN4924 with crosslinking agents represents a possible new strategy not only to increase the extent of DNA damage but also to inhibit checkpoint activation by ICLs to prevent their proper repair.

The future challenge is to develop selective CRL4 inhibitor to avoid adverse effects due to the blockage of other CRLs. Moreover, by exchanging its substrate receptors, CRL4 complexes can target a high number of proteins. A large-scale screen identified nearly 300 different CRL4 targets and many of those have functions in DNA metabolism, repair and replication (Emanuele et al., 2011). It is, therefore, possible that other CRL4 substrates than CDT1 contribute to the sensitizing effect toward ICLs. A comprehensive analysis of the involved substrates and substrate receptors would definitely be of great interest to achieve highest specificity of potential CRL4 inhibitors. We also have to consider that beside its function in protein degradation, some substrates including for example proliferating cell nuclear antigen (PCNA) or histones are monoubiquitinated by CRL4, thus exerting a regulatory function without affecting protein stability (Hu et al., 2012; Terai et al., 2010; Zeng et al., 2016). Another important goal for the next future is to identify cancer subtypes that are susceptible to the combined treatment strategy of CRL inhibitors with cisplatin. Overexpression of CRL4 subunits including the scaffolds CUL4A and CUL4B, the adaptor DDB1 or the substrate receptor CDT2 have been described for several tumors and were associated with poor treatment responses (Eastman, 1986; Hannah and Zhou, 2015; Yan et al., 2017). In particular, due to the enhance replication stress and DNA damage intrinsically present in cancer cells, some tumors might rely on a substantial CDT2 expression (Olivero et al., 2014; Yan et al., 2017). Of course, those cells might be particularly vulnerable to CRL4 inhibition. Thorough evaluation of biomarkers will be necessary to identify patients that would profit from such a combined treatment of CRLs inhibitors with cisplatin.

5 References

Abbas, T., and Dutta, A. (2011). CRL4 Cdt2: Master coordinator of cell cycle progression and genome stability. Cell Cycle 10, 241–249.

Akagi, H., Higuchi, H., Sumimoto, H., Igarashi, T., Kabashima, A., Mizuguchi, H., Izumiya, M., Sakai, G., Adachi, M., Funakoshi, S., et al. (2013). Suppression of myeloid cell leukemia-1 (Mcl-1) enhances chemotherapy-associated apoptosis in gastric cancer cells. Gastric Cancer 16, 100–110.

Akhoondi, S., Sun, D., von der Lehr, N., Apostolidou, S., Klotz, K., Maljukova, A., Cepeda, D., Fiegl, H., Dofou, D., Marth, C., et al. (2007). FBXW7/hCDC4 is a general tumor suppressor in human cancer. Cancer Res. 67, 9006–9012.

Albertella, M.R., Green, C.M., Lehmann, A.R., and O'Connor, M.J. (2005). A role for polymerase in the cellular tolerance to cisplatin-induced damage. Cancer Res. 65, 9799–9806.

Alexander, J.L., and Orr-Weaver, T.L. (2016). Replication fork instability and the consequences of fork collisions from rereplication. Genes Dev. 30, 2241–2252.

Apps, M.G., Choi, E.H.Y., and Wheate, N.J. (2015). The state-of-play and future of platin drugs. Endocr. Relat. Cancer 22, 219–233.

Archange, C., Nowak, J., Garcia, S., Moutardier, V., Calvo, E.L., Dagorn, J.-C., and Iovanna, J.L. (2008). The WSB1 gene is involved in pancreatic cancer progression. PLoS ONE 3, e2475.

Arentson, E., Faloon, P., Seo, J., Moon, E., Studts, J.M., Fremont, D.H., and Choi, K. (2002). Oncogenic potential of the DNA replication licensing protein CDT1. Oncogene 21, 1150–1158.

Arias, E.E., and Walter, J.C. (2006). PCNA functions as a molecular platform to trigger Cdt1 destruction and prevent re-replication. Nat. Cell Biol. 8, 84–90.

Ballabeni, A., Zamponi, R., Caprara, G., Melixetian, M., Bossi, S., Masiero, L., and Helin, K. (2009). Human CDT1 Associates with CDC7 and Recruits CDC45 to Chromatin during S Phase. J. Biol. Chem. 284, 3028–3036.

Bando, T., Iida, H., Tao, Z.-F., Narita, A., Fukuda, N., Yamori, T., and Sugiyama, H. (2003). Sequence specificity, reactivity, and antitumor activity of DNA-alkylating pyrrole-imidazole diamides. Chem. Biol. 10, 751–758.

Bao, L.-J., Jaramillo, M.C., Zhang, Z.-B., Zheng, Y.-X., Yao, M., Zhang, D.D., and Yi, X.-F. (2014). Nrf2 induces cisplatin resistance through activation of autophagy in ovarian carcinoma. Int J Clin Exp Pathol 7, 1502–13.

Barakat, B.M., Wang, Q.-E., Han, C., Milum, K., Yin, D.-T., Zhao, Q., Wani, G., Arafa, E.-S.A., El-Mahdy, M.A., and Wani, A.A. (2010). Overexpression of DDB2 enhances the sensitivity of human ovarian cancer cells to cisplatin by augmenting cellular apoptosis. Int. J. Cancer 127, 977–988.

Barckhausen, C., Roos, W.P., Naumann, S.C., and Kaina, B. (2013). Malignant melanoma cells acquire resistance to DNA interstrand cross-linking chemotherapeutics by p53-triggered upregulation of DDB2/XPC-mediated DNA repair. Oncogene 1–11.

Bartkova, J., Hořejší, Z., Koed, K., Krämer, A., Tort, F., Zieger, K., Guldberg, P., Sehested, M., Nesland, J.M., Lukas, C., et al. (2005). DNA damage response as a candidate anti-cancer barrier in early human tumorigenesis. Nature 434, 864–870.

Basu, A., and Krishnamurthy, S. (2010). Cellular responses to cisplatin-induced DNA damage. J. Nucleic Acids 2010, 1–16.

Ben-Yehoyada, M., Wang, L.C., Kozekov, I.D., Rizzo, C.J., Gottesman, M.E., and Gautier, J. (2009). Checkpoint Signaling from a Single DNA Interstrand Crosslink. Mol. Cell 35, 704–715.

Biehs, R., Steinlage, M., Barton, O., Juhász, S., Künzel, J., Spies, J., Shibata, A., Jeggo, P.A., and Löbrich, M. (2017). DNA Double-Strand Break Resection Occurs during Non-homologous End Joining in G1 but Is Distinct from Resection during Homologous Recombination. Mol. Cell 65, 671–684.e5.

Brinkmann, K., Schell, M., Hoppe, T., and Kashkar, H. (2015). Regulation of the DNA damage response by ubiquitin conjugation. Front. Genet. 6.

Brown, E.J. (2003). Essential and dispensable roles of ATR in cell cycle arrest and genome maintenance. Genes Dev. 17, 615–628.

Brown, J.S., and Jackson, S.P. (2015). Ubiquitylation, neddylation and the DNA damage response. Open Biol. 5, 150018–150018.

Brown, D.P.G., Chin-Sinex, H., Nie, B., Mendonca, M.S., and Wang, M. (2009). Targeting superoxide dismutase 1 to overcome cisplatin resistance in human ovarian cancer. Cancer Chemother. Pharmacol. 63, 723–730.

Cardozo, T., and Pagano, M. (2004). The SCF ubiquitin ligase: insights into a molecular machine. Nat. Rev. Mol. Cell Biol. 5, 739–751.

Cavadini, S., Fischer, E.S., Bunker, R.D., Potenza, A., Lingaraju, G.M., Goldie, K.N., Mohamed, W.I., Faty, M., Petzold, G., Beckwith, R.E.J., et al. (2016). Cullin–RING ubiquitin E3 ligase regulation by the COP9 signalosome. Nature 531, 598–603.

Ceccaldi, R., Sarangi, P., and D'Andrea, A.D. (2016). The Fanconi anaemia pathway: new players and new functions. Nat. Rev. Mol. Cell Biol.

Chan, C.-H., Morrow, J.K., Li, C.-F., Gao, Y., Jin, G., Moten, A., Stagg, L.J., Ladbury, J.E., Cai, Z., Xu, D., et al. (2013). Pharmacological inactivation of Skp2 SCF ubiquitin ligase restricts cancer stem cell traits and cancer progression. Cell 154, 556–568.

Chao, A., and Wang, T.-H. (2016). Molecular mechanisms for synergistic effect of proteasome inhibitors with platinum-based therapy in solid tumors. Taiwan. J. Obstet. Gynecol. 55, 3–8.

Chen, H.H.W., and Kuo, M.T. (2010). Role of glutathione in the regulation of cisplatin resistance in cancer chemotherapy. Met.-Based Drugs 2010, 1–7.

Chen, Q.-R., Bilke, S., Wei, J.S., Greer, B.T., Steinberg, S.M., Westermann, F., Schwab, M., and Khan, J. (2006). Increased WSB1 copy number correlates with its over-expression which associates with increased survival in neuroblastoma. Genes. Chromosomes Cancer 45, 856–862.

Chen, X., Velmurugu, Y., Zheng, G., Park, B., Shim, Y., Kim, Y., Liu, L., Van Houten, B., He, C., Ansari, A., et al. (2015). Kinetic gating mechanism of DNA damage recognition by Rad4/XPC. Nat. Commun. 6, 5849.

Cheung-Ong, K., Giaever, G., and Nislow, C. (2013). DNA-Damaging Agents in Cancer Chemotherapy: Serendipity and Chemical Biology. Chem. Biol. 20, 648–659.

Choi, D.W., Seo, Y.-M., Kim, E.-A., Sung, K.S., Ahn, J.W., Park, S.-J., Lee, S.-R., and Choi, C.Y. (2008). Ubiquitination and degradation of homeodomain-interacting protein kinase 2 by WD40 repeat/SOCS box protein WSB-1. J. Biol. Chem. 283, 4682–4689.

Chou, J.-L., Su, H.-Y., Chen, L.-Y., Liao, Y.-P., Hartman-Frey, C., Lai, Y.-H., Yang, H.-W., Deatherage, D.E., Kuo, C.-T., Huang, Y.-W., et al. (2010). Promoter hypermethylation of FBXO32, a novel TGF-b/ SMAD4 target gene and tumor suppressor, is associated with poor prognosis in human ovarian cancer. Lab. Invest. 90, 414–425.

Chung, D., and Dellaire, G. (2015). The Role of the COP9 Signalosome and Neddylation in DNA Damage Signaling and Repair. Biomolecules 5, 2388–2416.

Ciccia, A., and Elledge, S.J. (2010). The DNA Damage Response: Making It Safe to Play with Knives. Mol. Cell 40, 179–204.

Ciechanover, A. (1998). The ubiquitin–proteasome pathway: on protein death and cell life. EMBO J. 17, 7151–7160.

Clauson, C., Schärer, O.D., and Niedernhofer, L. (2013). Advances in understanding the complex mechanisms of DNA interstrand cross-link repair. Cold Spring Harb. Perspect. Biol. 5, a012732.

Cortez, D., Wang, Y., Qin, J., and Elledge, S.J. (1999). Requirement of ATM-Dependent Phosphorylation of Brca1 in the DNA Damage Response to Double-Strand Breaks. Science 286, 1162–1166.

Dasari, S., and Tchounwou, P.B.T. (2014). Cisplatin in cancer therapy: Molecular mechanisms of action. Eur. J. Pharmacol. 740, 364–378.

Dash, A., Pettus, J.A., Herr, H.W., Bochner, B.H., Dalbagni, G., Donat, S.M., Russo, P., Boyle, M.G., Milowsky, M.I., and Bajorin, D.F. (2008). A role for neoadjuvant gemcitabine plus cisplatin in muscle-invasive urothelial carcinoma of the bladder: A retrospective experience. Cancer 113, 2471–2477.

Davies, A.M., Chansky, K., Lara, P.N., Gumerlock, P.H., Crowley, J., Albain, K.S., Vogel, S.J., and Gandara, D.R. (2009). Bortezomib plus gemcitabine/carboplatin as first-line treatment of advanced non-small cell lung cancer: a phase II Southwest Oncology Group Study (S0339). J. Thorac. Oncol. 4, 87–92.

Day, R.S., Ziolkowski, C.H.J., Scudiero, D.A., Meyer, S.A., Lubiniecki, A.S., Girardi, A.J., Galloway, S.M., and Bynum, G.D. (1980). Defective repair of alkylated DNA by human tumour and SV40-transformed human cell strains. Nature 288, 724–727.

Dilruba, S., and Kalayda, G.V. (2016). Platinum-based drugs: past, present and future. Cancer Chemother. Pharmacol. 77, 1103–1124.

Ding, Q., He, X., Hsu, J.-M., Xia, W., Chen, C.-T., Li, L.-Y., Lee, D.-F., Liu, J.-C., Zhong, Q., Wang, X., et al. (2007). Degradation of Mcl-1 by -TrCP Mediates Glycogen Synthase Kinase 3-Induced Tumor Suppression and Chemosensitization. Mol. Cell. Biol. 27, 4006–4017.

Ding, Z., Zu, S., and Gu, J. (2016). Evaluating the molecule-based prediction of clinical drug responses in cancer. Bioinformatics btw344.

Donawho, C.K., Luo, Y., Luo, Y., Penning, T.D., Bauch, J.L., Bouska, J.J., Bontcheva-Diaz, V.D., Cox, B.F., DeWeese, T.L., Dillehay, L.E., et al. (2007). ABT-888, an Orally Active Poly(ADP-Ribose) Polymerase Inhibitor that Potentiates DNA-Damaging Agents in Preclinical Tumor Models. Clin. Cancer Res. 13, 2728–2737.

Dou, Q.P., and Zonder, J.A. (2014). Overview of proteasome inhibitor-based anti-cancer therapies: perspective on bortezomib and second generation proteasome inhibitors versus future generation inhibitors of ubiquitin-proteasome system. Curr. Cancer Drug Targets 14, 517–536.

Duan, L., Perez, R.E., Hansen, M., Gitelis, S., and Maki, C.G. (2014). Increasing cisplatin sensitivity by schedule-dependent inhibition of AKT and Chk1. Cancer Biol. Ther. 15, 1600–1612.

Duda, D.M., Borg, L.A., Scott, D.C., Hunt, H.W., Hammel, M., and Schulman, B.A. (2008). Structural insights into NEDD8 activation of cullin-RING ligases: conformational control of conjugation. Cell 134, 995–1006.

Eastman, A. (1986). Reevaluation of Interaction of cis-Dichloro(ethylenediamine)platinum(II) with DNA. Biochemistry (Mosc.) 25, 3912–39115.

Emanuele, M.J., Elia, A.E.H., Xu, Q., Thoma, C.R., Izhar, L., Leng, Y., Guo, A., Chen, Y.-N., Rush, J., Hsu, P.W.-C., et al. (2011). Global Identification of Modular Cullin-RING Ligase Substrates. Cell 147, 459–474.

Enchev, R.I., Schulman, B.A., and Peter, M. (2014). Protein neddylation: beyond cullin–RING ligases. Nat. Rev. Mol. Cell Biol. 16, 30–44.

Fichtinger-Schepman, A.M.J., Van der Veer, J.L., Den Hartog, J.H., Lohman, P.H., and Reedijk, J. (1985). Adducts of the antitumor drug cis-diamminedichloroplatinum (II) with DNA: formation, identification, and quantitation. Biochemistry (Mosc.) 24, 707–713.

Fischer, E.S., Scrima, A., Böhm, K., Matsumoto, S., Lingaraju, G.M., Faty, M., Yasuda, T., Cavadini, S., Wakasugi, M., Hanaoka, F., et al. (2011). The molecular basis of CRL4 DDB2/CSA ubiquitin ligase architecture, targeting, and activation. Cell 147, 1024–1039.

Friedman, A.A., Letai, A., Fisher, D.E., and Flaherty, K.T. (2015). Precision medicine for cancer with next-generation functional diagnostics. Nat. Rev. Cancer 15, 747–756.

Fuchs, S.Y., Chen, A., Xiong, Y., Pan, Z.-Q., and Ronai, Z. ’ev (1999). HOS, a human homolog of Slimb, forms an SCF complex with Skp1 and Cullin1 and targets the phosphorylation-dependent degradation of IkB and beta-catenin. Oncogene 18, 2039–2046.

Furfaro, A.L., Traverso, N., Domenicotti, C., Piras, S., Moretta, L., Marinari, U.M., Pronzato, M.A., and Nitti, M. (2016). The Nrf2/HO-1 axis in cancer cell growth and chemoresistance. Oxid. Med. Cell. Longev. 2016, 1–14.

Galluzzi, L., Senovilla, L., Vitale, I., Michels, J., Martins, I., Kepp, O., Castedo, M., and Kroemer, G. (2012). Molecular mechanisms of cisplatin resistance. Oncogene 31, 1869–1883.

Garcia, K., Blank, J.L., Bouck, D.C., Liu, X.J., Sappal, D.S., Hather, G., Cosmopoulos, K., Thomas, M.P., Kuranda, M., Pickard, M.D., et al. (2014). Nedd8-Activating Enzyme Inhibitor MLN4924 Provides Synergy with Mitomycin C through Interactions with ATR, BRCA1/BRCA2, and Chromatin Dynamics Pathways. Mol. Cancer Ther. 13, 1625–1635.

Genschik, P., Sumara, I., and Lechner, E. (2013). The emerging family of CULLIN3-RING ubiquitin ligases (CRL3s): cellular functions and disease implications. EMBO J. 32, 2307–2320.

Ghezraoui, H., Piganeau, M., Renouf, B., Renaud, J.-B., Sallmyr, A., Ruis, B., Oh, S., Tomkinson, A.E., Hendrickson, E., Giovannangeli, C., et al. (2014). Chromosomal Translocations in Human Cells Are Generated by Canonical Nonhomologous End-Joining. Mol. Cell 55, 829–842.

Gospodinov, A., and Herceg, Z. (2013). Shaping Chromatin for Repair. Mutat. Res. Mutat. Res. 752, 45–60.

Guan, L., Zhang, L., Gong, Z., Hou, X., Xu, Y., Feng, X., Wang, H., and You, H. (2016). FoxO3 inactivation promotes human cholangiocarcinoma tumorigenesis and chemoresistance via Keap1-Nrf2 signaling. Hepatology 63, 1914–1927.

Han, C., Wani, G., Zhao, R., Qian, J., Sharma, N., He, J., Zhu, Q., Wang, Q.-E., and Wani, A.A. (2015). Cdt2-mediated XPG degradation promotes gap-filling DNA synthesis in nucleotide excision repair. Cell Cycle 14, 1103–1115.

Hannah, J., and Zhou, P. (2015). Distinct and overlapping functions of the cullin E3 ligase scaffolding proteins CUL4A and CUL4B. Gene 573, 33–45.

Hansson, J., and Wood, R.D. (1989). Repair synthesis by human cell extracts in DNA damaged by cis-and trans-diamminedichloroplatinum (II). Nucleic Acids Res. 17, 8073–8091.

Hayden, A., Douglas, J., Sommerlad, M., Andrews, L., Gould, K., Hussain, S., Thomas, G.J., Packham, G., and Crabb, S.J. (2014). The Nrf2 transcription factor contributes to resistance to cisplatin in bladder cancer. Urol. Oncol. Semin. Orig. Investig. 32, 806–814.

Heo, J., Eki, R., and Abbas, T. (2016). Deregulation of F-box proteins and its consequence on cancer development, progression and metastasis. Semin. Cancer Biol. 36, 33–51.

Hidalgo, M., Bruckheimer, E., Rajeshkumar, N.V., Garrido-Laguna, I., De Oliveira, E., Rubio-Viqueira, B., Strawn, S., Wick, M.J., Martell, J., and Sidransky, D. (2011). A pilot clinical study of treatment guided by personalized tumorgrafts in patients with advanced cancer. Mol. Cancer Ther. 10, 1311–1316.

Higa, L.A.A., Mihaylov, I.S., Banks, D.P., Zheng, J., and Zhang, H. (2003). Radiation-mediated proteolysis of CDT1 by CUL4–ROC1 and CSN complexes constitutes a new checkpoint. Nat. Cell Biol. 5, 1008–1015.

Higgs, M.R., Reynolds, J.J., Winczura, A., Blackford, A.N., Borel, V., Miller, E.S., Zlatanou, A., Nieminuszczy, J., Ryan, E.L., Davies, N.J., et al. (2015). BOD1L Is Required to Suppress Deleterious Resection of Stressed Replication Forks. Mol. Cell 59, 462–477.

Ho, I.-L., Kuo, K.-L., Liu, S.-H.-, Chang, H.-C., Hsieh, J.-T., Wu, J.-T., Chiang, C.-K., Lin, W.-C., Tsai, Y.-C., Chou, C.-T., et al. (2015). MLN4924 Synergistically Enhances Cisplatin-induced Cytotoxicity via JNK and Bcl-xL Pathways in Human Urothelial Carcinoma. Sci. Rep. 5, 16948.

Hong, X., Liu, W., Song, R., Shah, J.J., Feng, X., Tsang, C.K., Morgan, K.M., Bunting, S.F., Inuzuka, H., Zheng, X.F.S., et al. (2016). SOX9 is targeted for proteasomal degradation by the E3 ligase FBW7 in response to DNA damage. Nucleic Acids Res. gkw748.

Howell, S.B., Safaei, R., Larson, C.A., and Sailor, M.J. (2010). Copper transporters and the cellular pharmacology of the platinum-containing cancer drugs. Mol. Pharmacol. 77, 887–894.

Hu, J., and Xiong, Y. (2006). An evolutionarily conserved function of proliferating cell nuclear antigen for Cdt1 degradation by the Cul4-Ddb1 ubiquitin ligase in response to DNA damage. J. Biol. Chem. 281, 3753–3756.

Hu, H., Yang, Y., Ji, Q., Zhao, W., Jiang, B., Liu, R., Yuan, J., Liu, Q., Li, X., Zou, Y., et al. (2012). CRL4B Catalyzes H2AK119 Monoubiquitination and Coordinates with PRC2 to Promote Tumorigenesis. Cancer Cell 22, 781–795.

Huang, X., and Dixit, V.M. (2016). Drugging the undruggables: exploring the ubiquitin system for drug development. Cell Res. 26, 484–498.

Huang, M., Kim, J.M., Shiotani, B., Yang, K., Zou, L., and D'Andrea, A.D. (2010). The FANCM/FAAP24 Complex Is Required for the DNA Interstrand Crosslink-Induced Checkpoint Response. Mol. Cell 39, 259–268.

Hung, M.-S., Chen, I.-C., You, L., Jablons, D.M., Li, Y.-C., Mao, J.-H., Xu, Z., Lung, J.-H., Yang, C.-T., and Liu, S.-T. (2016). Knockdown of cullin 4A inhibits growth and increases chemosensitivity in lung cancer cells. J. Cell. Mol. Med. 20, 1295–1306.

Huntoon, C.J., Flatten, K.S., Wahner Hendrickson, A.E., Huehls, A.M., Sutor, S.L., Kaufmann, S.H., and Karnitz, L.M. (2013). ATR Inhibition Broadly Sensitizes Ovarian Cancer Cells to Chemotherapy Independent of BRCA Status. Cancer Res. 73, 3683–3691.

Iso, T., Suzuki, T., Baird, L., and Yamamoto, M. (2016). Absolute Amounts and Status of the Nrf2-Keap1-Cul3 Complex within Cells. Mol. Cell. Biol. 36, 3100–3112.

Itoh, K., Wakabayashi, N., Katoh, Y., Ishii, T., Igarashi, K., Engel, J.D., and Yamamoto, M. (1999). Keap1 represses nuclear activation of antioxidant responsive elements by Nrf2 through binding to the amino-terminal Neh2 domain. Genes Dev. 13, 76–86.

Jackson, S., and Xiong, Y. (2009). CRL4s: the CUL4-RING E3 ubiquitin ligases. Trends Biochem. Sci. 34, 562–570.

Jazaeri, A.A., Shibata, E., Park, J., Bryant, J.L., Conaway, M.R., Modesitt, S.C., Smith, P.G., Milhollen, M.A., Berger, A.J., and Dutta, A. (2013). Overcoming platinum resistance in preclinical models of ovarian cancer using the neddylation inhibitor MLN4924. Mol. Cancer Ther. 12, 1958–1967.

Jeong, H.-S., Ryoo, I., and Kwak, M.-K. (2015). Regulation of the expression of renal drug transporters in KEAP1-knockdown human tubular cells. Toxicol. In Vitro 29, 884–892.

Jiang, T., Chen, N., Zhao, F., Wang, X.-J., Kong, B., Zheng, W., and Zhang, D.D. (2010). High levels of Nrf2 determine chemoresistance in type II endometrial cancer. Cancer Res. 70, 5486–5496.

Jin, J., Arias, E.E., Chen, J., Harper, J.W., and Walter, J.C. (2006). A Family of Diverse Cul4-Ddb1-Interacting Proteins Includes Cdt2, which Is Required for S Phase Destruction of the Replication Factor Cdt1. Mol. Cell 23, 709–721.

Jones, K.L., Zhang, L., Seldeen, K.L., and Gong, F. (2010). Detection of bulky DNA lesions: DDB2 at the interface of chromatin and DNA repair in eukaryotes. IUBMB Life 62, 803–811.

Joo, W., Xu, G., Persky, N.S., Smogorzewska, A., Rudge, D.G., Buzovetsky, O., Elledge, S.J., and Pavletich, N.P. (2011). The Mosaic of Surface Charge in Contact Electrification. Science 333, 312–316.

Kamura, T., Maenaka, K., Kotoshiba, S., Matsumoto, M., Kohda, D., Conaway, R.C., Conaway, J.W., and Nakayama, K.I. (2004). VHL-box and SOCS-box domains determine binding specificity for Cul2-Rbx1 and Cul5-Rbx2 modules of ubiquitin ligases. Genes Dev. 18, 3055–3065.

Kaustov, L., Lukin, J., Lemak, A., Duan, S., Ho, M., Doherty, R., Penn, L.Z., and Arrowsmith, C.H. (2007). The Conserved CPH Domains of Cul7 and PARC Are Protein-Protein Interaction Modules That Bind the Tetramerization Domain of p53. J. Biol. Chem. 282, 11300–11307.

Kee, Y., Huang, M., Chang, S., Moreau, L.A., Park, E., Smith, P.G., and D'Andrea, A.D. (2012). Inhibition of the Nedd8 system sensitizes cells to DNA interstrand cross-linking agents. Mol. Cancer Res. 10, 369–377.

Kelland, L. (2007). The resurgence of platinum-based cancer chemotherapy. Nat. Rev. Cancer 7, 573–584.

Kitagawa, K., Hiramatsu, Y., Uchida, C., Isobe, T., Hattori, T., Oda, T., Shibata, K., Nakamura, S., Kikuchi, A., and Kitagawa, M. (2009). Fbw7 promotes ubiquitin-dependent degradation of c-Myb: involvement of GSK3-mediated phosphorylation of Thr-572 in mouse c-Myb. Oncogene 28, 2393–2405.

Kitagawa, M., Lee, S.H., and McCormick, F. (2008). Skp2 suppresses p53-dependent apoptosis by inhibiting p300. Mol. Cell 29, 217–231.

Knipscheer, P., Räschle, M., Smogorzewska, A., Enoiu, M., Schärer, O.D., Elledge, S.J., Walter, J.C., and others (2009). The Fanconi anemia pathway promotes replication-dependent DNA interstrand cross-link repair. Science 326, 1698–1701.

Koepp, D.M., Schaefer, L.K., Ye, X., Keyomarsi, K., Chu, C., Harper, J.W., and Elledge, S.J. (2001). Phosphorylation-Dependent Ubiquitination of Cyclin E by the SCFFbw7 Ubiquitin Ligase. Science 294, 173–177.

Komander, D., and Rape, M. (2012). The ubiquitin code. Annu. Rev. Biochem. 81, 203–229.

Koo, J., Yue, P., Deng, X., Khuri, F.R., and Sun, S.-Y. (2015). mTOR complex 2 stabilizes Mcl-1 protein by suppressing its glycogen synthase kinase 3-dependent and SCF-FBXW7-mediated degradation. Mol. Cell. Biol. 35, 2344–2355.

Kossatz, U., Dietrich, N., Zender, L., Buer, J., Manns, M.P., and Malek, N.P. (2004). Skp2-dependent degradation of p27kip1 is essential for cell cycle progression. Genes Dev. 18, 2602–2607.

Lee, J., and Zhou, P. (2007). DCAFs, the Missing Link of the CUL4-DDB1 Ubiquitin Ligase. Mol. Cell 26, 775–780.

Lee, J., and Zhou, P. (2010). Cullins and cancer. Genes Cancer 1, 690–699.

Lee, C.H., Jeon, Y.-T., Kim, S.-H., and Song, Y.-S. (2007). NF-κB as a potential molecular target for cancer therapy. Biofactors 29, 19–35.

Lee, D.-F., Kuo, H.-P., Liu, M., Chou, C.-K., Xia, W., Du, Y., Shen, J., Chen, C.-T., Huo, L., Hsu, M.-C., et al. (2009). KEAP1 E3 Ligase-Mediated Downregulation of NF-κB Signaling by Targeting IKKβ. Mol. Cell 36, 131–140.

Li, C.-C., Yang, J.-C., Lu, M.-C., Lee, C.-L., Peng, C.-Y., Hsu, W.-Y., Dai, Y.-H., Chang, F.-R., Zhang, D.-Y., Wu, W.-J., et al. (2016a). ATR-Chk1 signaling inhibition as a therapeutic strategy to enhance cisplatin chemosensitivity in urothelial bladder cancer. Oncotarget 7, 1947.

Li, S., Ting, N.S.Y., Zheng, L., Chen, P.-L., Ziv, Y., Shiloh, Y., Lee, E.Y.-H.P., and Lee, W.-H. (2000). Functional link of BRCA1 and ataxia telangiectasia gene product in DNA damage response. Nature 406, 210–215.

Li, Z., Pearlman, A.H., and Hsieh, P. (2016b). DNA mismatch repair and the DNA damage response. DNA Repair 38, 94–101.

Liang, C.-C., Zhan, B., Yoshikawa, Y., Haas, W., Gygi, S.P., and Cohn, M.A. (2015). UHRF1 Is a Sensor for DNA Interstrand Crosslinks and Recruits FANCD2 to Initiate the Fanconi Anemia Pathway. Cell Rep. 10, 1947–1956.

Liao, H., Liu, X.J., Blank, J.L., Bouck, D.C., Bernard, H., Garcia, K., and Lightcap, E.S. (2011). Quantitative proteomic analysis of cellular protein modulation upon inhibition of the NEDD8-activating enzyme by MLN4924. Mol. Cell. Proteomics 10, M111.009183.

Lin, J.J., and Dutta, A. (2007). ATR Pathway Is the Primary Pathway for Activating G2/M Checkpoint Induction After Re-replication. J. Biol. Chem. 282, 30357–30362.

Lin, J.J., Milhollen, M.A., Smith, P.G., Narayanan, U., and Dutta, A. (2010). NEDD8-Targeting Drug MLN4924 Elicits DNA Rereplication by Stabilizing Cdt1 in S Phase, Triggering Checkpoint Activation, Apoptosis, and Senescence in Cancer Cells. Cancer Res. 70, 10310–10320.

Lin, W.-C., Kuo, K.-L., Shi, C.-S., Wu, J.-T., Hsieh, J.-T., Chang, H.-C., Liao, S.-M., Chou, C.-T., Chiang, C.-K., Chiu, W.-S., et al. (2015). MLN4924, a Novel NEDD8-activating enzyme inhibitor, exhibits antitumor activity and enhances cisplatin-induced cytotoxicity in human cervical carcinoma: in vitro and in vivo study. Am. J. Cancer Res. 5, 3350–3362.

Liontos, M., Koutsami, M., Sideridou, M., Evangelou, K., Kletsas, D., Levy, B., Kotsinas, A., Nahum, O., Zoumpourlis, V., Kouloukoussa, M., et al. (2007). Deregulated Overexpression of hCdt1 and hCdc6 Promotes Malignant Behavior. Cancer Res. 67, 10899–10909.

Liu, E., Lee, A.Y.-L., Chiba, T., Olson, E., Sun, P., and Wu, X. (2007). The ATR-mediated S phase checkpoint prevents rereplication in mammalian cells when licensing control is disrupted. J. Cell Biol. 179, 643–657.

Liu, J., Hanne, J., Britton, B.M., Bennett, J., Kim, D., Lee, J.-B., and Fishel, R. (2016). Cascading MutS and MutL sliding clamps control DNA diffusion to activate mismatch repair. Nature 539, 583–587.

Lo, J.Y., Spatola, B.N., and Curran, S.P. (2017). WDR23 regulates NRF2 independently of KEAP1. PLOS Genet. 13, e1006762.

Lopez-Martinez, D., Liang, C.-C., and Cohn, M.A. (2016). Cellular response to DNA interstrand crosslinks: the Fanconi anemia pathway. Cell. Mol. Life Sci. 73, 3097–3114.

Lovejoy, C.A., Lock, K., Yenamandra, A., and Cortez, D. (2006). DDB1 Maintains Genome Integrity through Regulation of Cdt1. Mol. Cell. Biol. 26, 7977–7990.

Maréchal, A., and Zou, L. (2015). RPA-coated single-stranded DNA as a platform for post-translational modifications in the DNA damage response. Cell Res. 25, 9–23.

Markkanen, E., Meyer, U., and Dianov, G. (2016). DNA Damage and Repair in Schizophrenia and Autism: Implications for Cancer Comorbidity and Beyond. Int. J. Mol. Sci. 17, 856.

Marullo, R., Werner, E., Degtyareva, N., Moore, B., Altavilla, G., Ramalingam, S.S., and Doetsch, P.W. (2013). Cisplatin induces a mitochondrial-ROS response that contributes to cytotoxicity depending on mitochondrial redox status and bioenergetic functions. PLoS ONE 8, e81162.

Matsuoka, S., Ballif, B.A., Smogorzewska, A., McDonald, E.R., Hurov, K.E., Luo, J., Bakalarski, C.E., Zhao, Z., Solimini, N., Lerenthal, Y., et al. (2007). ATM and ATR Substrate Analysis Reveals Extensive Protein Networks Responsive to DNA Damage. Science 316, 1160–1166.

Michels, J., Obrist, F., Vitale, I., Lissa, D., Garcia, P., Behnam-Motlagh, P., Kohno, K., Wu, G.S., Brenner, C., Castedo, M., et al. (2014). MCL-1 dependency of cisplatin-resistant cancer cells. Biochem. Pharmacol. 92, 55–61.

Miknyoczki, S.J., Jones-Bolin, S., Pritchard, S., Hunter, K., Zhao, H., Wan, W., Ator, M., Bihovsky, R., Hudkins, R., Chatterjee, S., et al. (2003). Chemopotentiation of temozolomide, irinotecan, and cisplatin activity by CEP-6800, a poly (ADP-ribose) polymerase inhibitor. Mol. Cancer Ther. 2, 371–382.

Milhollen, M.A., Narayanan, U., Soucy, T.A., Veiby, P.O., Smith, P.G., and Amidon, B. (2011). Inhibition of NEDD8-Activating Enzyme Induces Rereplication and Apoptosis in Human Tumor Cells Consistent with Deregulating CDT1 Turnover. Cancer Res. 71, 3042–3051.

Miller, R.P., Tadagavadi, R.K., Ramesh, G., and Reeves, W.B. (2010). Mechanisms of Cisplatin Nephrotoxicity. Toxins 2, 2490–2518.

Mladenov, E., Magin, S., Soni, A., and Iliakis, G. (2016). DNA double-strand-break repair in higher eukaryotes and its role in genomic instability and cancer: Cell cycle and proliferation-dependent regulation. Semin. Cancer Biol.

Moding, E.J., Castle, K.D., Perez, B.A., Oh, P., Min, H.D., Norris, H., Ma, Y., Cardona, D.M., Lee, C.-L., and Kirsch, D.G. (2015). Tumor cells, but not endothelial cells, mediate eradication of primary sarcomas by stereotactic body radiation therapy. Sci. Transl. Med. 7, 278ra34–278ra34.

Mohni, K.N., Thompson, P.S., Luzwick, J.W., Glick, G.G., Pendleton, C.S., Lehmann, B.D., Pietenpol, J.A., and Cortez, D. (2015). A Synthetic Lethal Screen Identifies DNA Repair Pathways that Sensitize Cancer Cells to Combined ATR Inhibition and Cisplatin Treatments. PLOS ONE 10, e0125482.

Moldovan, G.-L., and D'Andrea, A.D. (2009). FANCD2 Hurdles the DNA Interstrand Crosslink. Cell 139, 1222–1224.

Möller, A., Sirma, H., Hofmann, T.G., Staege, H., Gresko, E., Lüdi, K.S., Klimczak, E., Dröge, W., Will, H., and Schmitz, M.L. (2003a). Sp100 is important for the stimulatory effect of homeodomain-interacting protein kinase-2 on p53-dependent gene expression. Oncogene 22, 8731–8737.

Möller, A., Sirma, H., Hofmann, T.G., Rueffer, S., Klimczak, E., Dröge, W., Will, H., and Schmitz, M.L. (2003b). PML is required for homeodomain-interacting protein kinase 2 (HIPK2)-mediated p53 phosphorylation and cell cycle arrest but is dispensable for the formation of HIPK domains. Cancer Res. 63, 4310–4314.

Moriwaki, S. (2016). Human DNA repair disorders in dermatology: A historical perspective, current concepts and new insight. J. Dermatol. Sci. 81, 77–84.

Mouw, K.W., and D'Andrea, A.D. (2014). Crosstalk between the nucleotide excision repair and Fanconi anemia/BRCA pathways. DNA Repair 19, 130–134.

Murina, O., von Aesch, C., Karakus, U., Ferretti, L.P., Bolck, H.A., Hänggi, K., and Sartori, A.A. (2014). FANCD2 and CtIP Cooperate to Repair DNA Interstrand Crosslinks. Cell Rep. 7, 1030–1038.

Murphy, A.K., Fitzgerald, M., Ro, T., Kim, J.H., Rabinowitsch, A.I., Chowdhury, D., Schildkraut, C.L., and Borowiec, J.A. (2014). Phosphorylated RPA recruits PALB2 to stalled DNA replication forks to facilitate fork recovery. J. Cell Biol. 206, 493–507.

Myung, K., Chen, C., and Kolodner, R.D. (2001). Multiple pathways cooperate in the suppression of genome instability in Saccharomyces cerevisiae. Nature 411, 1073–1076.

Naegeli, H., and Sugasawa, K. (2011). The xeroderma pigmentosum pathway: Decision tree analysis of DNA quality. DNA Repair 10, 673–683.

Nawrocki, S.T., Kelly, K.R., Smith, P.G., Espitia, C.M., Possemato, A., Beausoleil, S.A., Milhollen, M., Blakemore, S., Thomas, M., Berger, A., et al. (2013). Disrupting protein NEDDylation with MLN4924 is a novel strategy to target cisplatin resistance in ovarian cancer. Clin. Cancer Res. 19, 3577–3590.

Neelsen, K.J., Zanini, I.M.Y., Mijic, S., Herrador, R., Zellweger, R., Ray Chaudhuri, A., Creavin, K.D., Blow, J.J., and Lopes, M. (2013). Deregulated origin licensing leads to chromosomal breaks by rereplication of a gapped DNA template. Genes Dev. 27, 2537–2542.

Nishitani, H., Sugimoto, N., Roukos, V., Nakanishi, Y., Saijo, M., Obuse, C., Tsurimoto, T., Nakayama, K.I., Nakayama, K., Fujita, M., et al. (2006). Two E3 ubiquitin ligases, SCF-Skp2 and DDB1-Cul4, target human Cdt1 for proteolysis. EMBO J. 25, 1126–1136.

Ohta, T., Iijima, K., Miyamoto, M., Nakahara, I., Tanaka, H., Ohtsuji, M., Suzuki, T., Kobayashi, A., Yokota, J., Sakiyama, T., et al. (2008). Loss of Keap1 function activates Nrf2 and provides advantages for lung cancer cell growth. Cancer Res. 68, 1303–1309.

Okumura, F., Matsuzaki, M., Nakatsukasa, K., and Kamura, T. (2012). The role of elongin BC-containing ubiquitin ligases. Front. Oncol. 2.

Olivero, M., Dettori, D., Arena, S., Zecchin, D., Lantelme, E., and Di Renzo, M.F. (2014). The stress phenotype makes cancer cells addicted to CDT2, a substrate receptor of the CRL4 ubiquitin ligase. Oncotarget 5, 5992–6002.

Olson, E., Nievera, C.J., Klimovich, V., Fanning, E., and Wu, X. (2006). RPA2 Is a Direct Downstream Target for ATR to Regulate the S-phase Checkpoint. J. Biol. Chem. 281, 39517–39533.

Pan, W.-W., Zhou, J.-J., Yu, C., Xu, Y., Guo, L.-J., Zhang, H.-Y., Zhou, D., Song, F.-Z., and Fan, H.-Y. (2013). Ubiquitin E3 Ligase CRL4 CDT2/DCAF2 as a potential

chemotherapeutic target for ovarian surface epithelial cancer. J. Biol. Chem. 288, 29680–29691.

Parsons, J.L., and Dianov, G.L. (2013). Co-ordination of base excision repair and genome stability. DNA Repair 12, 326–333.

Payne, A., and Chu, G. (1994). Xeroderma pigmentosum group E binding factor recognizes a broad spectrum of DNA damage. Mutat. Res. 310, 89–102.

Petroski, M.D., and Deshaies, R.J. (2005). Function and regulation of cullin–RING ubiquitin ligases. Nat. Rev. Mol. Cell Biol. 6, 9–20.

Pierce, N.W., Lee, J.E., Liu, X., Sweredoski, M.J., Graham, R.L.J., Larimore, E.A., Rome, M., Zheng, N., Clurman, B.E., Hess, S., et al. (2013). Cand1 promotes assembly of new SCF complexes through dynamic exchange of F box proteins. Cell 153, 206–215.

Pignon, J.-P., Tribodet, H., Scagliotti, G.V., Douillard, J.-Y., Shepherd, F.A., Stephens, R.J., Dunant, A., Torri, V., Rosell, R., Seymour, L., et al. (2008). Lung adjuvant cisplatin evaluation: A pooled analysis by the LACE collaborative group. J. Clin. Oncol. 26, 3552–3559.

Piperdi, B., Walsh, W.V., Bradley, K., Zhou, Z., Bathini, V., Hanrahan-Boshes, M., Hutchinson, L., and Perez-Soler, R. (2012). Phase-I/II study of bortezomib in combination with carboplatin and bevacizumab as first-line therapy in patients with advanced non–small-cell lung cancer. J. Thorac. Oncol. 7, 1032–1040.

Puumalainen, M.-R., Rüthemann, P., Min, J.-H., and Naegeli, H. (2016). Xeroderma pigmentosum group C sensor: unprecedented recognition strategy and tight spatiotemporal regulation. Cell. Mol. Life Sci. 73, 547–566.

Randle, S.J., and Laman, H. (2016). F-box protein interactions with the hallmark pathways in cancer. Semin. Cancer Biol. 36, 3–17.

Roukos, V., Kinkhabwala, A., Colombelli, J., Kotsantis, P., Taraviras, S., Nishitani, H., Stelzer, E., Bastiaens, P., and Lygerou, Z. (2011). Dynamic recruitment of licensing factor Cdt1 to sites of DNA damage. J. Cell Sci. 124, 422–434.

Roy, N., Stoyanova, T., Dominguez-Brauer, C., Park, H.J., Bagchi, S., and Raychaudhuri, P. (2010). DDB2, an essential mediator of premature senescence. Mol. Cell. Biol. 30, 2681–2692.

Rubbi, C.P., and Milner, J. (2001). Xeroderma pigmentosum group E binding factor recognizes a broad spectrum of DNA damage. Carcinogenesis 22, 1789–1796.

Rüthemann, P., Balbo Pogliano, C., and Naegeli, H. (2016). Global-genome Nucleotide Excision Repair Controlled by Ubiquitin/Sumo Modifiers. Front. Genet. 7.

Sarikas, A., Hartmann, T., and Pan, Z.-Q. (2011). The cullin protein family. Genome Biol 12, 220.

Sawant, A., Kothandapani, A., Zhitkovich, A., Sobol, R.W., and Patrick, S.M. (2015). Role of mismatch repair proteins in the processing of cisplatin interstrand cross-links. DNA Repair 35, 126–136.

Schaerer, O.D. (2013). Nucleotide excision repair in eukaryotes. Cold Spring Harb. Perspect. Biol. 5, a012609.

Shah, J.J., Jakubowiak, A.J., O'Connor, O.A., Orlowski, R.Z., Harvey, R.D., Smith, M.R., Lebovic, D., Diefenbach, C., Kelly, K., Hua, Z., et al. (2016). Phase I Study of the Novel Investigational NEDD8-Activating Enzyme Inhibitor Pevonedistat (MLN4924) in Patients with Relapsed/Refractory Multiple Myeloma or Lymphoma. Clin. Cancer Res. 22, 34–43.

Shibata, T., Ohta, T., Tong, K.I., Kokubu, A., Odogawa, R., Tsuta, K., Asamura, H., Yamamoto, M., and Hirohashi, S. (2008). Cancer related mutations in NRF2 impair its recognition by Keap1-Cul3 E3 ligase and promote malignancy. Proc. Natl. Acad. Sci. 105, 13568–13573.

Shichrur, K., Feinberg-Gorenshtein, G., Luria, D., Ash, S., Yaniv, I., and Avigad, S. (2014). Potential role of WSB1 isoforms in growth and survival of neuroblastoma cells. Pediatr. Res. 75, 482–486.

Shukuya, T., Yamanaka, T., Seto, T., Daga, H., Goto, K., Saka, H., Sugawara, S., Takahashi, T., Yokota, S., Kaneda, H., et al. (2015). Nedaplatin plus docetaxel versus cisplatin plus docetaxel for advanced or relapsed squamous cell carcinoma of the lung (WJOG5208L): a randomised, open-label, phase 3 trial. Lancet Oncol. 16, 1630–1638.

Silver, D.P., Richardson, A.L., Eklund, A.C., Wang, Z.C., Szallasi, Z., Li, Q., Juul, N., Leong, C.-O., Calogrias, D., Buraimoh, A., et al. (2010). Efficacy of neoadjuvant cisplatin in triple-negative breast cancer. J. Clin. Oncol. 28, 1145–1153.

Skaar, J.R., Florens, L., Tsutsumi, T., Arai, T., Tron, A., Swanson, S.K., Washburn, M.P., and DeCaprio, J.A. (2007). PARC and CUL7 form atypical cullin RING ligase complexes. Cancer Res. 67, 2006–2014.

Skaar, J.R., Pagan, J.K., and Pagano, M. (2013). Mechanisms and function of substrate recruitment by F-box proteins. Nat. Rev. Mol. Cell Biol. 14, 369–381.

Skaar, J.R., Pagan, J.K., and Pagano, M. (2014). SCF ubiquitin ligase-targeted therapies. Nat. Rev. Drug Discov. 13, 889–903.

Sokol, A.M., Cruet-Hennequart, S., Pasero, P., and Carty, M.P. (2013). DNA polymerase η modulates replication fork progression and DNA damage responses in platinum-treated human cells. Sci. Rep. 3.

Soldatenkov, V.A., Dritschilo, A., Ronai, Z. 've, and Fuchs, S.Y. (1999). Inhibition of homologue of slimb (HOS) function sensitizes human melanoma cells for apoptosis. Cancer Res. 59, 5085–5088.

Soucy, T.A., Smith, P.G., Milhollen, M.A., Berger, A.J., Gavin, J.M., Adhikari, S., Brownell, J.E., Burke, K.E., Cardin, D.P., Critchley, S., et al. (2009). An inhibitor of NEDD8-activating enzyme as a new approach to treat cancer. Nature 458, 732–736.

Stathopoulou, A., Roukos, V., Petropoulou, C., Kotsantis, P., Karantzelis, N., Nishitani, H., Lygerou, Z., and Taraviras, S. (2012). Cdt1 Is Differentially Targeted for Degradation by Anticancer Chemotherapeutic Drugs. PLoS ONE 7, e34621.

Stogios, P.J., Downs, G.S., Jauhal, J.J., Nandra, S.K., and Privé, G.G. (2005). Sequence and structural analysis of BTB domain proteins. Genome Biol. 6, R82.

Stoyanova, T., Roy, N., Kopanja, D., Bagchi, S., and Raychaudhuri, P. (2009). DDB2 decides cell fate following DNA damage. Proc. Natl. Acad. Sci. 106, 10690–10695.

Sun, C.-L., and Chao, C.C.-K. (2005). Potential attenuation of p38 signaling by DDB2 as a factor in acquired TNF resistance. Int. J. Cancer 115, 383–387.

Suryo Rahmanto, A., Savov, V., Brunner, A., Bolin, S., Weishaupt, H., Malyukova, A., Rosén, G., Čančer, M., Hutter, S., Sundström, A., et al. (2016). FBW7 suppression leads to SOX9 stabilization and increased malignancy in medulloblastoma. EMBO J. e201693889.

Takahara, P.M., Rosenzwelg, A.C., Frederick, C.A., and Lippard, S.J. (1995). Crystal structure of double-stranded DNA containing the major adduct of the anticancer drug cisplatin. Nature 377, 649–652.

Takimoto, R., MacLachlan, T.K., Dicker, D.T., Niitsu, Y., Mori, T., and El-Deiry, W.S. (2002). BRCA1 transcriptionally regulates damaged DNA binding protein (DDB2) in the DNA repair response following UV-irradiation. Cancer Biol. Ther. 1, 177–186.

Tan, J., Yang, X., Zhuang, L., Jiang, X., Chen, W., Lee, P.L., Karuturi, R.K.M., Tan, P.B.O., Liu, E.T., and Yu, Q. (2007). Pharmacologic disruption of Polycomb-repressive complex 2-mediated gene repression selectively induces apoptosis in cancer cells. Genes Dev. 21, 1050–1063.

Tan, P., Fuchs, S.Y., Chen, A., Wu, K., Gomez, C., Ronai, Z., and Pan, Z.-Q. (1999). Recruitment of a ROC1–CUL1 ubiquitin ligase by Skp1 and HOS to catalyze the ubiquitination of IκBα. Mol. Cell 3, 527–533.

Tanaka, T., Nakatani, T., and Kamitani, T. (2012). Inhibition of NEDD8-conjugation pathway by novel molecules: Potential approaches to anticancer therapy. Mol. Oncol. 6, 267–275.

Terai, K., Abbas, T., Jazaeri, A.A., and Dutta, A. (2010). CRL4 Cdt2 E3 ubiquitin ligase monoubiquitinates PCNA to promote translesion DNA synthesis. Mol. Cell 37, 143–149.

Tian, Y., Paramasivam, M., Ghosal, G., Chen, D., Shen, X., Huang, Y., Akhter, S., Legerski, R., Chen, J., Seidman, M.M., et al. (2015). UHRF1 Contributes to DNA Damage Repair as a Lesion Recognition Factor and Nuclease Scaffold. Cell Rep. 10, 1957–1966.

Tian, Y., Wu, K., Liu, Q., Han, N., Zhang, L., Chu, Q., and Chen, Y. (2016). Modification of platinum sensitivity by KEAP1/NRF2 signals in non-small cell lung cancer. J. Hematol. Oncol.J Hematol Oncol 9.

Toledo, L.I., Murga, M., Zur, R., Soria, R., Rodriguez, A., Martinez, S., Oyarzabal, J., Pastor, J., Bischoff, J.R., and Fernandez-Capetillo, O. (2011). A cell-based screen identifies ATR inhibitors with synthetic lethal properties for cancer-associated mutations. Nat. Struct. Mol. Biol. 18, 721–727.

Tubbs, J.L., Latypov, V., Kanugula, S., Butt, A., Melikishvili, M., Kraehenbuehl, R., Fleck, O., Marriott, A., Watson, A.J., Verbeek, B., et al. (2009). Flipping of alkylated DNA damage bridges base and nucleotide excision repair. Nature 459, 808–813.

van Twest, S., Murphy, V.J., Hodson, C., Tan, W., Swuec, P., O'Rourke, J.J., Heierhorst, J., Crismani, W., and Deans, A.J. (2017). Mechanism of Ubiquitination and Deubiquitination in the Fanconi Anemia Pathway. Mol. Cell 65, 247–259.

Unno, J., Itaya, A., Taoka, M., Sato, K., Tomida, J., Sakai, W., Sugasawa, K., Ishiai, M., Ikura, T., Isobe, T., et al. (2014). FANCD2 Binds CtIP and Regulates DNA-End Resection during DNA Interstrand Crosslink Repair. Cell Rep. 7, 1039–1047.

Veena, M.S., Wilken, R., Zheng, J.-Y., Gholkar, A., Venkatesan, N., Vira, D., Ahmed, S., Basak, S.K., Dalgard, C.L., Ravichandran, S., et al. (2014). p16 protein and gigaxonin are associated with the ubiquitination of NFκB in cisplatin-induced senescence of cancer cells. J. Biol. Chem. 289, 34921–34937.

Wang, D., and Lippard, S.J. (2005). Cellular processing of platinum anticancer drugs. Nat. Rev. Drug Discov. 4, 307–320.

Wang, S., Xia, W., Wang, X., Jiang, F., Yin, R., and Xu, L. (2016). Atlas on substrate recognition subunits of CRL2 E3 ligases. Oncotarget.

Wang, X.-J., Sun, Z., Villeneuve, N.F., Zhang, S., Zhao, F., Li, Y., Chen, W., Yi, X., Zheng, W., Wondrak, G.T., et al. (2008). Nrf2 enhances resistance of cancer cells to chemotherapeutic drugs, the dark side of Nrf2. Carcinogenesis 29, 1235–1243.

Wang, Y., Zhang, P., Liu, Z., Wang, Q., Wen, M., Wang, Y., Yuan, H., Mao, J.-H., and Wei, G. (2014a). CUL4A overexpression enhances lung tumor growth and sensitizes lung cancer cells to erlotinib via transcriptional regulation of EGFR. Mol. Cancer 13, 252.

Wang, Z., Liu, P., Inuzuka, H., and Wei, W. (2014b). Roles of F-box proteins in cancer. Nat. Rev. Cancer 14, 233–247.

van de Wetering, M., Francies, H.E., Francis, J.M., Bounova, G., Iorio, F., Pronk, A., van Houdt, W., van Gorp, J., Taylor-Weiner, A., Kester, L., et al. (2015). Prospective Derivation of a living organoid biobank of colorectal cancer patients. Cell 161, 933–945.

Wheate, N.J., Walker, S., Craig, G.E., and Oun, R. (2010). The status of platinum anticancer drugs in the clinic and in clinical trials.docx. Dalton Trans. 39, 8113–8127.

Wilkinson, Ke.D. (1997). Regulation of ubiquitin-dependent processes by deubiquitinating enzymes. FASEB J. 11, 1245–1256.

Willmarth, N.E., Albertson, D.G., and Ethier, S.P. (2004). Chromosomal instability and lack of cyclin E regulation in hCdc4 mutant human breast cancer cells. Breast Cancer Res 6, R531–R539.

Woo, M.G., Xue, K., Liu, J., McBride, H., and Tsang, B.K. (2012). Calpain-mediated processing of p53-associated parkin-like cytoplasmic protein (PARC) affects chemosensitivity of human ovarian cancer cells by promoting p53 subcellular trafficking. J. Biol. Chem. 287, 3963–3975.

Wu, B., Liu, Z.-Y., Cui, J., Yang, X.-M., Jing, L., Zhou, Y., Chen, Z.-N., and Jiang, J.-L. (2017). F-Box Protein FBXO22 Mediates Polyubiquitination and Degradation of CD147 to Reverse Cisplatin Resistance of Tumor Cells. Int. J. Mol. Sci. 18, 212.

Wu, C.-C., Li, T.-K., Farh, L., Lin, T.-S., Yu, Y.-J., Yen, T.-J., Chiang, C.-W., and Chan, N.-L. (2011). Structural Basis of Type II Topoisomerase Inhibition by the Anticancer Drug Etoposide. Science 333, 456–459.

Wu, S., Zhu, W., Nhan, T., Toth, J.I., Petroski, M.D., and Wolf, D.A. (2013). CAND1 controls in vivo dynamics of the cullin 1-RING ubiquitin ligase repertoire. Nat. Commun. 4, 1642.

Xia, M., Yu, H., Gu, S., Xu, Y., Su, J., Li, H., Kang, J., and Cui, M. (2014). p62/SQSTM1 is involved in cisplatin resistance in human ovarian cancer cells via the Keap1-Nrf2-ARE system. Int. J. Oncol. 45, 2341–2348.

Xiong, L., Edwards, C., and Zhou, L. (2014). The Biological Function and Clinical Utilization of CD147 in Human Diseases: A Review of the Current Scientific Literature. Int. J. Mol. Sci. 15, 17411–17441.

Xu, L., Wei, Y., Reboul, J., Vaglio, P., Shin, T.-H., Vidal, M., Elledge, S.J., and Harper, J.W. (2003). BTB proteins are substrate-specific adaptors in an SCF-like modular ubiquitin ligase containing CUL-3. Nature 425, 316–321.

Xu, Y., Wang, Y., Ma, G., Wang, Q., and Wei, G. (2014). CUL4A is overexpressed in human pituitary adenomas and regulates pituitary tumor cell proliferation. J. Neurooncol. 116, 625–632.

Yan, H., Bi, L., Wang, Y., Zhang, X., Hou, Z., Wang, Q., Snijders, A.M., and Mao, J.-H. (2017). Integrative analysis of multi-omics data reveals distinct impacts of DDB1-CUL4 associated factors in human lung adenocarcinomas. Sci. Rep. 7.

Yang, Y.-L., Hung, M.-S., Wang, Y., Ni, J., Mao, J.-H., Hsieh, D., Au, A., Kumar, A., Quigley, D., Fang, L.T., et al. (2014). Lung tumourigenesis in a conditional Cul4A transgenic mouse model: Cul4A in lung tumourigenesis. J. Pathol. 233, 113–123.

Yi, J., Lu, G., Li, L., Wang, X., Cao, L., Lin, M., Zhang, S., and Shao, G. (2015). DNA damage-induced activation of CUL4B targets HUWE1 for proteasomal degradation. Nucleic Acids Res. 43.

You, Z., and Masai, H. (2008). Cdt1 Forms a Complex with the Minichromosome Maintenance Protein (MCM) and Activates Its Helicase Activity. J. Biol. Chem. 283, 24469–24477.

Yu, H.-G., Wei, W., Xia, L.-H., Han, W.-L., Zhao, P., Wu, S.-J., Li, W.-D., and Chen, W. (2013). FBW7 upregulation enhances cisplatin cytotoxicity in non-small cell lung cancer cells. Asian Pac. J. Cancer Prev. 14, 6321–6326.

Yun, M.H., and Hiom, K. (2009). CtIP-BRCA1 modulates the choice of DNA double-strand-break repair pathway throughout the cell cycle. Nature 459, 460–463.

Zellweger, R., Dalcher, D., Mutreja, K., Berti, M., Schmid, J.A., Herrador, R., Vindigni, A., and Lopes, M. (2015). Rad51-mediated replication fork reversal is a global response to genotoxic treatments in human cells. J. Cell Biol. 208, 563–579.

Zeng, M., Ren, L., Mizuno, K., Nestoras, K., Wang, H., Tang, Z., Guo, L., Kong, D., Hu, Q., He, Q., et al. (2016). CRL4Wdr70 regulates H2B monoubiquitination and facilitates Exo1-dependent resection. Nat. Commun. 7, 11364.

Zhang, L., and Wang, C. (2006). F-box protein Skp2: a novel transcriptional target of E2F. Oncogene 25, 2615–2627.

Zhang, H.-F., Tomida, A., Koshimizu, R., Ogiso, Y., Lei, S., and Tsuruo, T. (2004). Cullin 3 promotes proteasomal degradation of the topoisomerase I-DNA covalent complex. CANCER Res. 64, 1114–1121.

Zhang, P.-F., Sheng, L.-L., Wang, G., Tian, M., Zhu, L.-Y., Zhang, R., Zhang, J., and Zhu, J.-S. (2016a). miR-363 promotes proliferation and chemo-resistance of human gastric cancer via targeting of FBW7 ubiquitin ligase expression. Oncotarget 7, 35284–35292.

Zhang, W., Cao, L., Sun, Z., Xu, J., Tang, L., Chen, W., Luo, J., Yang, F., Wang, Y., and Guan, X. (2016b). Skp2 is over-expressed in breast cancer and promotes breast cancer cell proliferation. Cell Cycle 15, 1344–1351.

Zhao, Y., and Sun, Y. (2013). Cullin-RING ligases as attractive anti-cancer targets. Curr. Pharm. Des. 19, 3215–3225.

Zhao, R., Han, C., Eisenhauer, E., Kroger, J., Zhao, W., Yu, J., Selvendiran, K., Liu, X., Wani, A.A., and Wang, Q.-E. (2013). DNA damage-binding complex recruits HDAC1 to repress Bcl-2 transcription in human ovarian cancer cells. Mol. Cancer Res. 12.

Zhou, H., Liu, Y., Zhu, R., Ding, F., Wan, Y., Li, Y., and Liu, Z. (2017). FBXO32 suppresses breast cancer tumorigenesis through targeting KLF4 to proteasomal degradation. Oncogene 36, 3312–3321.

Zhou, X., Jin, W., Jia, H., Yan, J., and Zhang, G. (2015). MiR-223 promotes the cisplatin resistance of human gastric cancer cells via regulating cell cycle by targeting FBXW7. J. Exp. Clin. Cancer Res. 34.

Zhu, W., and Dutta, A. (2006). An ATR- and BRCA1-Mediated Fanconi Anemia Pathway Is Required for Activating the G2/M Checkpoint and DNA Damage Repair upon Rereplication. Mol. Cell. Biol. 26, 4601–4611.

Zou, L., and Elledge, S.J. (2003). Sensing DNA Damage Through ATRIP Recognition of RPA-ssDNA Complexes. Science 300, 1542–1548.

6 Curricullum Vitae

Personal Information

Name	CODILUPI
First Name	Tamara
Date of birth	13.04.1983
Heimatort	Rupperswil, AG

Education

06/2013 - present **PhD**
University of Zurich
Life Science Zurich Graduate School, Cancer Biology PhD Program
Laboratory of Prof. Hanspeter Naegeli

Thesis: CRL4 Ubiquitin Ligase Promotes Fanconi Anemia Pathway-Induced Single-Stranded DNA Signaling at Interstrand Crosslinks.

9/2010 - 9/2012 **Master of Sciences**
University of Zurich
Molecular and Cellular Biology Master Program

Thesis in the laboratory of Prof. Dr. Martin Pruschy, Molecular Radiobiology, University Hospital Zurich: The role of MVP in drug- and radiation resistance.

9/2007 - 9/2010 **Bachelor of Science**
University of Applied Sciences Northwestern Switzerland
Molecular Life Sciences, Molecular Bioanalytics Program

Thesis: in the Laboratory of Prof. Dr. Davide Corona and Prof. Dr. Rosa Alduina; Erasmus exchange in the University of Palermo, Italy: Identification and characterization of bacterial endosymbionts present in the model system *Drosophila melanogaster*.

Teaching and mentoring experience

2017	Supervision of a semester student, University of Konstanz
2015	Assistance of a practical course: Genetics course BIO111 / 117
2015	Supervision of a master student, ETH Zürich
2015	Planning and teaching of a practical cell culture course, Universitiy of Zurich
2013 and 2014	Supervision of oral exams: Krebs: Grundlagen, Ursachen und Therapie, ETH Zürich

7 Acknowledgments

First, I would like to acknowledge my supervisor Hanspeter Naegeli for giving me the opportunity to do my PhD in his laboratory and to work on an interesting project. His continuous guidance, encouragement and confidence contributed substantially to the success of my PhD. Next, I would like to thank my PhD committee Lorenza Penengo, Pavel Janscak and Martin Pruschy for their great support and valuable discussions throughout the project. Special thanks to Martin who also supervised my Master's thesis. His enthusiasm and positivity encouraged me to continue my scientific career.

A big thank you to all former and current colleagues from the Nägeli group: Chiara, Elena, Parisa, Inigo, Peter, Hans, Sandro, Julian, Doreen and Lukas for having a great time in the lab and all the scientific and non-scientific discussions; Zuzana for her great job in managing the lab and her almost endless patience; Enni for helpful scientific discussions and great inputs. Thanks to everyone of the Institute of Veterinary Pharmacology and Toxicology for providing a friendly working environment and sharing many social events.

Finally, a special thanks to all my friends and family for the unlimited support and encouragement. Mein besonderer Dank gilt meiner Familie und meinem Freund, insbesondere Yves, Papi und Angi die mich in all meinen Entscheidungen unterstützt haben. Ohne eure moralische Unterstützung, kontinuierliche Motivation und Verständins in den letzten Jahren wäre dies nicht möglich gewesen. Jasmin, thanks for sharing so many nice moments throughout our students life and even before. Thanks that I could always count on you. Thanks to everyone I did not mention here. I am greatful for your support and happy moments we shared together.